

1. Report No. FHWA/TX-86/16+316-1		2. Government Accession No.		3. Recipient's Catalog No.	
4. Title and Subtitle DURABILITY OF PRESTRESSED BRIDGE DECKS				5. Report Date July 1985	
				6. Performing Organization Code	
7. Author(s) R. W. Poston, R. L. Carrasquillo, and J. E. Breen				8. Performing Organization Report No. Research Report 316-1	
9. Performing Organization Name and Address Center for Transportation Research The University of Texas at Austin Austin, Texas 78712-1075				10. Work Unit No.	
				11. Contract or Grant No. Research Study 3-5-82-316	
12. Sponsoring Agency Name and Address Texas State Department of Highways and Public Transportation; Transportation Planning Division P. O. Box 5051 Austin, Texas 78763				13. Type of Report and Period Covered Interim	
				14. Sponsoring Agency Code	
15. Supplementary Notes Study conducted in cooperation with the U. S. Department of Transportation, Federal Highway Administration Research Study Title: "Application of Transverse Prestressing to Bridge Decks"					
16. Abstract It is estimated that \$500 million dollars is spent annually for repair of bridge decks which suffer from deterioration. The major cause of bridge deck deterioration is corrosion of reinforcing steel induced by exposure to chlorides from deicers and salt water spray. Dissolved salts seep into bridge decks primarily at crack locations and cause steel corrosion which sets up splitting forces because of the volumetric expansion and eventually breaks the concrete sport. This report briefly presents background information on the mechanism of corrosion of steel reinforcement in concrete, and summarizes the observations and findings from an experimental corrosion study. A simple test specimen was developed to simulate the behavior of a transversely prestressed bridge deck subjected to an aggressive deicing salt exposure. The experimental program investigated the primary variables affecting corrosion of steel in prestressed concrete: concrete cover, crack width, protective coatings for steel reinforcement, type of prestressing protective system, concrete quality, and level of prestressing. Behavioral trends are presented as determined from half cell potential measurement of the nonprestressed reinforcement, chloride analysis of the concrete, and visual observation from a post mortem autopsy of the specimens.					
17. Key Words bridge decks, prestressed, durability, corrosion, reinforcing steel, concrete, salt, splitting			18. Distribution Statement No restrictions. This document is available to the public through the National Technical Information Service, Springfield, Virginia 22161.		
19. Security Classif. (of this report) Unclassified		20. Security Classif. (of this page) Unclassified		21. No. of Pages 176	22. Price

DURABILITY OF PRESTRESSED BRIDGE DECKS

by

R. W. Poston
R. L. Carrasquillo
and
J. E. Breen

Research Report 316-1

Research Project No. 3-5-82-316

"Application of Transverse Prestressing to Bridge Decks"

Conducted for

Texas

State Department of Highways and Public Transportation

In cooperation with the
U. S. Department of Transportation
Federal Highway Administration

by

CENTER FOR TRANSPORTATION RESEARCH
BUREAU OF ENGINEERING RESEARCH
THE UNIVERSITY OF TEXAS AT AUSTIN

July 1985

The contents of this report reflect the views of the authors who are responsible for the facts and accuracy of the data presented herein. The contents do not necessarily reflect the views or policies of the Federal Highway Administration. This report does not constitute a standard, specification, or regulation.

P R E F A C E

This report is the first in a series which summarizes a detailed investigation assessing the use of deck prestressing as a method of improving durability of bridge decks. This report briefly reviews the mechanism of steel reinforcement corrosion in concrete, and summarizes an extensive experimental corrosion study which was conducted to assess the use of deck prestressing as a method of improving bridge deck durability. The second report in the series summarizes an extensive analytical and experimental program which was performed to document the structural behavior of bridge decks utilizing transverse prestressing. The third and final report in the series draws on the findings from the durability and structural studies. The final report develops design recommendations and suggested AASHTO Specification provisions to use combined longitudinal and transverse prestressing for economical and durable bridge decks. The third report also contains several design examples to illustrate the application of the design recommendations and procedures.

This work is part of Research Project 3-5-82-316, entitled "Application of Transverse Prestressing to Bridge Decks." The study was conducted at the Phil M. Ferguson Structural Engineering Laboratory as part of the overall research program of the Center for Transportation Research, Bureau of Engineering Research, of The University of Texas at Austin. The work was sponsored jointly by the Texas State Department of Highways and Public Transportation and the Federal Highway Administration.

Liaison with the SDHPT was maintained through the contact representative, Mr. James C. Wall; the Area IV Committee Chairman, Mr. Robert L. Reed; and the State Bridge Engineer, Mr. Wayne Henneberger. Mr. Jerry W. Bowman was the contact representative for the Federal Highway Administration.

The overall study was directed by Dr. Ramon L. Carrasquillo, Associate Professor of Civil Engineering, and Dr. John E. Breen, who holds the Nasser I. Al-Rashid Chair in Civil Engineering. The detailed work was carried out under the immediate supervision of Dr. Randall W. Poston, research engineer, Center for Transportation Research.

S U M M A R Y

It is estimated that \$500 million dollars is spent annually for repair of bridge decks which suffer from deterioration. The major cause of bridge deck deterioration is corrosion of reinforcing steel induced by exposure to chlorides from deicers and salt water spray.

Dissolved salts seep into bridge decks primarily at crack locations and cause steel corrosion which sets up splitting forces because of the volumetric expansion and eventually breaks the concrete spout.

This report briefly presents background information on the mechanism of corrosion of steel reinforcement in concrete, and summarizes the observations and findings from an experimental corrosion study. A simple test specimen was developed to simulate the behavior of a transversely prestressed bridge deck subjected to an aggressive deicing salt exposure. The experimental program investigated the primary variables affecting corrosion of steel in prestressed concrete: concrete cover, crack width, protective coatings for steel reinforcement, type of prestressing protective system, concrete quality, and level of prestressing. Behavioral trends are presented as determined from half cell potential measurement of the nonprestressed reinforcement, chloride analysis of the concrete, and visual observation from a post mortem autopsy of the specimens.

I M P L E M E N T A T I O N

This report is the first in a series which summarizes a major experimental and analytical study aimed at developing specific recommendations for design of post-tensioned bridge decks. The recommendations should be considered by the Texas State Department of Highways and Public Transportation and by AASHTO for inclusion in design specifications and design manuals of practice. The specific recommendations are included in the third and concluding report of this series.

This report contains background information of interest to those responsible for deciding on specifications and codes. It contains documentation of the durability study on which many of the design recommendations are based. In addition, it contains specific information regarding the behavior of reinforced and prestressed concrete subjected to an aggressive chloride-containing corrosive environment. Control of corrosion of deck steel reinforcement will lead to more durable bridge decks and should result in important savings in both maintenance and replacement funds.

C O N T E N T S

Part	Page
1 INTRODUCTION	1
1.1 Problems with Bridge Deck Durability	1
1.2 Deck Prestressing for Improving Deck Durability	1
1.3 Design Needs for Transverse Prestressing	3
1.4 Objectives of this Research	5
1.5 Report Contents	7
2 CORROSION OF STEEL IN CONCRETE	9
2.1 Introduction	9
2.2 Nature and Mechanics of Galvanic Corrosion of Steel in Concrete	9
2.2.1 Typical Chemical Reactions	12
2.2.2 Rate of Corrosion	15
2.2.3 Influence of Cracking	15
2.3 Corrosion Induced Distress	19
2.3.1 Staining	19
2.3.2 Concrete Cracking, Spalling, Delamination and Decomposition	20
2.3.3 Steel Pitting and Fracture	22
2.4 Detection and Evaluation of Corrosion Distress	22
2.4.1 Visual Inspection	23
2.4.2 Chloride Determination	24
2.4.3 Half Cell Potential	24
2.4.4 Post-Mortem Examination	25
3 DURABILITY TEST PROGRAM	27
3.1 Introduction	27
3.2 Test Variables	27
3.2.1 Effect of Prestressing	27
3.2.2 Cracking	29
3.2.3 Concrete Cover	29
3.2.4 Type of Nonprestressed Reinforcement	29
3.2.5 Type of Prestressing System	30
3.3 General Description	30
3.4 Specimen Design and Details	34

Part	Page	
3.5	Materials	37
3.5.1	Concrete	37
3.5.2	Nonprestressed Reinforcement	37
3.5.3	Prestressing Strand	37
3.5.4	Anchorage	41
3.5.5	Galvanized Duct	41
3.5.6	Grout	41
3.5.7	Mortar Plug	41
3.5.8	Salt	44
3.5.9	Other Materials	44
3.6	Fabrication	44
3.6.1	Speciman Fabrication	44
3.6.2	Posttensioning Operation	44
3.6.3	Grouting	48
3.6.4	Pocket Patch	48
3.7	Half Cell Potential Instrumentation	48
3.8	Test Setup	50
3.9	Testing	50
3.9.1	Cracking of Specimens	50
3.9.2	Exposure	55
3.9.3	Post-Mortem Examination	55
4	PRESENTATION OF DURABILITY TEST RESULTS	61
4.1	Introduction	61
4.2	Specimen Initial Cracking Cycle	61
4.3	Exposure Testing	65
4.3.1	Half Cell Potential Readings	65
4.3.2	Visual Examination	68
4.4	Post-Mortem Examination	68
4.4.1	Chloride Content Determination	68
4.4.2	Visual Inspection of Reinforcement	72
5	EVALUATION OF DURABILITY STUDY TEST RESULTS	105
5.1	Introduction	105
5.2	Initial Cracking	105
5.3	Exposure Testing	107
5.3.1	Visual Inspection	107
5.3.2	Half Cell Potentials for Nonprestressed Reinforcement	109
5.3.2.1	Predictive Capability	110
5.3.2.2	Comparisons	110
5.3.2.3	Time to Corrosion	120

Part	Page
5.4 Post-Mortem Examination	120
5.4.1 Chloride Content	120
5.4.1.1 Cracked Concrete	123
5.4.1.2 Uncracked Concrete	125
5.4.1.3 Penetration with Depth	127
5.4.1.4 Relationship Between Chloride Level and Concrete Quality	127
5.4.2 Visual Inspection	129
6 CONCLUSIONS AND RECOMMENDATIONS	139
6.1 Conclusions	139
6.2 Recommendations	140
APPENDIX A - Specimen Crack Maps, Saw Cut Locations, and Concrete Sample Locations for Chloride Content Tests	143
APPENDIX B - Summary of Mineral Studies Laboratory (MSL) Procedure for Determination of Chloride (Cl ⁻) Content in Concrete	151
REFERENCES	157

F I G U R E S

Figure		Page
1.1	Bridge deck deterioration	2
1.2	Corrosion protection mechanism of prestressing	4
1.3	Various components of overall research study on deck prestressing	6
1.4	Deck prestressing of a conventional slab-girder bridge	8
2.1	Basic galvanic cell	10
2.2	Corrosion of steel in concrete	14
2.3	Steel corrosion products	16
2.4	Influence of crack width on corrosion of concrete in marine environment after 10 years exposure	18
2.5	Concrete deterioration mechanism	21
3.1	Durability specimens	31
3.2	Durability specimens representing a component of a transversely prestressed bridge deck	33
3.3	Loading scheme for durability specimens	35
3.4	Durability specimen details	36
3.5	Compressive strength versus time	39
3.6	VSL anchorage S5N used in unbonded specimens	42
3.7	Details of grouted specimen anchorages	43
3.8	Reinforcement tied to chairs in unbonded specimen; wood positioning template and coil ties in place	45
3.9	Anchorage casting and pocket former on stressing end of unbonded specimen	45

Figure		Page
3.10	Reinforcement tied to chairs in grouted specimens; wood positioning template in place	46
3.11	Cast-in dead end anchorage and chucks for grouted specimen; wires for half cell potential instrumentation in place	46
3.12	Specimen posttensioning	47
3.13	Grouting tank	47
3.14a	Electrical connection to a reinforcing bar	49
3.14b	Electrical connections to prestressing strand and galvanized duct	49
3.15	Exposure facility	51
3.16	Actual loading system	51
3.17	Schematic of loading system	52
3.18	Painted surfaces; half cell potential stations	53
3.19	Levee system on specimens	54
3.20	Cracks marked on specimens during initial cracking	54
3.21	Basic exposure cycle	57
3.22	Half cell potential readings	57
3.23	Saw used to crosscut specimens at crack zones	59
3.24	Concrete section removed from crack zone	59
4.1a	Induced cracks for Specimen 1	62
4.1b	Induced cracks for Specimen 13	62
4.2a	Induced cracks for Specimen 2	63
4.2b	Induced cracks for Specimen 18	63

Figure		Page
4.3	Moment versus crack width upon reloading after initial cracking	64
4.4	Half cell potentials with time for left reinforcing bar in Specimen 13	66
4.5	Half cell potentials with time for right reinforcing bar in Specimen 11	67
4.6	Rust staining on specimen surface above anchorage	69
4.7	Surface rust staining and hairline crack along direction of specimen length	70
4.8	Discoloration of mortar anchorage plug in some areas after prolonged exposure	71
4.9	Typical heavy corrosion of uncoated nonprestressed reinforcement in the region near cracks	77
4.10	Very light surface corrosion on epoxy-coated reinforcing bar	78
4.11	Surface corrosion of zinc coating on galvanized duct of grouted specimens	78
4.12	Very light surface corrosion on unbonded tendon removed from Specimen 8	79
4.13	Corrosion of loaded end anchorage of unbonded specimens	80
4.14	Description of component codes used in Table 4.3	83
5.1	Moment versus crack width reloading after initial cracking	106
5.2	Migration path of salt water	108
5.3	Comparison of incidence of corrosion of uncoated and epoxy-coated reinforcement	118
5.4	Comparison of incidence of corrosion of reinforcement in nonprestressed and prestressed specimens	119

Figure		Page
5.5	Comparison of incidence of corrosion of reinforcement in specimens with 2 in. and 3 in. concrete covers without regard to other test variables	121
5.6	Effect of precleaning uncoated reinforcement on incidence of corrosion	122
5.7	Cl ⁻ content at level of reinforcement at the crack location in the specimens (see Appendix A for crack locations)	124
5.8	Cl ⁻ content at level of reinforcement at the uncracked location in the specimens (see Appendix A for core locations)	126
5.9	Cl ⁻ penetration with depth in uncracked concrete	128
5.10	Comparison of Cl ⁻ penetration with depth in uncracked sections	130
5.11	Spreading effect of corrosion of uncoated reinforcement	133
5.12a	Histogram of corrosion of uncoated reinforcement	134
5.12b	Histogram of corrosion of epoxy-coated reinforcement ..	134
5.13	Histogram of nonprestressed reinforcement corrosion in specimens	135
5.14a	Histogram of nonprestressed reinforcement corrosion with 2 in. cover	136
5.14b	Histogram of nonprestressed reinforcement corrosion with 3 in. cover	136

T A B L E S

Table		Page
2.1	Standard EMF Series of Metals	11
3.1	Summary of Durability Study Test Variables	28
3.2	Durability Specimen Summary	32
3.3	Concrete Mix Design for Durability Specimens	38
3.4	Estimated 28-Day Strengths	38
3.5	Durability Specimens Cast from Each Batch	40
3.6	Summary of Interior Support Positions	40
3.7	Summary of Specimen Loads	56
4.1	Chloride Ion (Cl ⁻) Content in Concrete Samples Taken from Durability Specimens	73
4.2	Evaluation System for the Visual Inspection of the Components Removed from the Durability Specimens	81
4.3	Results of the Evaluation of the Components Removed from the Durability Specimens	84
5.1	Evaluation of the Half Cell Potentials for the Mild Reinforcement in the Secimens	111
5.2	Comparison of Corrosion Activity by Half Cell Potential (HCP) Method to that Observed by Visual Inspection of the Exposed Steel	113
5.3	Evaluation of Incidence of Corrosion of the Nonprestressed Reinforcement in the Durability Specimens	115
5.4	ACI Recommendations for Reinforced and Prestressed Concrete Slabs Exposed to Corrosive Environments	131

CHAPTER 1

INTRODUCTION

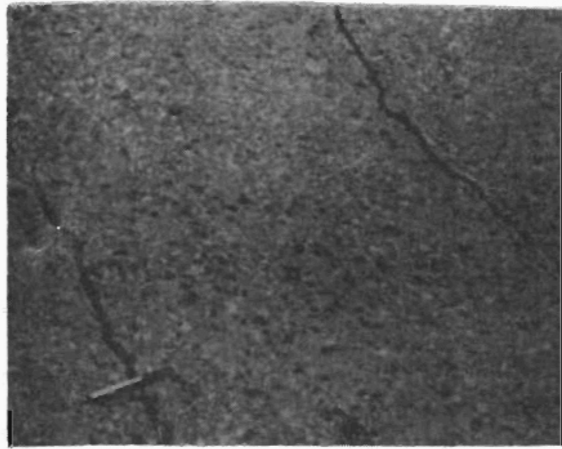
1.1 Problems with Bridge Deck Durability

There are approximately 560,000 bridges in the U.S., of which 45 percent are structurally deficient or functionally obsolete requiring close to \$50 billion in repair [1,2,3]. Additionally, the interstate highway system that stretches over 40,000 miles across the country will require close to \$500 billion in repairs over the next decade according to the U.S. Department of Transportation [1]. State highway agencies expect bridges to last 50 years or more, but many show signs of corrosion of reinforcement and concrete delamination in five years or less [3]. The problem has become so severe that the phrase "the bridge deck problem" has been coined to specifically imply the distress suffered by bridge decks [3,4].

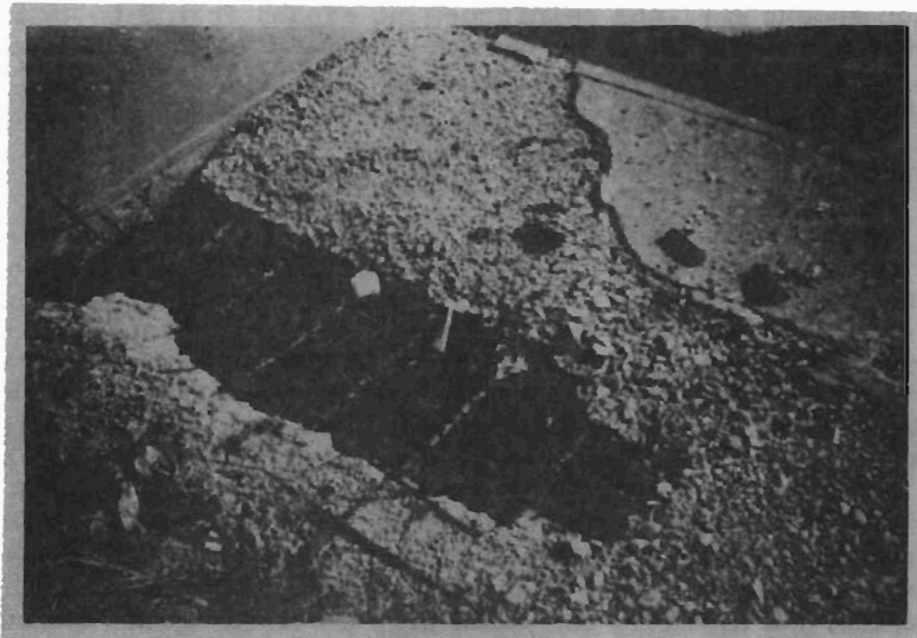
The major cause of the bridge deck deterioration is chloride containing deicing salts that have been applied to maintain trafficable winter roadway conditions [3]. In coastal areas, decks in the splash zones suffer similar attacks. The rate of corrosion accelerates rapidly when chlorides combine with moisture and oxygen and disrupt the passivity of reinforcing steel. In turn, the corrosion products of the reinforcement expand from 2 to 15 times, resulting in stresses large enough to crack and subsequently spall a concrete bridge deck, as seen in Fig. 1.1.

1.2 Deck Prestressing for Improving Deck Durability

Most efforts in improving the corrosion distress suffered by bridge decks have focused on improving the quality of concrete, increasing the concrete cover over the reinforcing steel, or providing other forms of corrosion protection ranging from coatings for the steel reinforcement and the use of exotic types of concrete to active cathodic protection. However, these alternatives have met with only moderate success for several reasons. The cost of many of these alternatives adds significantly to the construction cost of the bridge deck. In addition, many of the corrosion protection alternatives become ineffective when cracking of the bridge deck occurs under moving vehicular loads. The cracking suffered by bridge decks facilitates the penetration of water, oxygen, and chloride ions into the concrete, resulting in corrosion of the reinforcement and surface spalling. One suggestion for improving bridge deck durability is the



a) cracking in a bridge deck



b) bridge deck spalling

Fig. 1.1 Bridge deck deterioration

application of deck prestressing [5.6]. In composite slab and girder bridges, the decks would be longitudinally and transversely prestressed. In post-tensioned box girder bridges, the decks are now longitudinally prestressed and only transverse prestressing would have to be added. "Active Reinforcement" of a deck by prestressing would minimize or possibly eliminate cracking of the bridge deck.

Figure 1.2 illustrates the corrosion protection mechanism of prestressing. Since corrosion producing elements can penetrate uncracked concrete with insufficient cover, concrete quality or compaction, it is assumed throughout this report that all normal precautions involving provision of adequate cover and concrete quality will be observed. Even in such a well-designed and constructed conventional reinforced concrete slab, which more than likely cracks under service load conditions, water, oxygen and salt can penetrate the concrete with subsequent corrosion of the reinforcing steel. However, under the action of prestressing the applied compressive force prevents cracks from forming or closes the cracks preventing penetration of the corrosion-producing elements.

In addition, prestressing provides an auxiliary level of corrosion protection. Even if cracks do form under load in a prestressed concrete member, upon removal of the load the cracks completely close. This is in contrast to a reinforced concrete member where once a crack forms, the crack never completely closes. In non-prestressed members, there will generally be a residual crack opening at the concrete surface allowing penetration of the corrosion-producing elements.

Unlike many of the other corrosion protection alternatives, there are possible economic advantages in using deck prestressing because of the use of "high efficiency" materials. Prestressing tendons carry substantially more force per unit area of material than conventional mild reinforcing steel. The utilization of prestressing with smaller, more efficient steel elements would tend to reduce congestion and make concrete placement easier. Moreover, it is believed that the benefits of possible increased durability of bridge decks would more than offset the higher cost of prestressing steel, higher strength concrete and extra labor operations associated with prestressing.

1.3 Design Needs for Transverse Prestressing

Anton Tedesko [6] in 1976 was the first person to clearly expound both the durability and economic benefits of transverse prestressing. And although Tedesko suggested the advantages of transverse prestressing have a reasonable theoretical basis, there are

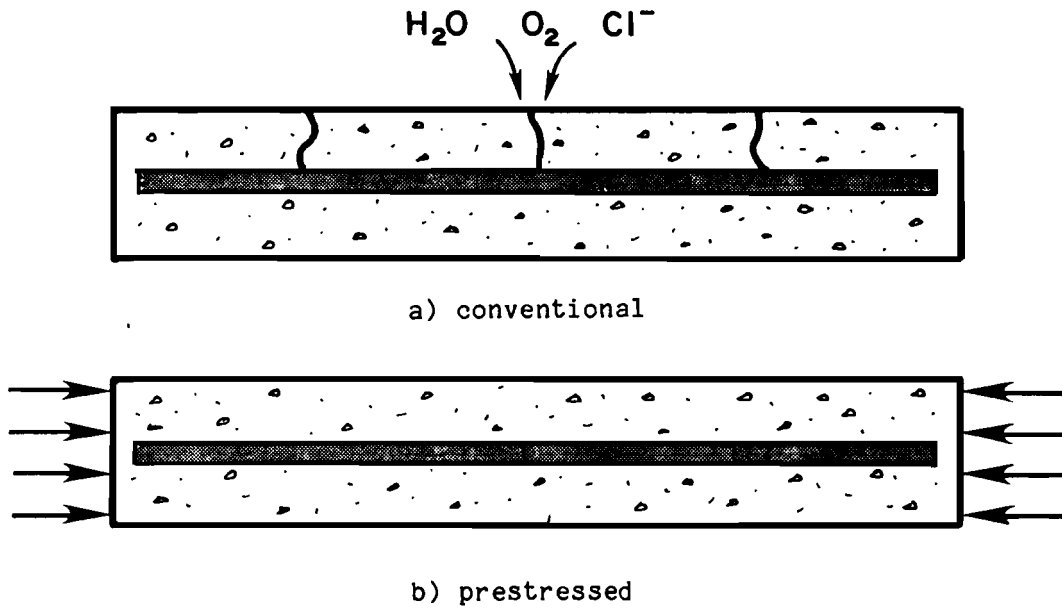


Fig. 1.2 Corrosion protection mechanism of prestressing

few documented studies and observations of the actual behavior of such a bridge system [6,7,8,9]. When one examines the present AASHTO Design Specifications [10] for prestressed concrete, it is clear that the provisions have been basically developed for longitudinal prestressing. While the provisions may be utilized for transverse prestressing, they do not account for many important variables. For instance, no guidance is given on the distribution of prestressing across the slab. Other questions include how much does the lateral stiffness of the longitudinal girders and transverse diaphragms influence the actual distribution of the transverse prestress? If nominal uniform compressive stresses are applied along the edge of the bridge slab, how much is still actually effective at the region over the middle girder? If transverse prestressing is from one edge only, what level of transverse prestressing exists at the far end of the bridge?

Additional questions exist which are fundamentally related to the combination of structural effects and durability requirements. Are the allowable tensile stresses for precompressed tension zones recommended in the AASHTO Specifications [10] valid for the design of transverse prestressing? These limits were basically set to address flexural cracking problems in longitudinal girders and do not consider the possible damaging penetration of salt or other contaminant solutions in thin cover zones over top deck reinforcement. Also, is there a threshold value of precompression that is desirable in order to achieve increased durability?

1.4 Objectives of this Research

The principal objective of this research was to examine the concept of improving the durability of bridge decks with deck prestressing. This principal objective can be further categorized into:

1. Evaluation of the effect of major variables on corrosion protection
2. Evaluation of the structural effects of transverse prestressing
3. Recommendation of design criteria for the economic application of deck prestressing considering the interrelationship between the structural and durability aspects

To help fulfill these objectives, the overall research program was divided into three areas, as shown in Fig. 1.3. The first

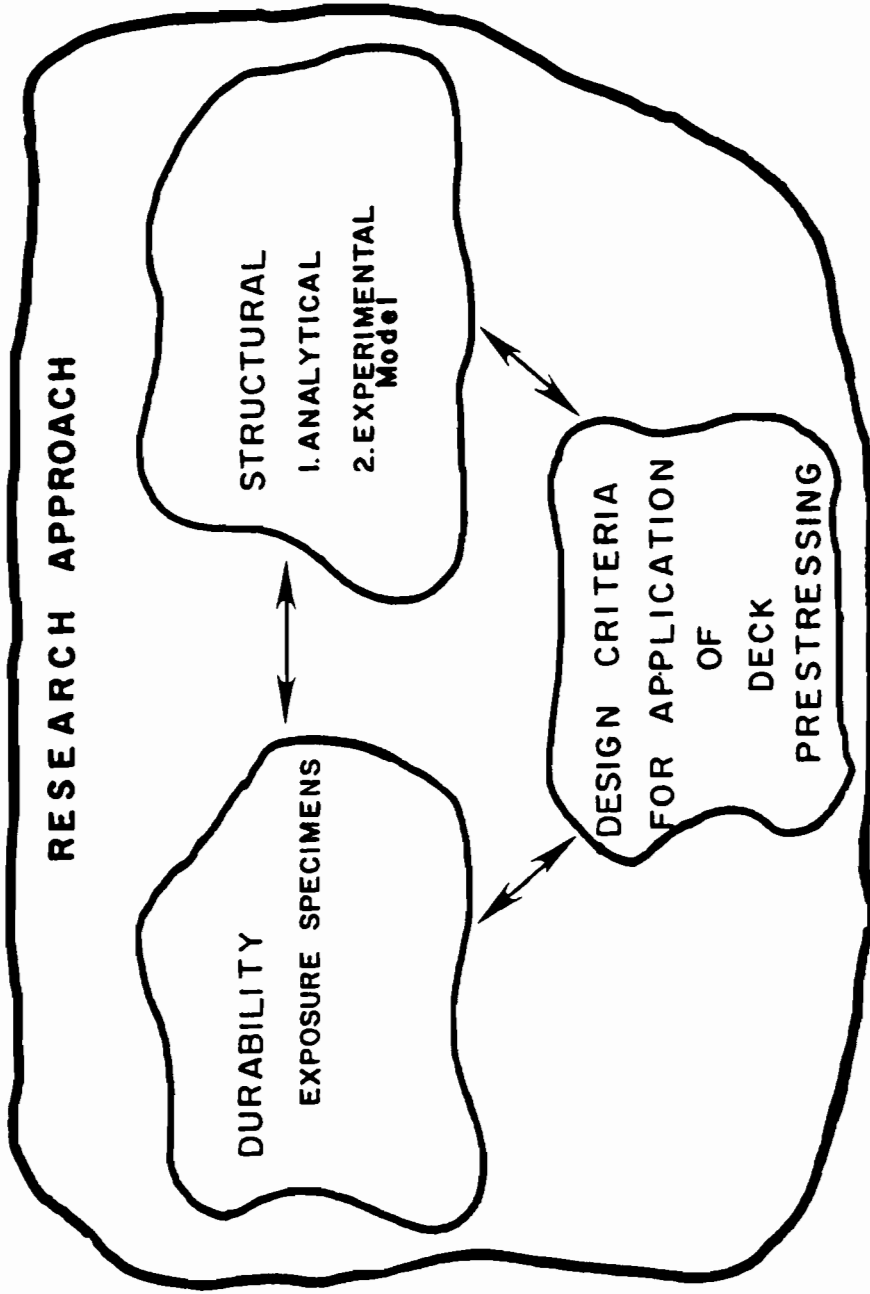


Fig. 1.3 Various components of overall research study on deck prestressing

area was the structural phase, in which both analytical and experimental studies were conducted. The second area was the durability phase, in which the main emphasis was the experimental investigation of prestressed concrete exposure specimens. The final area was the formulation of design recommendations for deck prestressing incorporating the results from both the structural and the durability studies.

The scope of the research primarily covers prestressing of composite cast-in-place bridge decks over multiple girders of the general configuration shown in Fig. 1.4. However, many of the conclusions and recommendations relating to the durability aspects are equally applicable to decks of other bridge types.

1.5 Report Contents

This report primarily covers the durability phase of the research study shown in Fig. 1.3. A very brief review of the corrosion mechanism of steel reinforcement in concrete is presented in Chapter 2. Details of the fabrication, instrumentation, and testing of 24 prestressed concrete exposure specimens is presented in Chapter 3. Test results are summarized in Chapter 4. Chapter 5 presents the evaluation of the durability test results. The major conclusions from the durability phase of the research study are summarized in Chapter 6.

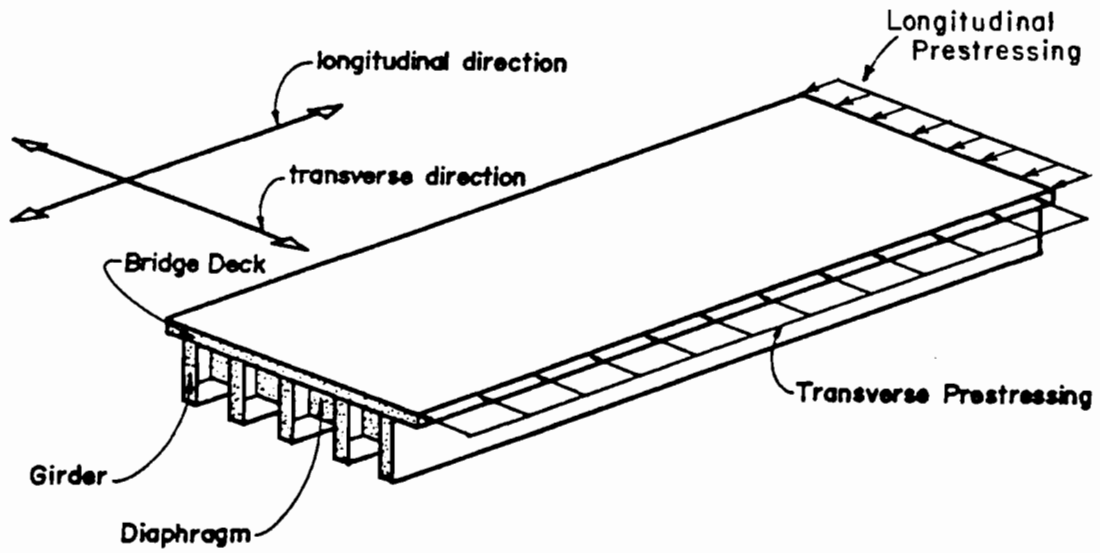


Fig. 1.4 Deck prestressing of a conventional slab-girder bridge

C H A P T E R 2

CORROSION OF STEEL IN CONCRETE

2.1 Introduction

Corrosion is defined as the deterioration of a substance, usually a metal, because of a reaction with its environment [11]. In the case of the corrosion of steel in concrete, the metal is low-carbon steel reinforcement and the environment is the concrete. Normally, concrete provides a high degree of protection against corrosion. Concrete with its inherently high alkalinity protects and passivates the steel reinforcement from corrosion. Because of the inherent protection quality of concrete, corrosion of steel does not occur in a majority of reinforced and prestressed concrete structures. However, outside environmental factors such as the use of deicing salts on bridge decks or exposure to marine environments can destroy this corrosion protection.

There are eight basic forms by which corrosion can occur [12]. The main form of the corrosion of steel in concrete is electrochemical or galvanic corrosion and is believed to be the cause of essentially all corrosion distress that occurs [13]. The corrosion of steel in concrete due to stress corrosion, hydrogen embrittlement, or electrolysis due to stray electrical currents is rare, even though some cases and studies can be found [14,15,16].

In this chapter, the nature and mechanics of galvanic corrosion of steel in concrete are detailed, followed by an examination of the effects of corrosion. The various methods which were used for evaluating corrosion distress in the durability specimens are also discussed.

2.2 Nature and Mechanics of Galvanic Corrosion of Steel in Concrete

The most common form of corrosion attack of steel embedded in concrete is galvanic or two-metal corrosion. In this process, the driving forces are electromechanical in nature.

A galvanic cell is formed when two dissimilar electrodes, separated by an electrolyte, are electrically connected by a conductor. Figure 2.1 illustrates a galvanic cell consisting of iron and copper in oxygenated water. Because of their relative positions in the electromotive force series as seen in Table 2.1, iron serves as

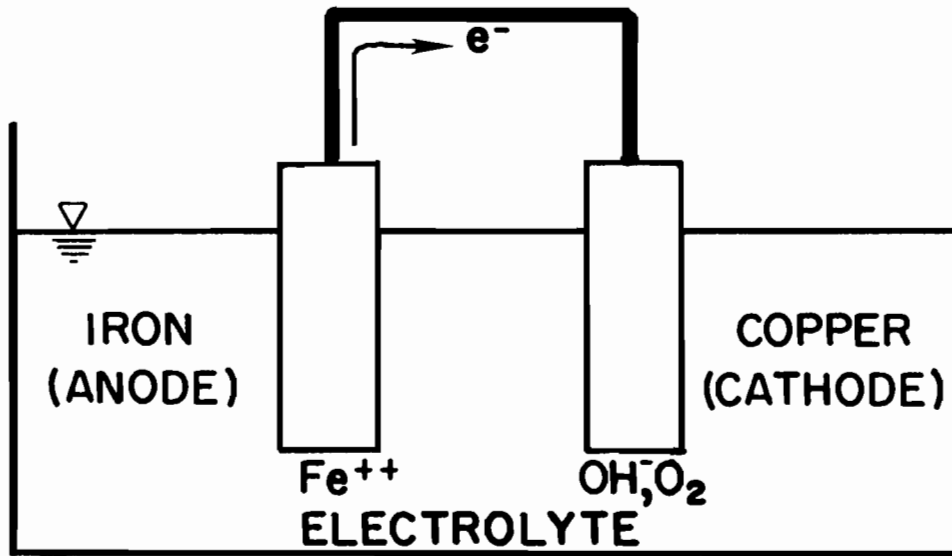




Fig. 2.1 Basic galvanic cell

TABLE 2.1 Standard EMF Series of Metals (from Ref. 12)

Metal-Metal Ion Equilibrium (Unit Activity)	Electrode Potential vs. Normal Hydrogen Electrode at 25°C (volts)
 Noble or cathodic	Au-Au ⁺³ +1.498
	Pt-Pt ⁺² +1.2
	Pd-Pd ⁺² +0.987
	Ag-Ag ⁺ +0.799
	Hg-Hg ₂ ⁺² +0.788
	Cu-Cu ⁺² +0.337
H ₂ -H ⁺ 0.000	
Active or anodic 	Pb-Pb ⁺² -0.126
	Sn-Sn ⁺² -0.136
	Ni-Ni ⁺² -0.250
	Co-Co ⁺² -0.277
	Cd-Cd ⁺² -0.403
	Fe-Fe ⁺² -0.440
Cr-Cr ⁺³ -0.744	
Zn-Zn ⁺² -0.763	
Al-Al ⁺³ -1.662	
Mg-Mg ⁺² -2.363	
Na-Na ⁺ -2.714	
K-K ⁺ -2.925	

the anode and copper as the cathode. The result is electrochemical corrosion of iron resulting in an iron plating of the copper.

A galvanic cell also exists when two similar metals are separated by dissimilar electrolytes. This is the more appropriate analogy for corrosion of steel in concrete. Instead of two different metals in concrete, different locations of the reinforcing steel become anodic and cathodic to each other.

For an electrochemical mechanism to occur, three conditions must exist: 1) there must be a potential difference between two metallic areas (the reason for the name "two-metal" corrosion); 2) there must be a conductive path; and 3) there must be appropriate electrode reactions taking place. A difference in potential may arise from almost any heterogeneity in the system. Differences in materials or nonuniformities of the physical or chemical environment surrounding the steel in concrete, or both, produce a difference in potential. Thus, in a medium of perfect uniformity, corrosion would not occur. However, reinforced or prestressed concrete are by no means homogeneous materials and corrosion cells are set up when certain conditions exist. There are numerous reasons for the corrosion enhancing nonuniformities in concrete. Concrete may be honeycombed, porous, or unevenly wet and dry. Cracking causes differences in steel stress, differential aeration, and allows easy entrance of applied salts. Also, there are always nonuniformities in the steel itself due to residual stresses from the manufacturing process. As a result, regions of lower potential become anodic and regions of higher potential become cathodic. Moist concrete acts as an electrolyte, the action of which is further accelerated if chloride ions from salts are present.

2.2.1 Typical Chemical Reactions. The tendency of a metal to oxidize to a metal ion in an aqueous solution of normal ionic activity is given by its position in the electromotive force (EMF) series (see Table 2.1). The hydrogen electrode is normally selected as an arbitrary reference and thus has an electrode potential of 0.000 volts. Any metal which is more negative or lower in Table 2.1 will have a greater tendency to corrode. Consequently, iron, which has an electrode potential of -0.440 volts relative to the hydrogen electrode, has a substantial tendency to enter into solution. The area where the iron ions go into solution becomes the anode. The ionization of the iron at the anode is referred to as oxidation and is given by the following anodic reaction:



In this primary stage of corrosion the iron is said to have lost its valence and thus produces electrons. Any reaction which produces electrons is an oxidation reaction.

The anodic region of the reinforcing steel now has an excess of electrons. To maintain an equilibrium of charge, an equivalent quantity of hydrogen is plated at adjacent surfaces of the steel. This results in a thin invisible film of hydrogen around the cathode, and this protective film inhibits further progress of the reaction, as shown in Fig. 2.2b. Any subsequent reaction ceases unless the hydrogen film is removed. If the hydrogen film remains intact, reinforcing steel in concrete is in a very protective environment and enters a passive state, as shown in Fig. 2.2a. This process of impeding the corrosion process is known as activation polarization since the film forms at the steel and concrete interface.

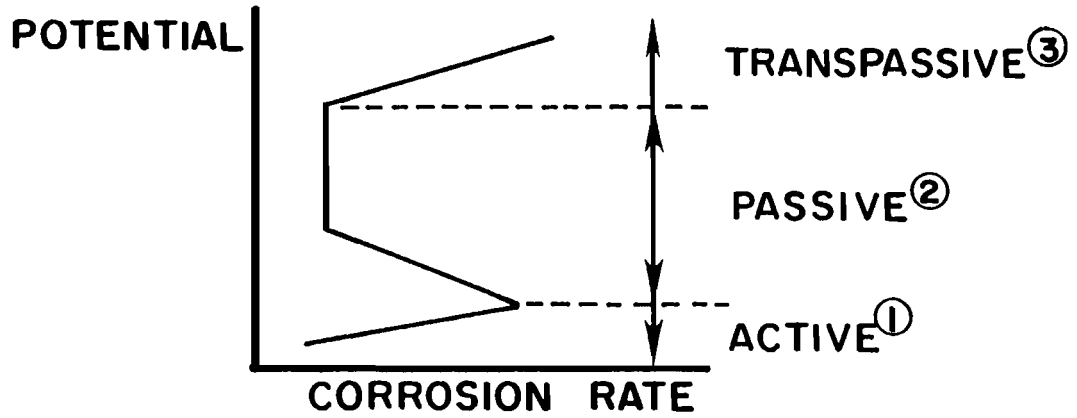
The destruction of the hydrogen film may take place in one of two ways: 1) oxygen reduction or depolarization at the cathode; or 2) hydrogen evolution as a gas. These cathodic reactions, also known as secondary reactions, are the reactions responsible for controlling the corrosion rate of structural steel and are as follows:



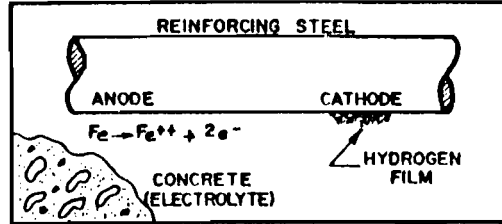
Corrosion controlled by the cathodic depolarization of oxygen in reaction (2.2) is more prevalent and the more important of the two reactions [17]. This reaction is shown in Fig. 2.2c. Reaction (2.3) is not normally characteristic of the corrosion of steel in concrete; however, it will take place in the presence of acid solutions. As a result of the destruction of the hydrogen film, corrosion enters the final stage known as the transpassive region as shown in Fig. 2.2a.

Reaction (2.2) is dependent on the concentration of dissolved oxygen next to the steel. Therefore, the reaction depends on the amount of oxygen entering the concrete, and as will be shown later, also depends on chloride ions from salts as well as many other factors. At this point, it is important to note that anything which limits and minimizes these factors will retard corrosion, keeping the steel in a passive state. This concept is fundamental to the corrosion protection offered by transverse prestressing on bridge decks.

If the cathodic reactions occur, the anodic reactions continue, resulting in an accumulation of ferrous ions, Fe^{++} , which in the presence of water and oxygen are oxidized and precipitated as rust. Two states of oxidation occur. In the first state, ferrous

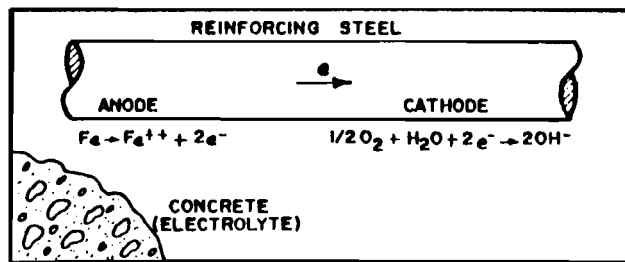


a) various phases of steel corrosion



① & ②

b) formation of protective film

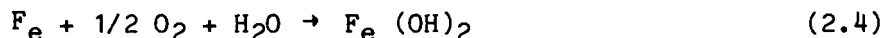


③

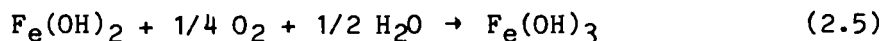
c) oxidation and reduction

Fig. 2.2 Corrosion of steel in concrete

hydroxide forms directly on the reinforcing steel surface. Equation (2.4) gives the reaction and Fig. 2.3 shows the formation of ferrous hydroxide.



Ferrous hydroxide is converted to the more soluble hydrated ferric hydroxide at a short distance from the steel surface where it is in contact with more oxygen. Equation (2.5) shows this reaction and Fig. 2.3 shows the formation of the ferric hydroxide.



The ferric hydroxide is the familiar rust normally associated with the corrosion of iron and steel. Reaction (2.5) occurs because the free energy of ferric hydroxide is less than that of ferrous hydroxide.

The structure and composition of the rust varies considerably and plays an important role in subsequent corrosion [17]. Hard, dry rust which adheres to the reinforcement surface may retard corrosion by forming a protective coating. This "rehealing" does not usually occur if an ample supply of oxygen and water are present. However, in general, the rust is spongy and fragile and thus easily detachable from the reinforcement surface [17]. In this case, no rehealing takes place and corrosion continues to occur.

2.2.2 Rate of Corrosion. In galvanic corrosion, the slower of the electrochemical reactions controls the rate of corrosion. In the case of steel corrosion in concrete, the primary oxidation reaction is much faster than the secondary reduction reactions. This implies that the environmental factors of oxygen concentration--water, salt and others--are the dominant influences on the corrosion processes. However, there are other factors which also are important. If the cathode is large and consequently exposed to a greater amount of oxygen, then the corrosion cell current is stronger relative to the size of the anode [12,17]. This intensifies the attack and results in a faster overall corrosion rate at the anode.

2.2.3 Influence of Cracking. The role of cracking in concrete on corrosion is quite controversial, but it can be divided into basically two schools of thought [18,19,20]. One point of view suggests that cracks provide access for chloride ions, water, and oxygen to the reinforcement. Thus, cracks accelerate the onset of corrosion. The other viewpoint suggests that while the onset of corrosion is accelerated by cracking, such corrosion is localized, and that eventually chloride ions penetrate even uncracked concrete and initiate even more widespread corrosion. According to this latter viewpoint, the result is that after a period of time, there is little

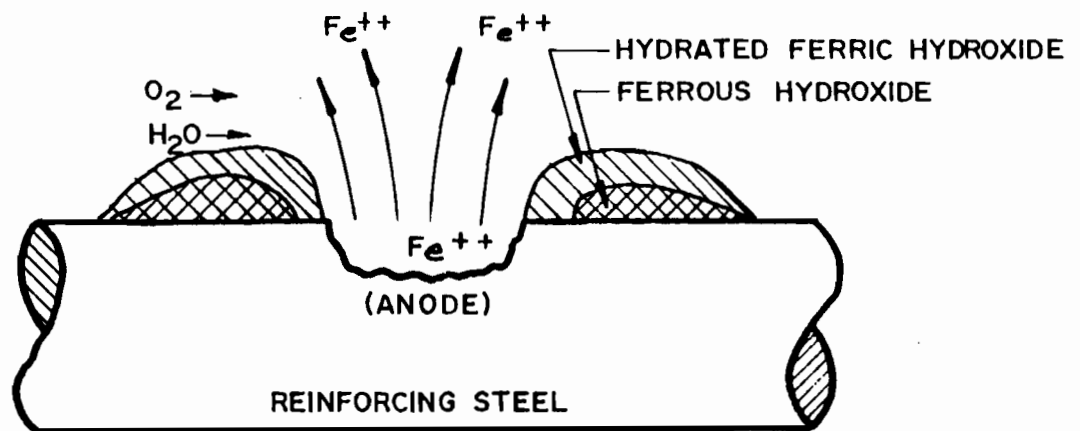


Fig. 2.3 Steel corrosion products

difference between the amount of corrosion in cracked and uncracked concrete.

In part, the different points of view can be explained by the origin, width, intensity and orientation of cracks. For cracks which are perpendicular to the reinforcement, the corroded length is not likely to exceed three bar diameters [18]. In contrast, cracks which follow the line of reinforcement are probably more damaging since the corroded length is greater, and, consequently, the concrete's resistance to spalling and delamination is reduced.

The subject of the influence of concrete cracking on corrosion is especially controversial when the results from various research studies are examined. Several studies [21,22,23,24,25] have shown that surface crack widths as small as 0.004 in. have led to significant corrosion of reinforcement. An extensive study conducted by the Concrete Technology Division of the U. S. Army Engineer Waterways Experiment Station at Treat Island in Maine revealed that concrete specimens with 0.01 in. surface crack widths lead to deterioration [26]. On the other hand, several studies have indicated the contrary; wider cracks have resulted in less corrosion than narrow cracks, and cracks up to 0.012 in. have little influence on corrosion of steel in concrete [24]. Furthermore, Beeby [19] presents data as shown in Fig. 2.4 which appear to indicate that crack width has little influence on corrosion of reinforcement in marine environments, and thus implies that current design recommendations are requiring unnecessary calculations for surface crack width as a measure of corrosion protection. In addition, several research studies have cited data which seems to indicate that limiting surface crack width to certain values is inappropriate since there is not a simple relationship between surface crack width and crack width at the level of the reinforcement [19,24,27].

However, most design codes recognize in some way that cracks can lead to corrosion. The uncertainty of the relationship between the level of cracking and corrosion is clearly evident when examining the maximum crack width recommended by various design codes. The recommended values range is between 0.003 in. and 0.015 in. [19], with current practice for North Sea structures approaching almost a "crack-free" design concept [28]. The current ACI Building Code [29] implicitly recommends a maximum crack width of 0.012 in. for exterior exposure. The value is based on years of field experience for normal exterior conditions. This recommendation for maximum crack width clearly did not envision aggressive chloride-containing environments as evidenced by a provision in the ACI Building Code that for structures subject to aggressive exposures that special investigation and precaution are required. The recommendations for maximum crack

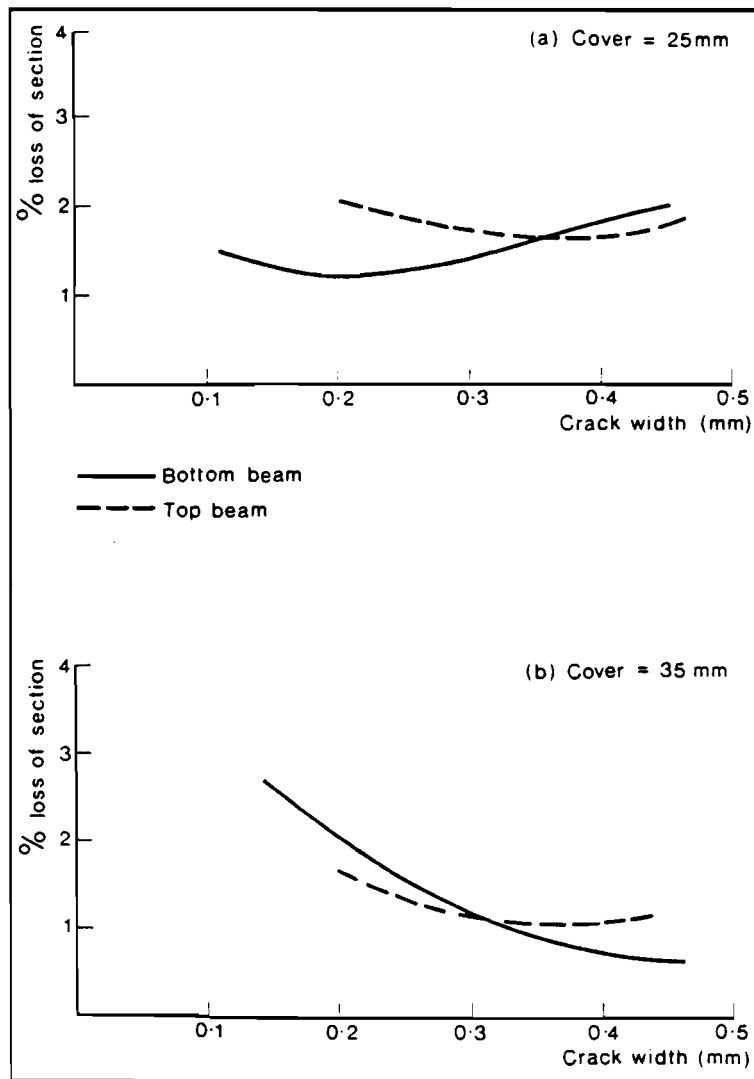


Fig. 2.4 Influence of crack width on corrosion of concrete in marine environment after 10 years exposure (from Ref. 19)

width in the current AASHTO Specifications [10] are slightly more restrictive than those in the ACI Building Code, limiting the crack width to about 0.011 in. However, AASHTO also has a special provision stating that concrete exposed to chlorides such as from deicers may require additional protection in the form of a waterproof membrane or other measures.

Thus, it is clear that at present there is no consensus on the role of cracking on corrosion and the acceptable crack width which will reduce corrosion. The durability tests which were a part of this research provided some additional data to help address this cracking/corrosion dilemma. However, it is important to note that the lack of conclusive evidence suggesting that there is a simple relationship between crack width and corrosion has resulted in several researchers suggesting that the only foolproof method for ensuring corrosion protection is to strive for a "crack free" design which would ensure that a structure would remain free of cracks throughout its entire service life [30,31]. This, of course, is the potential advantage of deck prestressing. It is implicit that such a "crack free" design can only ensure corrosion protection if adequate thickness of concrete cover, adequate concrete quality and adequate compaction exist so that "uncracked" concrete provides the necessary barrier to inhibit the corrosion mechanism.

2.3 Corrosion Induced Distress

Most concrete structures are largely unaffected by corrosion. Generally, the high alkalinity of concrete protects steel reinforcement from corrosion. However, if the external and internal conditions are such that a corrosive environment exists, a destructive action takes place at an ever increasing rate and creates serious problems. The use of deicing salts on bridge decks or salt water spray in coastal environments characterize perfect scenarios for internal and external factors conducive to corrosion.

The effects of corrosion are progressive. That is, the final stages of severe corrosion distress occur only after early corrosion signs which forecast the final stages. As corrosion progresses, the effects become more and more pernicious.

The following sections discuss the various stages of corrosion distress, which include staining, concrete cracking, and steel fracture.

2.3.1 Staining. Early symptoms of corrosion distress in concrete are surface discolorations. In general, the discoloration is a reddish-brown stain which is the familiar "rust" color associated

with rusting of the steel reinforcement. The rust products travel through cracks or any passageway in the concrete to the surface. The corrosion products which form, ferrous hydroxide and hydrated ferric hydroxide, produce the reddish-brown color (see Fig. 2.3).

In some cases, a whitish substance exudes at the concrete surface, suggesting a leaching or efflorescence. The corrosion process itself does not produce efflorescence. However, the presence of efflorescence is a sign of microcracks and microfissures in the concrete which allow corrosion producing substances to penetrate to the steel reinforcement. Efflorescence occurs on the concrete surface when water percolates through the concrete. Efflorescence consists of deposited salts that leach out of the concrete, which crystallize upon subsequent evaporation of water or interaction with carbon dioxide in the atmosphere. Typical salts include sulfates and carbonates of sodium, potassium, or calcium, the major constituent being calcium carbonate [32]. Also, for the case of bridge decks, the salts deposited are compounds of any applied deicing salts which are leached out to the surface. If there are signs of efflorescence in a bridge deck, rusting and further corrosion distress are likely in the future.

2.3.2 Concrete Cracking, Spalling, Delamination and Decomposition. Cracking, spalling, delamination and decomposition of concrete signal more advanced stages of corrosion distress. It is possible for each of these effects to be present individually, simultaneously or to develop in succession. They may appear at different locations and in varying and different degrees of development.

Severe corrosion of reinforcement usually results in cracking of the concrete in a direction parallel to the reinforcement. Initially, small cracks and fissures in the concrete as well as low concrete permeability allow the penetration of corrosive elements as shown in Fig. 2.5a. Mehta and Gerwick [33] propose a corrosion-cracking interaction model which suggests the need for small cracks in concrete to initiate corrosion. As the reinforcement corrodes in Fig. 2.5b, iron oxides form around the periphery of the steel bar or strand. The corrosion products occupy volumes anywhere from 2 to 15 times that of the base metals from which they come, as seen in Fig. 2.5c. Wide cracking, as shown in Fig. 2.5d, results from the internal pressures created by the oxide rust products occupying a greater volume. When the internal stresses exceed the concrete tensile capacity, concrete cracks.

Spalling is a physical disruption or splitting of the concrete. Usually, the coarse aggregate fractures and the uncracked concrete appears to be sound. Spalling is particularly detrimental to

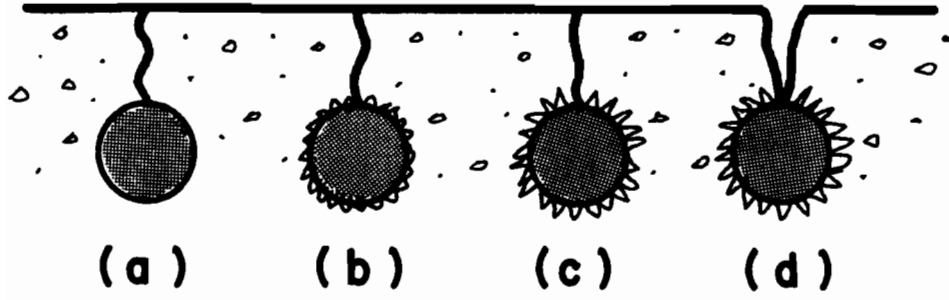


Fig. 2.5 Concrete deterioration mechanism

bridge decks because it affects riding quality and the structural integrity of the deck.

If the cracking and spalling are severe enough, layers of concrete split and separate. This is known as delamination and represents final stages of corrosion distress.

Decomposition exists when the cement loses its binding capacity, and after a period of deterioration the sand and cement begin to disappear, leaving exposed aggregate. As this process continues, it can result in a complete loss of cross section. However, there is little or no apparent fracturing of the coarse aggregates. A whitish calcium residue often appears, especially in aggregate pockets or depressions.

2.3.3 Steel Pitting and Fracture. The final stages of corrosion distress result in steel pitting and fracture. Intense corrosion activity produces localized deep pitting, and thus a severe loss of steel reinforcement cross section. The loss of reinforcement cross section reduces the tensile load carrying capacity of the reinforcement. This effect is particularly critical, if not catastrophic, for prestressing tendons in which small steel areas carry large tension forces. The actual fracture of the reinforcement can be accelerated by fatigue loading as would be the case for bridges carrying moving vehicular loads.

The final stages of corrosion distress which produce steel fracturing would be particularly pernicious in the case of unbonded prestressing tendons. The loss of an unbonded tendon does not allow for a smooth redistribution of load to other tension components compared to grouted tendons which ensure bond. Recent experimental evidence indicates that in bonded strands, individual wires can redevelop full strength in 2 to 3 feet [34]. The energy-absorption capability of a grouted tendon exceeds that of an unbonded tendon. For this reason, structural systems which are particularly susceptible to progressive collapse favor the use of bonded tendons.

2.4 Detection and Evaluation of Corrosion Distress

There are many methods which have been used for detecting and evaluating the effects of steel corrosion in concrete. These methods include visual inspection, chaining or sounding for delamination, chloride content determination, pH level determination, potential measurements, polarization techniques, petrographic examination, and x-ray spectography. However, many of these methods require concrete cores to be brought into the laboratory for testing. In addition, the

laboratory methods require significant technical expertise to perform them. Also, the evaluation of the results from many of the tests rely on subjective or statistical interpretations from previously reported tests.

Erlin and Verbeck [13], in a recent state-of-the-art review, suggest one of the real research needs for structures in service is the development of improved nondestructive methods for detecting corrosion that is in progress. They further emphasize the need for determining the degree of actual corrosion damage in structures. Spellman and Stratfull [35] further suggest that for every researcher studying corrosion of steel in concrete, there is a different test and evaluation method or variation thereof. In most instances, the different investigators using their own methods do not obtain clearly reproducible results. The corrosion of steel in concrete is a function of many variables, and is a highly complex phenomenon; therefore, reliable methods of corrosion detection and evaluation have developed slowly.

The following sections discuss some of the more common methods used in the field for corrosion detection and evaluation. These include visual inspection, half cell potential measurements, chloride level determination, and post-mortem examination.

2.4.1 Visual Inspection. The easiest and most straightforward method for detecting steel corrosion in reinforced and prestressed concrete structures is the visual inspection for rust staining and cracking. Rust stains that follow the line of reinforcement clearly indicate steel corrosion. When corrosion progresses further, cracking of the concrete cover occurs.

For a structure in which cracking exposes the reinforcement, a visual examination of the amount of steel pitting reveals a quantitative measurement of the reduction in tensile-carrying capacity. In addition, visual inspection results in a qualitative assessment of structural integrity. In the case of a bridge deck, the signs of heavy rust and a marked reduction in cross-sectional reinforcement area could imply an immediate need for reducing the load-carrying capacity of the bridge or implementation of strengthening procedures.

Corrosion progressing to an extent that surface stains and cracking occur suggests substantial damage. Thus, visual inspection is not an early corrosion detection method, but in reality a post-mortem procedure. By visual inspection, no corrosion of embedded steel can be observed before it is in an advanced stage. In addition, there are numerous cases cited in the literature [28] in which severe corrosion occurs without development of severe cracking and spalling.

Thus, for the case of prestressing tendons in which only a small amount of localized corrosion could cause fracture, visual inspection would not be a reliable detection method. Also, visual inspection by

itself does not provide definitive indication of the extent of corrosion distress.

2.4.2 Chloride Determination. Determining chloride content in concrete is not a detection method per se, but establishes the likelihood as to whether or not corrosion is occurring. In addition, it does not provide an indication of the extent of corrosion distress. The significance of a chloride analysis lies within the spectrum of simply determining that the concentration is sufficient to cause steel to change from a passive to an active corrosion state. Beyond the threshold value of chloride concentration necessary to cause corrosion, the rate of corrosion is a function of many variables, but in particular of moisture content. Therefore, even though a bridge slab may have more chlorides than the threshold value, it may not be in an active state when considering ambient and environmental factors which are necessary for corrosion. Likewise, if a bridge deck is in an active corrosion state, additional amounts of chlorides may have little effect on the corrosion.

Most researchers agree that the minimum chloride threshold concentration to induce corrosion ranges between 1.0 and 1.5 lbs/cu.yd. Stratfull et al. [36] elaborate that there is a good correlation between the maximum chloride content from a concrete sample to that calculated by a statistical distribution, using the maximum quantity at the 95% confidence limits of the data. Thus, determining the chloride content in a concrete sample and comparing that value to a threshold value is a good indication of whether or not the reinforcement is in an active or passive state of corrosion. If the chloride concentration exceeds the threshold value and other ambient conditions are conducive to corrosion, then the conclusion is that the reinforcement is in an active corrosion state. Chloride contents at the level of the reinforcement should be used when comparing to the threshold value.

2.4.3 Half Cell Potential. For an electrochemical mechanism such as galvanic corrosion to occur, there must be a potential difference. Potential methods such as the half cell potential method rely on this known condition for corrosion detection. In particular, the half cell potential method measures voltage gradients or drops by use of a high-impedance voltmeter and a constant voltage reference cell. The reference cell possesses a constant internal voltage, which allows voltage changes existing on the reinforcement to be measured. This method provides both an effective means for determining if corrosion is occurring and the extent of corrosion distress. However,

if corrosion has occurred and then was arrested by some means, the method proves ineffective in detecting this.

The half cell potential method can be used to indicate corrosion activity associated with steel embedded in field or laboratory concrete members. This method is applicable for members regardless of their size or the depth of cover over the reinforcing steel. It can be used in structures which show no visible signs of distress to determine when corrosion initiates, or in a structure which shows severe corrosion distress to determine the extent of corrosion.

Stratfull was the first person to describe the use of half cell potential measurements for corrosion detection [36,37,38]. His continuing work with the method resulted in ASTM C-876 [39], Standard Test Method for Half Cell Potentials of Reinforcing Steel in Concrete. Criteria for judging whether meaningful corrosion is occurring are discussed in Section 5.3.2.

2.4.4 Post-Mortem Examination. By definition, this procedure is not a corrosion detection method but a method of evaluating structures after suffering severe corrosion distress (i.e., post-mortem). The various tests in a structural post-mortem examination might include visual inspection for rust, measurement of reinforcement area reduction, chloride analysis, and petrographic examination. By performing a post-mortem examination of a structure suffering severe corrosion distress, the overriding reasons for the cause of corrosion might be identified. This information is helpful in preventing similar distress in future structures.

CHAPTER 3

DURABILITY TEST PROGRAM

3.1 Introduction

The principal objective of the durability test program was to gather information and data on the behavior and performance of prestressed deck slabs subjected to an aggressive corrosion-producing environment. The information from this study would then be used in the development and identification of the proper materials, design criteria, and construction practices which would effectively provide prestressing to bridge decks.

To study the effects of prestressing on durability performance, 24 full-thickness deck slab models were subjected to the accelerated corrosion testing of an aggressive deicing salt exposure. Some of the specimens utilized prestressing while others did not. In this way, the relative contribution of prestressing to the improvement of corrosion protection could be identified. All specimens contained conventionally reinforcement as well. Other test variables included the level of cracking, concrete cover, type of reinforcement, and type of prestressing system. A brief description of the variables is provided in the next section.

3.2 Test Variables

An extensive review of current literature and discussions with industry contacts, highway officials, and other researchers helped to identify the most relevant variables for study in the corrosion durability tests. Table 3.1 summarizes the test variables for the durability study.

3.2.1 Effect of Prestressing. The principal variable in the durability test was the effect of prestressing on corrosion protection. To qualitatively and quantitatively assess the effectiveness of prestressing as a means of improving corrosion protection, some specimens were prestressed, while others were nonprestressed. This allowed a direct comparison between the performance of a prestressed bridge deck and that of a conventionally reinforced bridge deck.

The mechanism by which it is believed that prestressing improves corrosion protection is that it eliminates or limits concrete cracking, and thus reduces the network by which aggressive

TABLE 3.1 Summary of Durability Study Test Variables

Test Variable	Comparison
Effect of prestressing	Nonprestressed (0 psi)
	Prestressed (160 psi)
Level of cracking	~ 0.002 in. surface crack width
	~ 0.015 in. surface crack width
Concrete cover	2 in.
	3 in.
Type of nonprestressed reinforcement	Uncoated (as manufactured)
	Uncoated (clean)
	Epoxy-coated
Type of prestressing system	Unbonded monostrand (plastic duct)
	Grouted multistrand (rigid galvanized duct)

substances can penetrate. Besides limiting the cracking in concrete, there may be a secondary level of protection offered by prestressing which involves the magnitude of compression. It is reasonable to assume that for higher levels of compression, the internal microstructure of the concrete is more "closely-packed." The concrete would contain fewer microcracks and voids, and thus would be less susceptible to the penetration of aggressive substances. However, this secondary level of protection of prestressing at the microstructure level was not a variable for direct study in the present research. Only the effect of prestressing on cracking was studied.

3.2.2 Cracking. Since the postulated mechanism by which the durability of a prestressed bridge deck is improved involves the elimination or at least the minimization of cracks in the concrete, it was necessary to somehow include cracking as a study parameter. A conventional reinforced concrete deck more than likely cracks under service load conditions. However, with a prestressed bridge deck, the induced compression would keep cracks from forming. Even if small cracks do form in a prestressed deck, the prestressing probably closes the crack upon load removal, and thus prevents the penetration of aggressive substances.

To introduce cracking as a variable, it was decided to first "precrack" all specimens before exposure testing. Then, during exposure testing, the nonprestressed specimens were loaded to produce surface crack widths of about 0.015 in., which is a value slightly greater than the acceptable level for environmental exposure [10]. Likewise, some of the prestressed specimens were loaded to produce crack widths of this magnitude. The cracks in the other prestressed specimens were opened to about 0.002 in. This was the crack width which resulted when the same load which was used to open cracks of 0.015 in. in the nonprestressed specimens was applied to these prestressed specimens.

3.2.3 Concrete Cover. Concrete cover was a variable in the test in order to study the possible improvement in corrosion protection with increasing concrete cover. Both 2 in. and 3 in. covers over the reinforcement were selected for study.

3.2.4 Type of Nonprestressed Reinforcement. One option for improving the corrosion protection of bridge decks which has received a great deal of attention is the use of epoxy-coated reinforcement. Hence, a comparison between the performance of epoxy-coated and uncoated reinforcement was another principal variable in the durability study. In addition, some of the uncoated reinforcement was cleaned of all mill scale to determine if it might exhibit better resistance to corrosion.

3.2.5 Type of Prestressing System. Another variable which was felt to be of interest in the durability study was the type of prestressing system. There is a growing use of posttensioned unbonded monostrand systems for prestressed concrete applications. The most popular system is a high-strength, seven-wire prestressing tendon wrapped in a viscous rust-inhibiting, low-friction grease, and covered by an extruded plastic duct. Because of its popularity, this type of system was selected for use in half of the specimens.

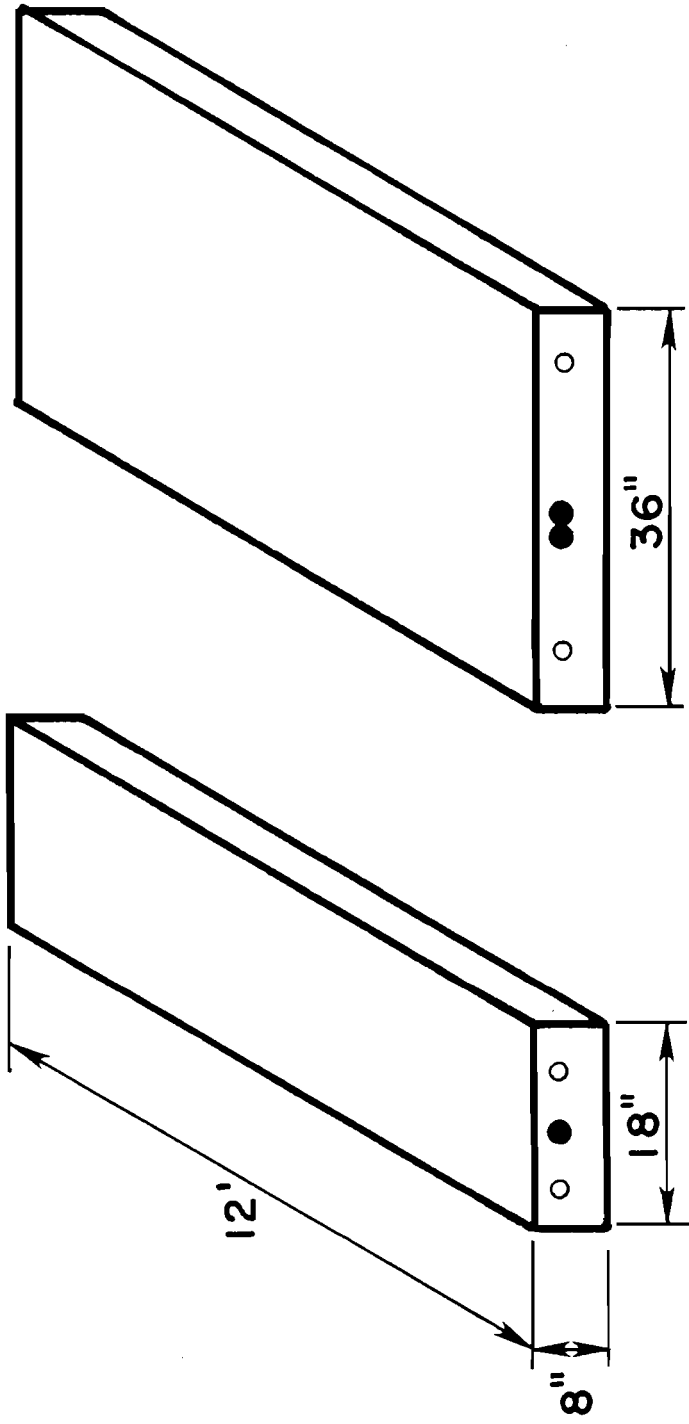
The other prestressing system identified for comparative testing was a posttensioned, grouted multistrand system. Much of the current literature regards a grouted system as the best form of protection for prestressing steel. In addition, a multistrand application has the potential for greatly reducing construction costs because of the fewer jacking operations and the fewer number of required anchorages. For the purposes of the laboratory durability tests, a two-strand system with a rigid galvanized duct was selected.

3.3 General Description

To study the relevant variables identified in the previous section required the construction and testing of 24 full-thickness durability specimens. Half of the specimens utilized the unbonded single-strand system as shown in Fig. 3.1a, whereas the other half of the specimens utilized the grouted multistrand system as shown in Fig. 3.1b. Table 3.2 summarizes the relevant characteristics of each of the durability specimens. The durability specimens will henceforth be identified by the specimen numbers given in Table 3.2.

The durability specimens were designed to simulate a small component of a bridge deck as shown in Fig. 3.2. The critical surface of a bridge deck exposed to deicing salts is the top surface. Any cracks which form in the top of the deck slab permit the ingress of deicing salts, water, and oxygen. Since it is anticipated that the primary top surface crack formation in a bridge deck will occur at the negative moment region over the girders, the durability specimens were specifically designed to simulate this region of the deck slab, as illustrated in Fig. 3.2.

The testing involved the exposure of the top surface of the durability specimens to a deicing salt water solution. The exposure consisted of alternating wet-dry periods. The alternating cycles represented an aggressive and accelerated exposure condition. During the exposure to the salt water, the specimens were loaded to open the cracks and allow the penetration of any aggressive elements.



POSTTENSIONED UNBONDED MONOSTRAND POSTTENSIONED GROUTED MULTISTRAND

- prestressing tendon
- reinforcing bar

Fig. 3.1 Durability specimens

TABLE 3.2 Durability Specimen Summary

Specimen No.	Pre-stressing System Type	Pre-stressed	Reinforcement Type	Approximate	
				Concrete Cover (in.)	Surface Crack Width under Load (0.001 in.)
1	Unbonded	No	Uncoated	2	15
2	Unbonded	No	Epoxy-coated	2	15
3	Unbonded	No	Uncoated	3	15
4	Unbonded	No	Epoxy-coated	3	15
5	Unbonded	Yes	Uncoated	2	15
6	Unbonded	Yes	Epoxy-coated	2	15
7	Unbonded	Yes	Uncoated	3	15
8	Unbonded	Yes	Epoxy-coated	3	15
9	Unbonded	Yes	Uncoated	2	2
10	Unbonded	Yes	Epoxy-coated	2	2
11	Unbonded	Yes	Uncoated	3	2
12	Unbonded	Yes	Epoxy-coated	3	2
13	Grouted	No	Uncoated	2	15
14	Grouted	No	Epoxy-coated	2	15
15	Grouted	No	Uncoated	3	15
16	Grouted	No	Epoxy-coated	3	15
17	Grouted	Yes	Uncoated	2	15
18	Grouted	Yes	Epoxy-coated	2	15
19	Grouted	Yes	Uncoated	3	15
20	Grouted	Yes	Epoxy-coated	3	15
21	Grouted	Yes	Uncoated	2	2
22	Grouted	Yes	Epoxy-coated	2	2
23	Grouted	Yes	Uncoated	3	2
24	Grouted	Yes	Epoxy-coated	3	2

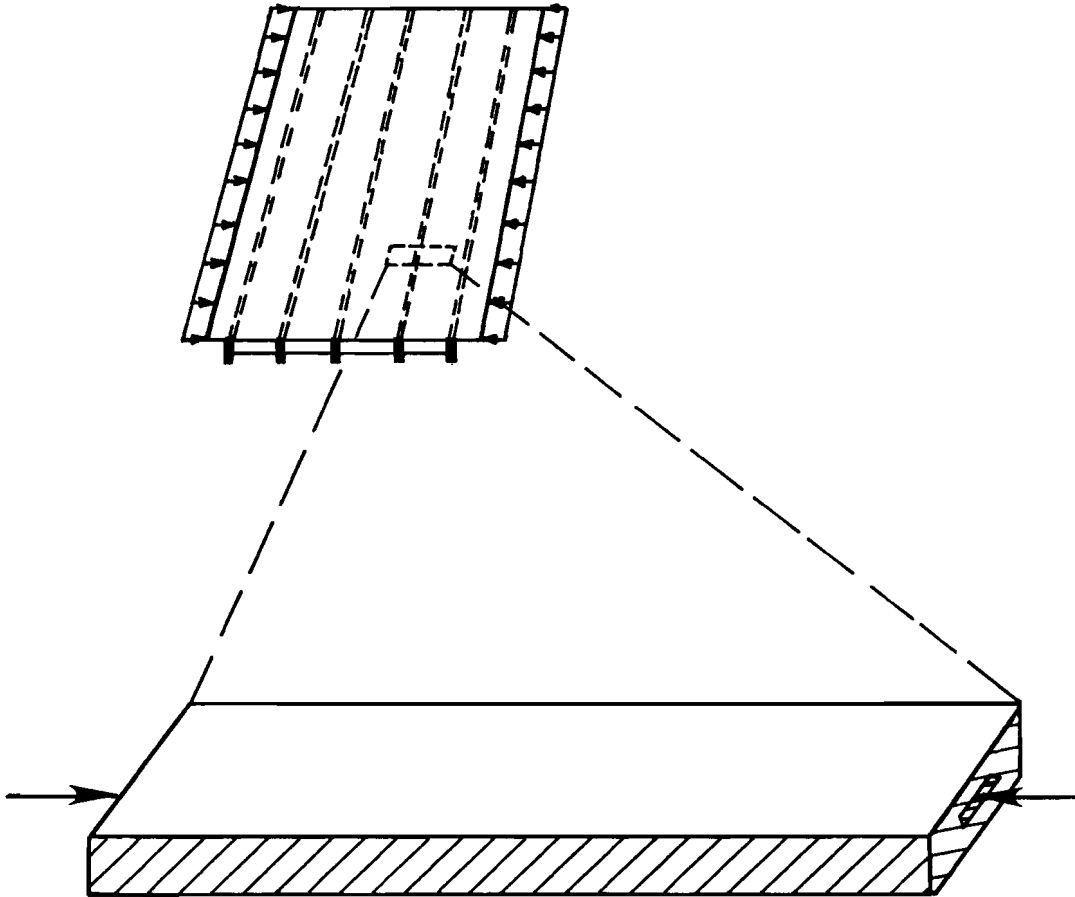


Fig. 3.2 Durability specimens representing a component of a transversely prestressed bridge deck

3.4 Specimen Design and Details

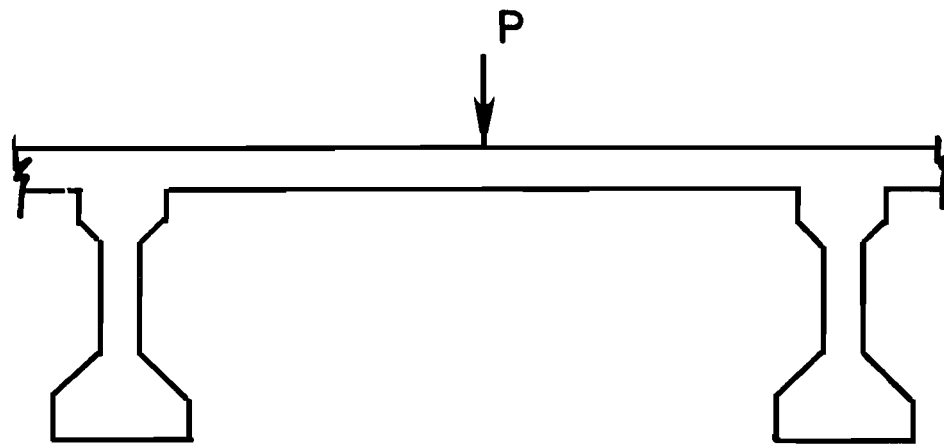
The basic requirement for the durability specimens was to approximately represent the behavior of a bridge deck exposed to deicing salts. As was shown in Fig. 3.2, each of the durability specimens represented only a small exposed portion of a transversely prestressed bridge deck. To simulate the effect of loads on a bridge deck, the loading condition for the durability specimens as shown in Fig. 3.3 was proposed. For this loading, there was a negative moment at the interior support B which approximated the behavior of the slab at the girders in a slab-girder bridge.

It was decided to build the durability specimens with full-thickness in order to represent as closely as possible existing available construction materials and to eliminate scaling effects. The slab thickness of a bridge deck varies depending primarily on the span length between girders. Additionally, it was decided to design the durability specimens with an 8 in. thickness to approximate the slab thickness in a full-scale representation of the laboratory structural bridge model.

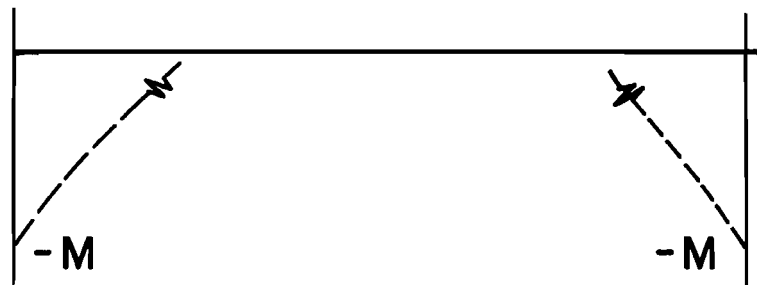
Each specimen was designed for a single representation of the prestressing system type in order to minimize the size of the specimens. Thus, the unbonded specimens contained a single unbonded plastic-coated tendon, whereas the grouted specimens contained one complete prestressing assembly consisting of two tendons in a rigid galvanized duct.

Nonprestressed reinforcement was included in the durability specimens since some conventional reinforcement would be required in a bridge deck in addition to the prestressing in order to carry dead loads before posttensioning, to control cracking from temperature and shrinkage stresses, to distribute cracks from structural loads, and to provide structural integrity. The concrete cover was the same for both prestressed and nonprestressed reinforcement as specified in Table 3.2. Two #4 bars were placed in the top of each of the unbonded specimens and four #4 bars in the top of each of the grouted specimens. Bottom reinforcement consisting of #4 bars was included primarily to prevent cracking during handling of the specimens prior to testing. No reinforcing representing the longitudinal steel in a deck slab was used in the durability specimens. This was to ensure that each nonprestressed bar and prestressing tendon was "electrically isolated" from each other, and thus would basically represent independent corrosion cells.

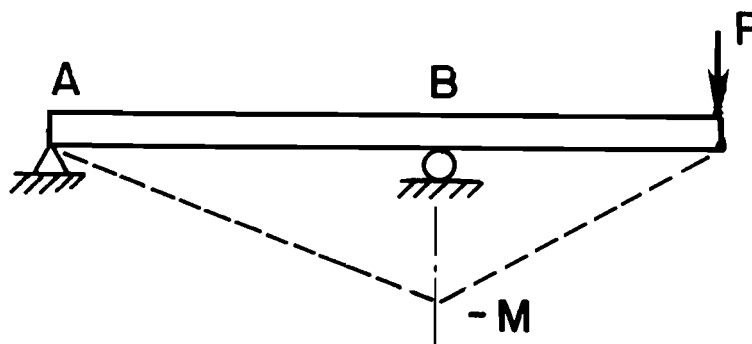
The final details of the durability specimens are shown in Fig. 3.4.



Prototype Bridge Cross Section

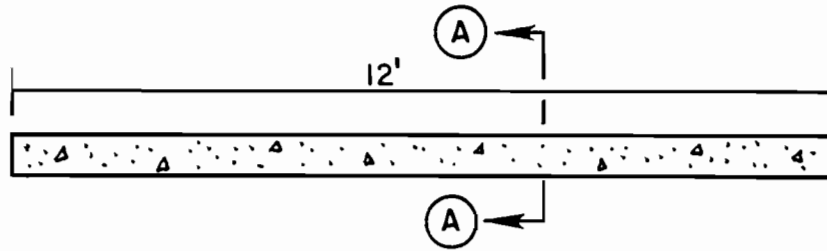


Negative Moment
in Slab at Girders

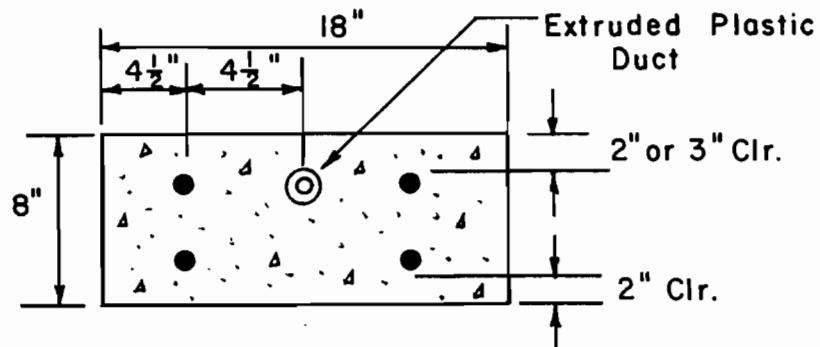


Negative Moment at B in Durability
Specimens to Simulate Negative
Moment in Bridge Slab at Girders

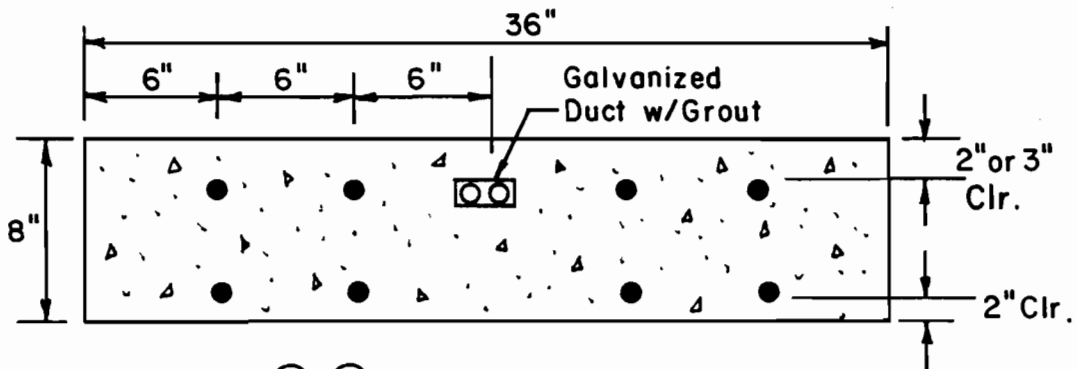
Fig. 3.3 Loading scheme for durability specimens



- #4 Uncoated or Epoxy-Coated Reinforcing Bar
- $\frac{1}{2}$ " diameter 270 K Prestressing Tendon



Section (A) (A) for Unbonded Specimens



Section (A) (A) for Grouted Specimens

Fig. 3.4 Durability specimen details

3.5 Materials

3.5.1 Concrete. A special concrete mix was used for the durability specimens since current TSDHPT Specifications [40] do not include a concrete specification for a prestressed concrete bridge deck application. The mix design called for a water-cement ratio (W/C) of 0.44 and a cement factor (CF) of 6.5 sacks/cu.yd. The desired 28-day compressive strength (f'_c) was 5000 psi with 4000 psi recommended at the time of prestressing. This represented a higher strength than normally specified for a conventionally reinforced bridge deck. The design also called for 5% air in the concrete. Other mix design parameters are shown in Table 3.3.

Six different concrete casts were required to construct all 24 durability specimens. The compressive strengths varied considerably between the six batches at all ages as shown in Fig. 3.5 even though all concrete batches had the same mix proportions. However, test cylinders from each cast were cured in the same manner and location as the specimens. The 28-day strengths, estimated from the strength-with time relationships shown in Fig. 3.5, are provided in Table 3.4. As can be seen, the estimated 28-day strength for batches 2, 5, and 6 fell below the 28-day design strength. However, at the time exposure testing began, only batches 2 and 5 fell below the specified design strength. As will be discussed in Chapter 5, corrosion occurred only at crack locations, and thus it is believed that these concrete strength variances did not significantly affect the test.

The specimens cast from each concrete batch are identified in Table 3.5.

3.5.2 Nonprestressed Reinforcement. Standard deformed GR60 #4 bars were used as the nonprestressed reinforcement in the durability specimens. The bars arrived at the laboratory with three different surface conditions. They were: 1) as manufactured; 2) cleaned of all rust and mill scale; and 3) epoxy-coated. All nonprestressed reinforcement was obtained from the same supplier. The epoxy-coated reinforcement clearly met the requirements for the acceptability of damage to coating as outlined in ASTM A775, Specification for Epoxy-Coated Reinforcing Steel Bars.

3.5.3 Prestressing Strand. The plastic-sheathed prestressing strand used in the unbonded single-strand specimens was purchased from a supplier in Texas. The prestressing tendon was a nominal 1/2 in. diameter, seven-wire strand with a minimum ultimate stress of 270 ksi. The thickness of the plastic sheathing as measured at several locations on the strand was between 0.026 and 0.042 in. The plastic duct surrounding the strand was heavily

TABLE 3.3 Concrete Mix Design for Durability Specimens

Material	Material Proportions
Cement (Type I)	611 lbs/cu.yd.
Water	32.5 gals/cu.yd.
Fine Aggregate	1265 lbs/cu.yd.
Coarse Aggregate	1720 lbs/cu.yd.
ASTM Type A Water-Reducing Admixture (Spec. 494)	26 oz/cu.yd.
Air-Entraining Admixture (SOLAIR)	3.5 oz/cu.yd.

TABLE 3.4 Estimated 28-Day Strengths

Batch Number	Estimated 28-Day Compressive Strength (psi)
1	6850
2	3750
3	5000
4	6200
5	4000
6	4900
Mean	5117

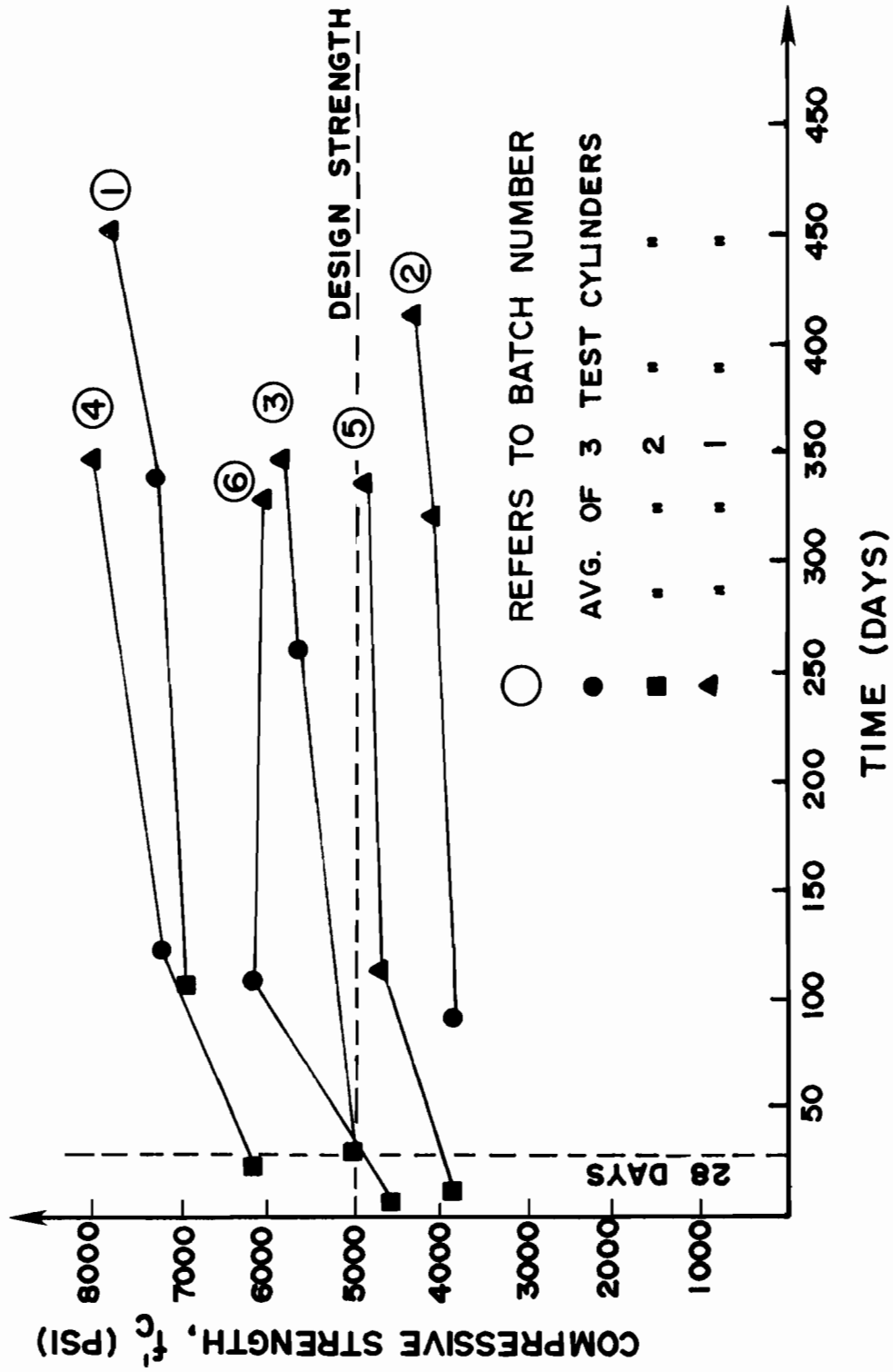


Fig. 3.5 Compressive strength versus time

TABLE 3.5 Durability Specimens Cast from Each Batch

Batch No.	Specimens Cast*
1	1, 3, 5, 6, 7, 8
2	2, 4, 9, 10, 11, 12
3	13, 17, 18
4	14, 21, 22
5	15, 16, 23
6	19, 20, 24

* Refer to Table 3.2

TABLE 3.6 Summary of Interior Support Positions

Interior Support Condition*	Specimens**
A	1, 2, 9, 10, 13, 14, 21, 22
B	3, 4, 11, 12, 15, 16, 23, 24
C	5, 6, 7, 8, 17, 18, 19, 20

* Refers to Fig. 3.17

** Refers to Table 3.2

damaged in many locations upon arrival at the laboratory. However, only undamaged duct was used in the specimens. But since it was apparent that this product probably arrives at any construction site with some damage to the plastic duct, it was decided to slit the plastic duct in known locations. Therefore, if corrosion was likely to occur, it would occur at these slit locations.

The prestressing tendon used in the grouted multistrand specimens was uncoated seven-wire stress-relieved strand with a nominal diameter of 1/2 in. and a specified minimum ultimate stress of 270 ksi. This strand was purchased from a commercial vendor in Texas.

3.5.4 Anchorage. The anchorage components used for the unbonded monostrand specimens were obtained from VSL Corporation. The anchorages consisted of a casting and a pair of wedges. A VSL pocket former grommet was used to leave the anchorage accessible for stressing on the stressing end of the specimens. Details of the VSL anchorages are provided in Fig. 3.6.

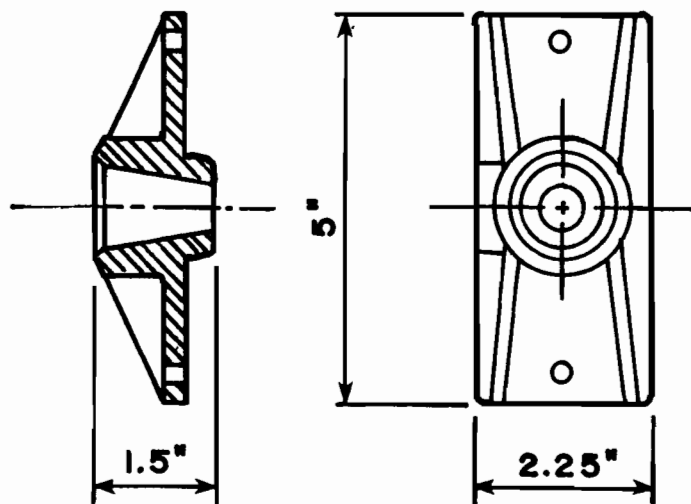
An anchorage for a two-strand application was not commercially available in the United States for the grouted multistrand specimens. The use of other larger anchors for four to seven strands was investigated, but these were found to be too expensive, large or inappropriate for thin bridge deck applications. Therefore, the anchorages for these specimens were fabricated in the laboratory. The details of the anchorages are shown in Fig. 3.7.

The galvanized rectangular duct was attached to the anchor plates by a flexible silicone adhesive caulking. A piece of high-density styrofoam 2-1/2" x 6" x 4" was used as a pocket former at the stressing end of the grouted specimens.

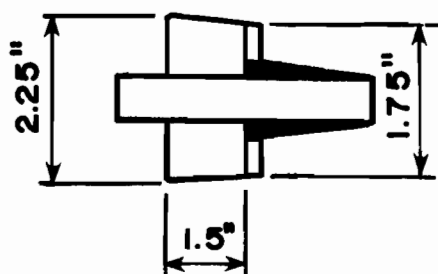
3.5.5 Galvanized Duct. The rigid, thin-walled, galvanized rectangular duct used for the grouted specimens was typical of that used for flat-plate building construction. The duct dimensions are shown in Fig. 3.7.

3.5.6 Grout. The mix used to grout the prestressing strands in the grouted specimens complied with TSDHPT Specifications [40]. The mix design used consisted of one sack of Type III portland cement, one pound of Sika Intraplast-N, an expanding admixture, and five gallons of water. The grout was mixed in a 3-1/2 cu.ft. mixer.

3.5.7 Mortar Plug. Mortar was used to plug the anchor recesses left by the pocket formers on the stressing end of all specimens and to fill the holes left after removing the grout pipes in the grouted specimens. The mix ratio for the mortar by weight of



Anchorage Casting



Grommet

Fig. 3.6 VSL anchorage S5N used in unbonded specimens

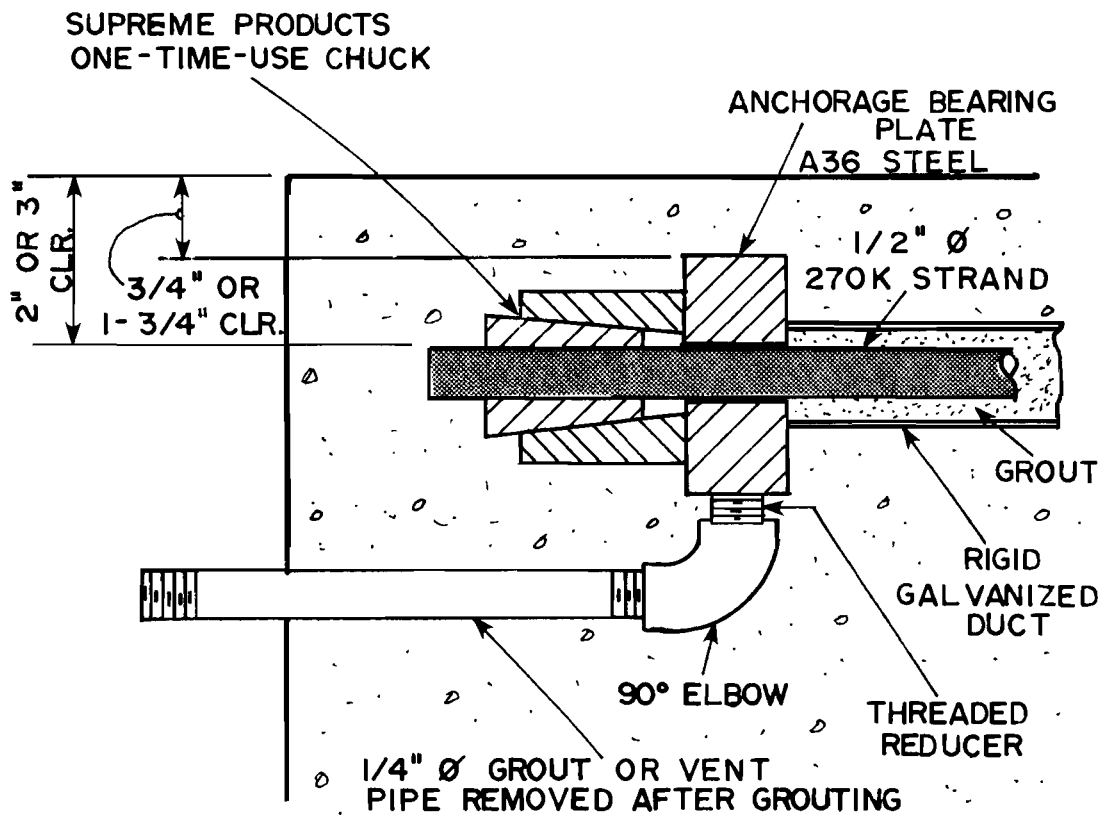
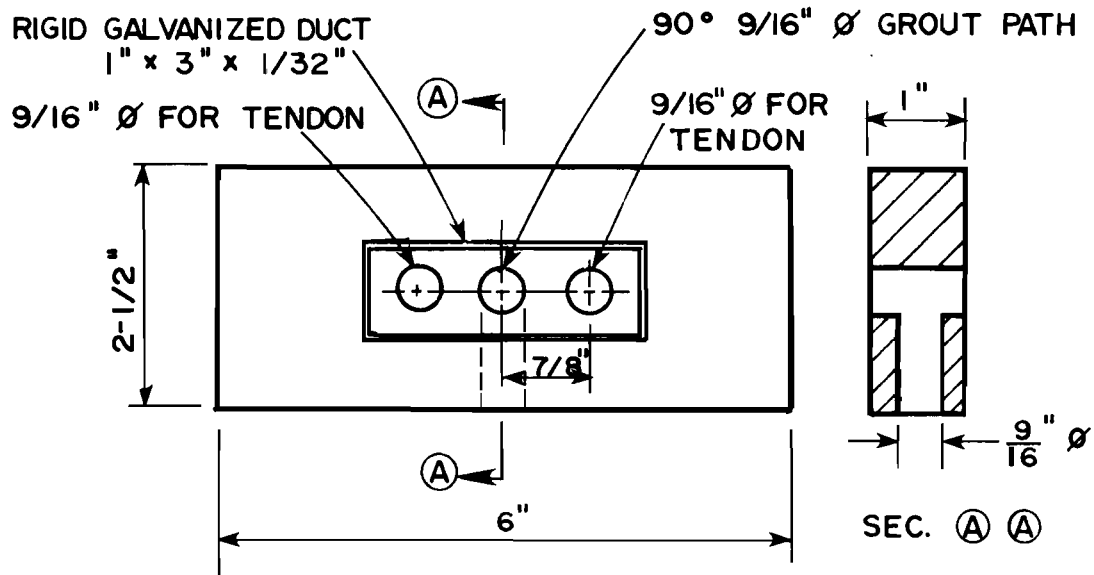


Fig. 3.7 Details of grouted specimen anchorages

sand to cement to water was approximately 3:1:0.5, as recommended for an anchorage plug in Ref. 41.

3.5.8 Salt. The salt used for exposure in the durability tests is the same salt used for deicing roads and bridges in Texas by TSDHPT. The sodium chloride (NaCl) content of the salt was approximately 96%. A 3.5% salt water solution was prepared using this salt and then applied to the surface of the specimens during the exposure cycle of testing.

3.5.9 Other Materials. Two different epoxies were used in the construction of the durability specimens. An industrial epoxy was used to paint certain areas of the specimens, mostly the sides and ends, to prevent salt water penetration. This epoxy was also used to coat the anchorages of the grouted specimens to prevent them from corroding. An epoxy bonding agent, No. A-103, made by the TSDHPT was applied to the inside walls of the anchor pockets on the stressing ends of the specimens before the mortar plug was placed.

Since corrosion is an electrochemical phenomenon, it was necessary to isolate the reinforcing steel, prestressing tendon, and metal duct from any possible electrical contact. This provided assurance from each component acting as an independent corrosion cell. Therefore, the conventional metal chairs used in construction to provide proper concrete covers were dipped in epoxy prior to placement of the steel. This prevented an electrical contact between the reinforcement and the chairs. In addition, plastic cable ties were used to tie the reinforcement to the chairs.

Though not in direct contact with the reinforcement in the specimens, the coil ties used for lifting purposes were coated with epoxy as well.

3.6 Fabrication

3.6.1 Specimen Fabrication. Figures 3.8 through 3.11 show various details of the formwork and reinforcement. The ready mixed concrete was consolidated using electrical internal vibrators. After finishing was completed, wet burlap was placed over the specimens, and then covered with plastic for curing. The specimens were cured for three to four days prior to formwork removal.

3.6.2 Posttensioning Operation. Specimens were posttensioned from one end using a hydraulic ram, electric pump and stressing chair as shown in Figs. 3.12. For the case of the grouted specimens, both strands were posttensioned simultaneously.

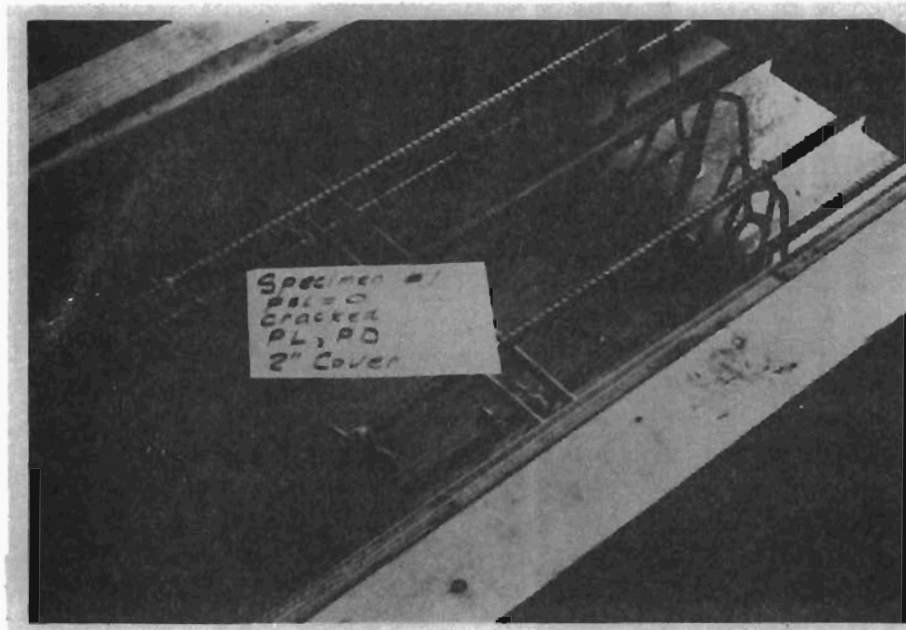


Fig. 3.8 Reinforcement tied to chairs in unbonded specimen; wood positioning template and coil ties in place

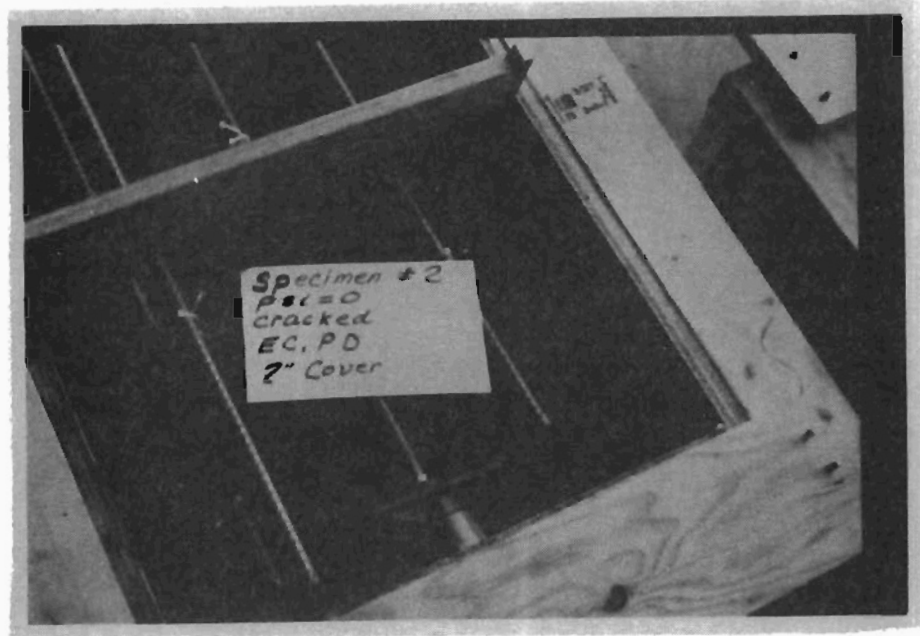


Fig. 3.9 Anchorage casting and pocket former on stressing end of unbonded specimen



Fig. 3.10 Reinforcement tied to chairs in grouted specimen;
wood positioning template in place

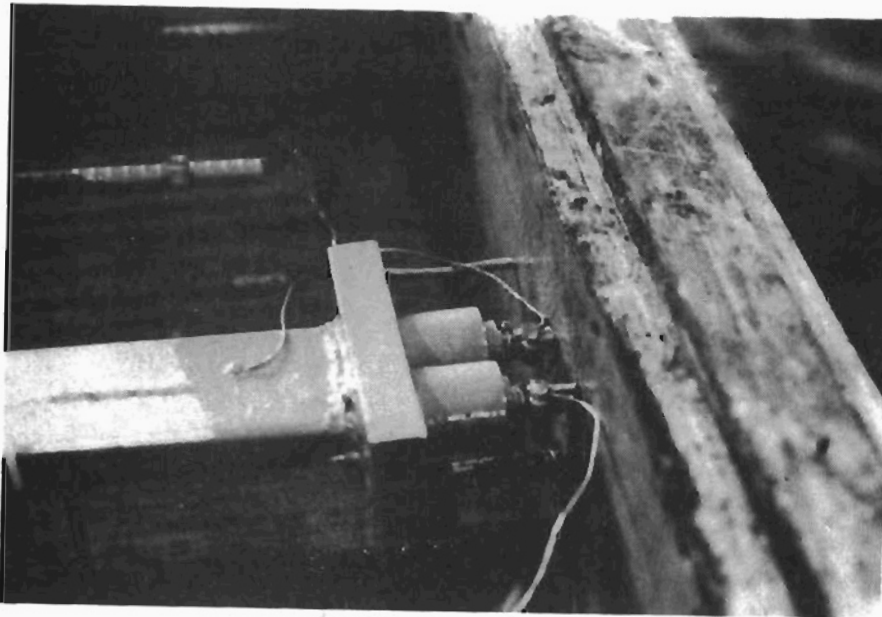


Fig. 3.11 Cast-in dead end anchorage and chucks for grouted
specimen; wires for half cell potential
instrumentation in place

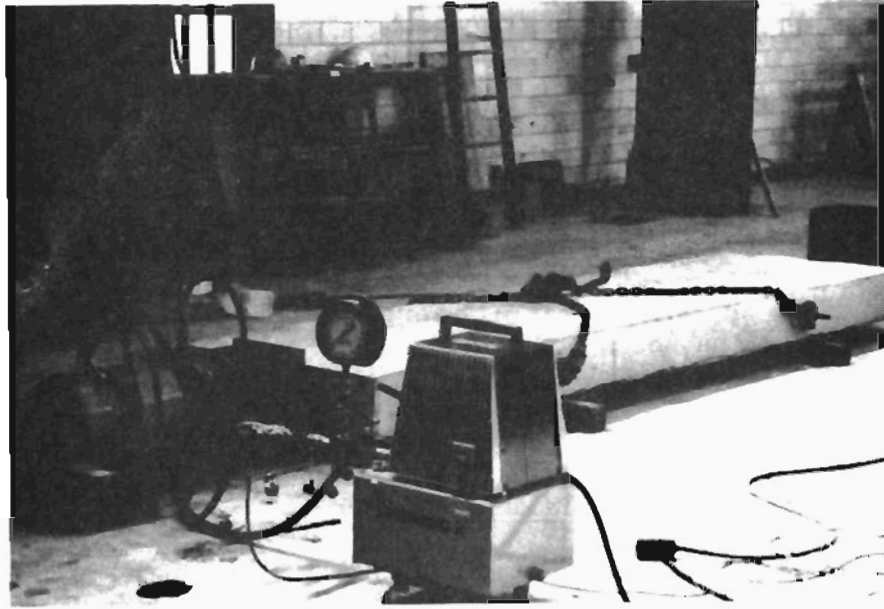


Fig. 3.12 Specimen posttensioning

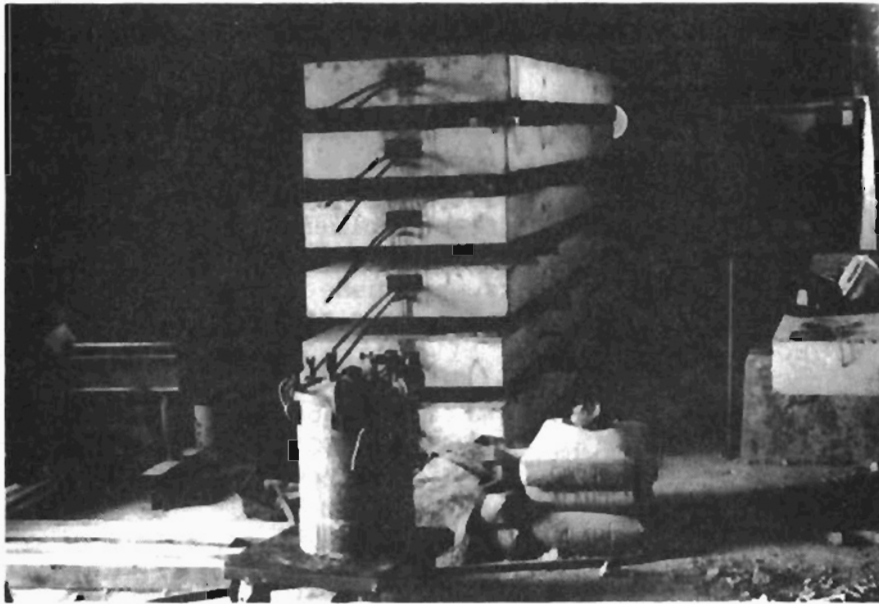


Fig. 3.13 Grouting tank

Special care was taken to ensure that the seating losses were minimized for the short tendon lengths. The strands were tensioned initially to $0.8 f_{pu}$ corresponding to 216 ksi for the 270K strand. The strand extensions were cut off within the pocket by using a torch.

3.6.3 Grouting. The grouted multistrand specimens were grouted using the pressurized grouting tank shown in Fig. 3.13. Conventional grouting procedures were used.

3.6.4 Pocket Patch. Mortar was used for filling the spaces left by the pocket formers on the stressing end of the specimens and the holes left by the grout tubes. Before placing the mortar, the inside walls of the pockets and the anchorages were painted with TSDHPT epoxy bonding agent.

3.7 Half Cell Potential Instrumentation

The half cell potentials of the top nonprestressed reinforcement, the prestressing strands, and the galvanized duct were monitored over the period of the exposure testing. The electrical connection to the reinforcement, strand and duct required to monitor the half cell potentials consisted of a single plastic-coated wire lead attached to the ends of the reinforcing bar and strand at the support end of the specimens using a small-diameter hose clamp. All electrical connections were epoxy-painted after completion. Typical electrical connections are shown in Figs. 3.14a and 3.14b.

The half cell potentials of both top reinforcing bars and the unbonded plastic-coated prestressing tendon in the unbonded specimens were monitored throughout the exposure period. Only the two top middle reinforcing bars, the two prestressing strands, and the galvanized duct in the grouted specimens were monitored.

The half cell readings were made in accordance with ASTM C-876-80, Standard Test Method for Half Cell Potentials of Reinforcing Steel in Concrete [39]. To eliminate the need for individual connections of each wire at each reading time, the leads from all specimens were attached to switching boxes. Half cell potential readings were made using a Beckman 3500 digital high-impedance voltmeter. A saturated calomel electrode (SCE) was used as the reference potential.

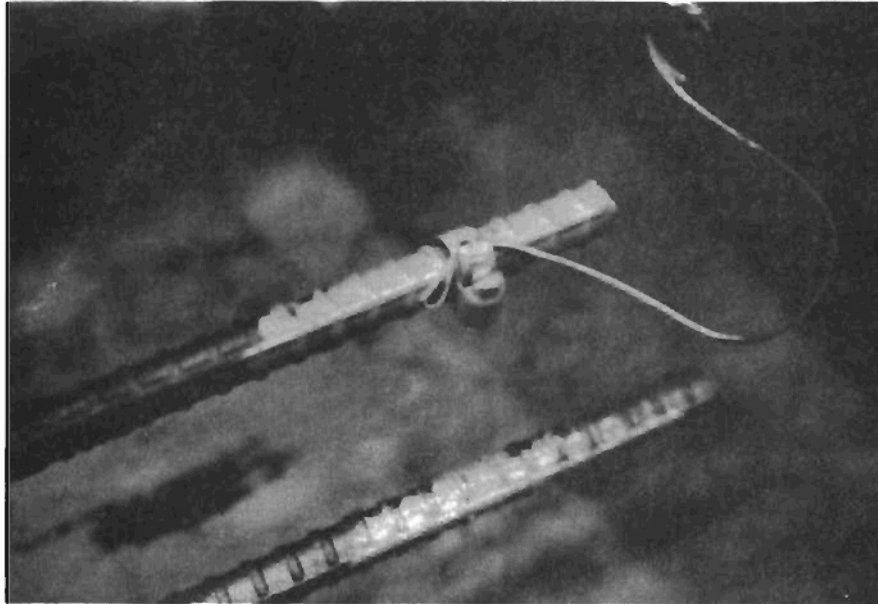


Fig. 3.14a Electrical connection to a reinforcing bar

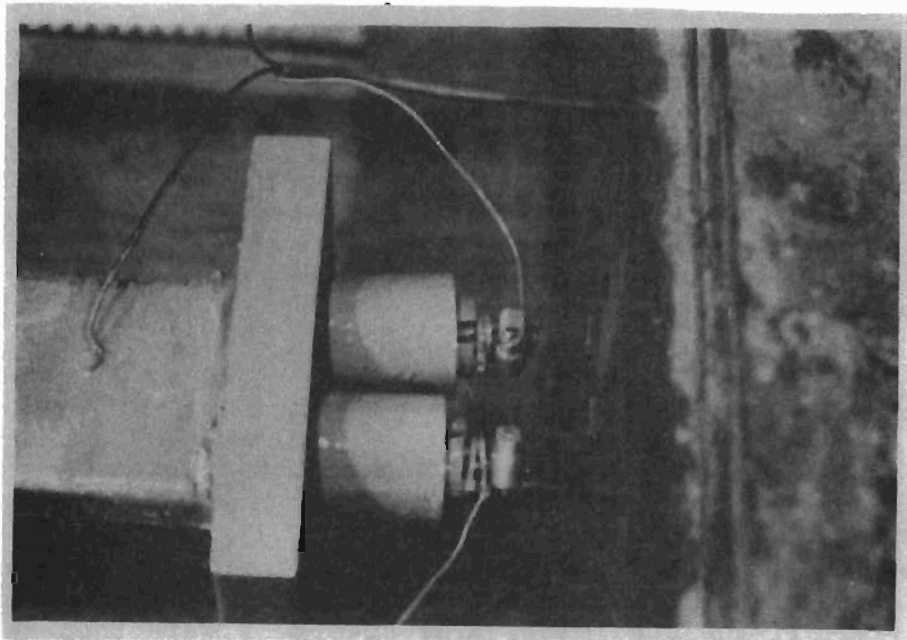


Fig. 3.14b Electrical connections to prestressing strand and galvanized duct

3.8 Test Setup

After fabrication, the durability specimens were moved to the exposure facility which contained separate "garages" in which four unbonded specimens or two grouted specimens were placed as shown in Fig. 3.15. The loading of the specimens to produce negative moment at the interior support and to open cracks was accomplished with the loading system shown in Figs. 3.16 and 3.17. The load was monitored using a pressure transducer attached to the pump.

The interior support position varied depending on the concrete cover and the desired crack width under load. The support locations for series A, B, and C in Fig. 3.17 were chosen to minimize the load required to open cracks to the specified level. The support arrangement used for each specimen is given in Table 3.6.

Since in an actual bridge deck the penetration of aggressive substance represents a one-dimensional flow problem, the side walls and ends of each specimen were epoxy-painted to better simulate the salt water flow condition in the field. The top surfaces at the tie-down beam locations were painted in all specimens. However, only for the grouted specimens were the top surfaces of the concrete at the tie-down and loaded ends painted. This was done to eliminate the corrosion susceptibility of the grouted specimen anchorages which were fabricated in the laboratory. The painted areas of the unbonded and grouted specimens are shown in Fig. 3.18.

A levee $3/4$ in. in height made of plastic molding was placed around the edges of the top exposed surfaces of the specimens. This levee as shown in Fig. 3.19 allowed the salt water to pond on the specimens during the exposure testing.

Spray paint was used to mark locations on the top surfaces of the specimens where half cell potential readings were to be taken. There were five stations for each individual reinforcing bar, strand or duct as shown in Fig. 3.20.

3.9 Testing

3.9.1 Cracking of Specimens. Before exposure testing began, the specimens were loaded until cracking occurred using the loading system shown in Figs. 3.16 and 3.17. After a specimen cracked, the load was removed and the crack locations were marked as shown in Fig. 3.20. Appendix A shows the locations of the induced cracks in all the specimens. The specimens were then reloaded gradually until the desired surface crack width was achieved as specified in Table 3.2. The crack widths were measured using a

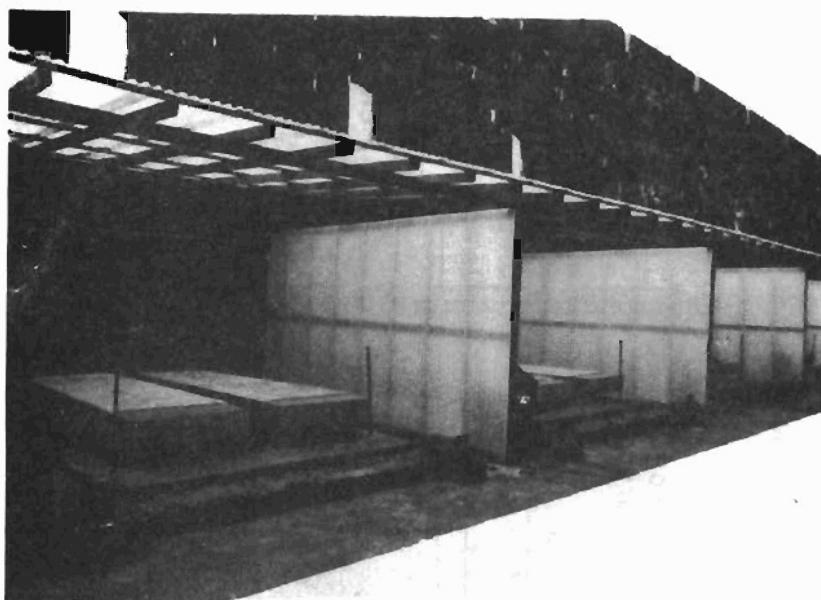


Fig. 3.15 Exposure facility

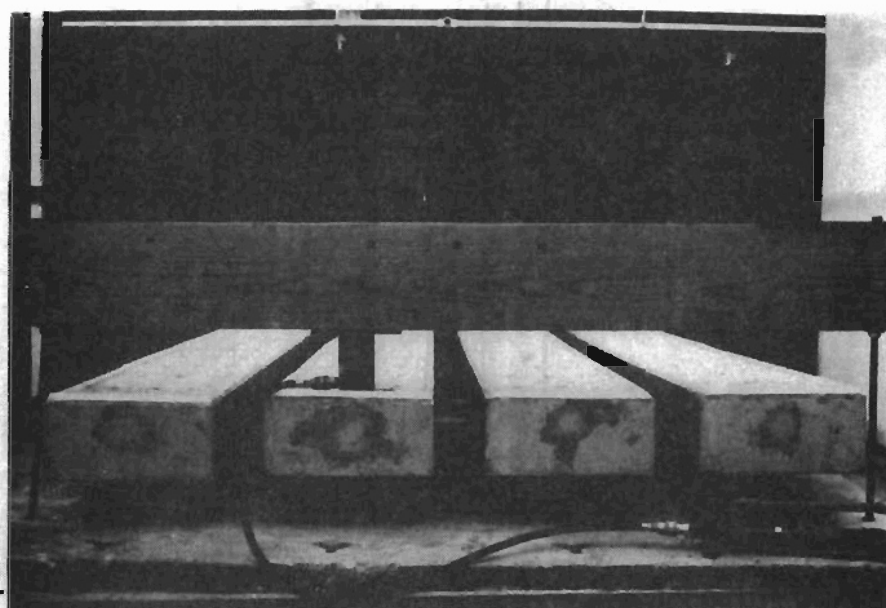


Fig. 3.16 Actual loading system

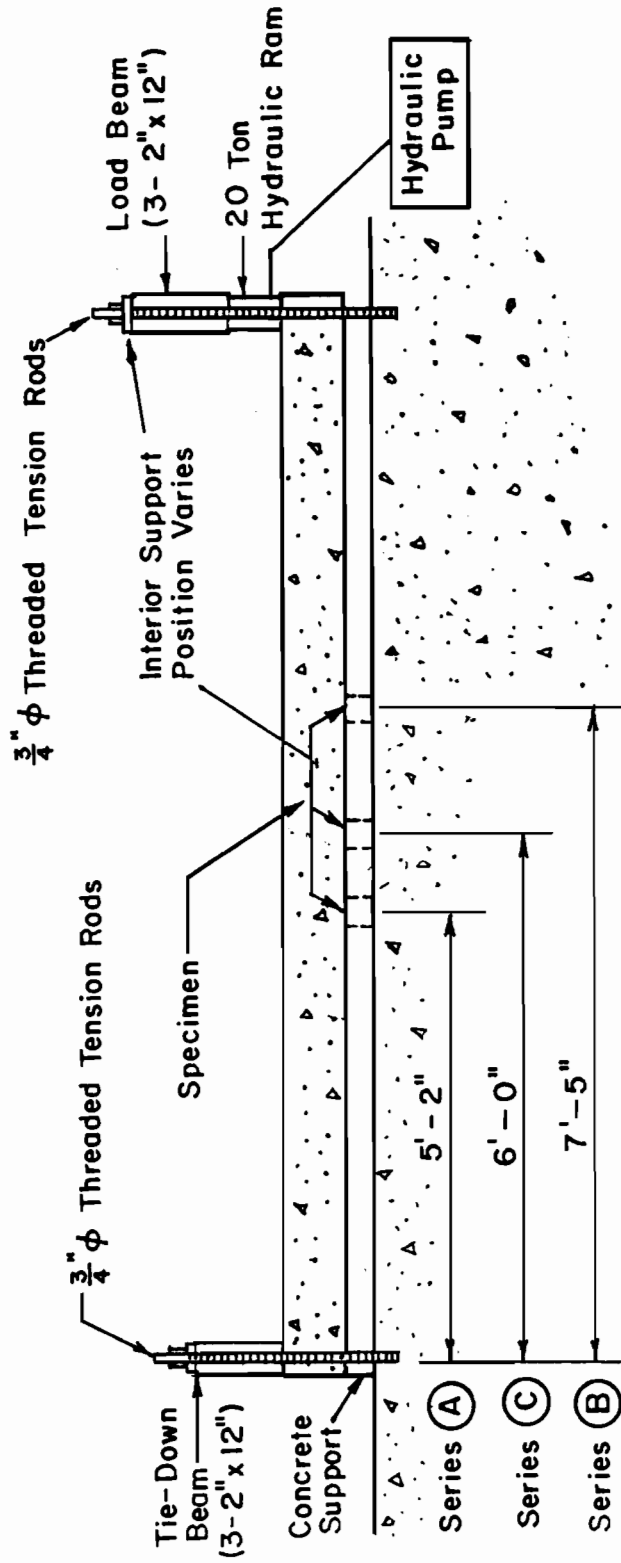


Fig. 3.17 Schematic of loading system

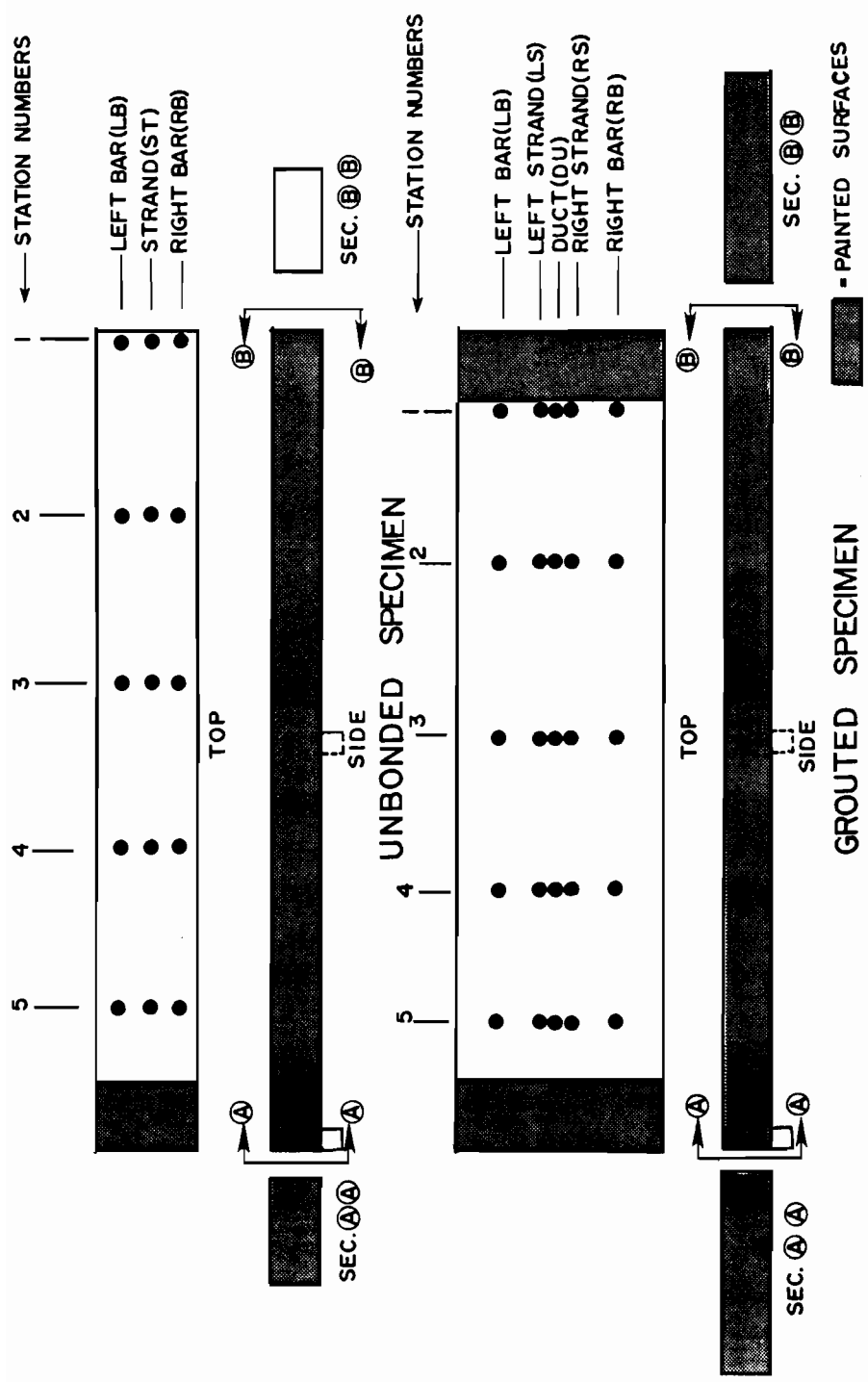


Fig. 3.18 Painted surfaces; half cell potential stations

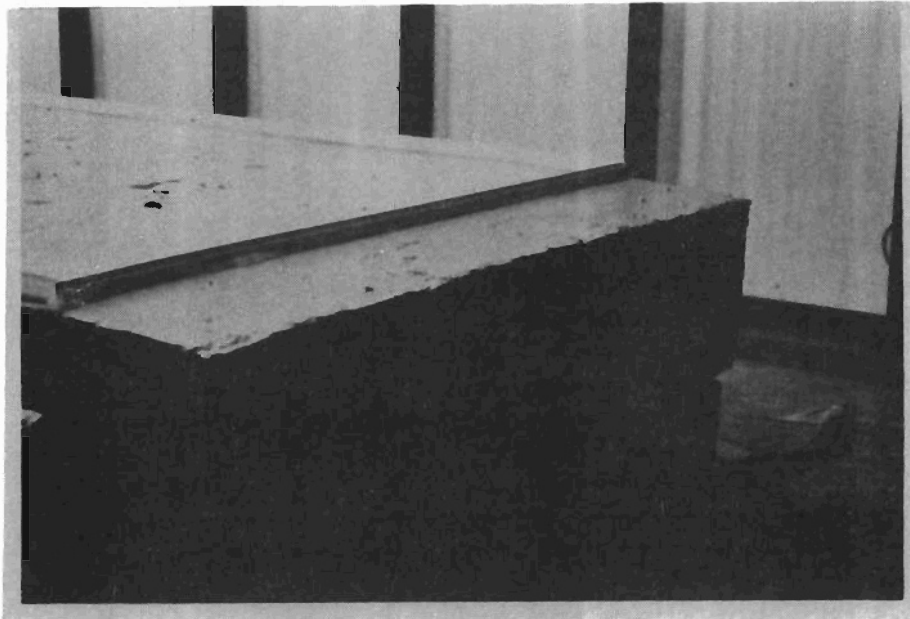


Fig. 3.19 Levee system on specimens

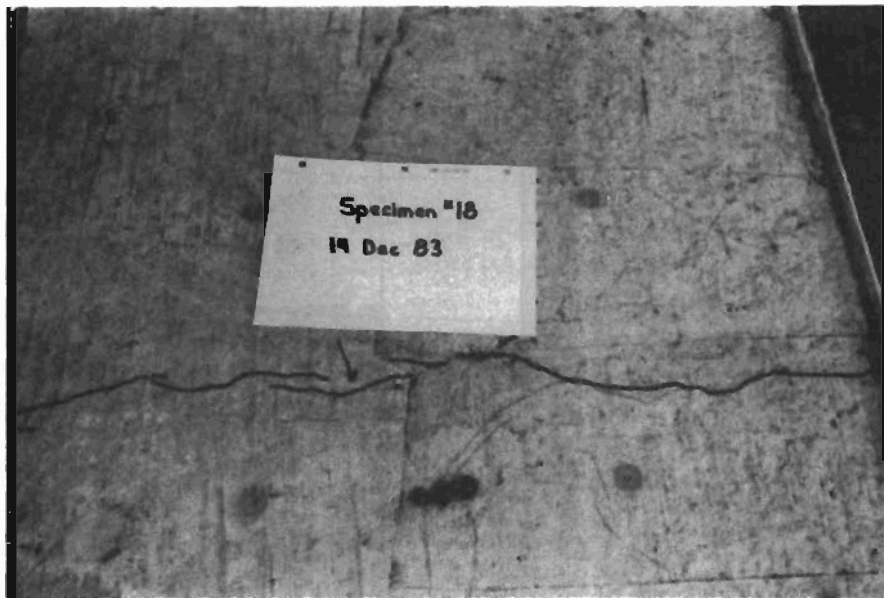


Fig. 3.20 Cracks marked on specimens during initial cracking

length comparator accurate to 0.001 in. The load to produce the desired crack width is reported in Table 3.7.

3.9.2 Exposure. Exposure testing consisted of subjecting each specimen to one wet-dry test cycle every fourteen days as shown in Fig. 3.21. On the first day, the salt water was ponded on the surface of the specimens to a depth of approximately 1/2 in. On the second day, specimens were subjected to five repeated loading cycles up to a load equal to that producing the desired crack width as determined during the initial cracking stage. During each load cycle, the maximum applied load was held constant for approximately five seconds prior to release. Any water lost during loading due to specimen deflections was replaced immediately after loading. After loading all specimens, half cell potential readings were taken, as shown in Fig. 3.22. Specimens were then allowed to dry out until the start of the next exposure test cycle. On the ninth day, five additional load cycles were applied to each specimen. In general, by this time the specimens had dried out with very little standing water left. However, the loading provided an oxygen path to the reinforcement by way of the cracks. The specimens continued to dry out from the ninth to the fourteenth days. Then the cycle was repeated. The surface of the specimens was thoroughly washed to remove any crystallized salt every third cycle. Fourteen cycles were completed for specimens in Series A and B of Table 3.6, and eight cycles for specimens in Series C before the exposure testing was stopped due to time constraints. In light of the extremely aggressive environment, this relatively limited time of exposure was felt to be adequate for determination of relative corrosion damage in the vicinity of cracks. The short time periods (196 days for Series A and B and 112 days for Series C) would not be adequate to determine the possibility of corrosion damage in uncracked concrete of adequate cover and quality.

3.9.3 Post-Mortem Examination. Upon completion of the exposure testing, a "post-mortem" examination of the durability specimens was carried out to assess their performance in the salt water environment. The examination included chloride content determination and visual inspection of all top reinforcement prestressing strands and prestressing anchorages for evidence of corrosion.

The chloride content tests were performed following the FHWA recommended procedure [42] for sampling and testing for chloride ions in concrete, except instead of using the recommended titration process for determining chloride content, an alternate, yet more accurate, colorimetric procedure was used. Concrete samples were taken at the level of the reinforcement at two locations for each specimen: at a crack near the interior support and in the uncracked concrete near the

TABLE 3.7 Summary of Specimen Loads

Specimen No.	Applied Load (lbs)
1	1250
2	1250
3	1850
4	1850
5	4425
6	4425
7	3000
8	3000
9	1250
10	1250
11	1850
12	1850
13	2500
14	2500
15	3700
16	3700
17	9650
18	9650
19	6050
20	6050
21	2500
22	2500
23	3700
24	3700

* refers to the total applied load required to produce the specified crack width given in Table 3.2

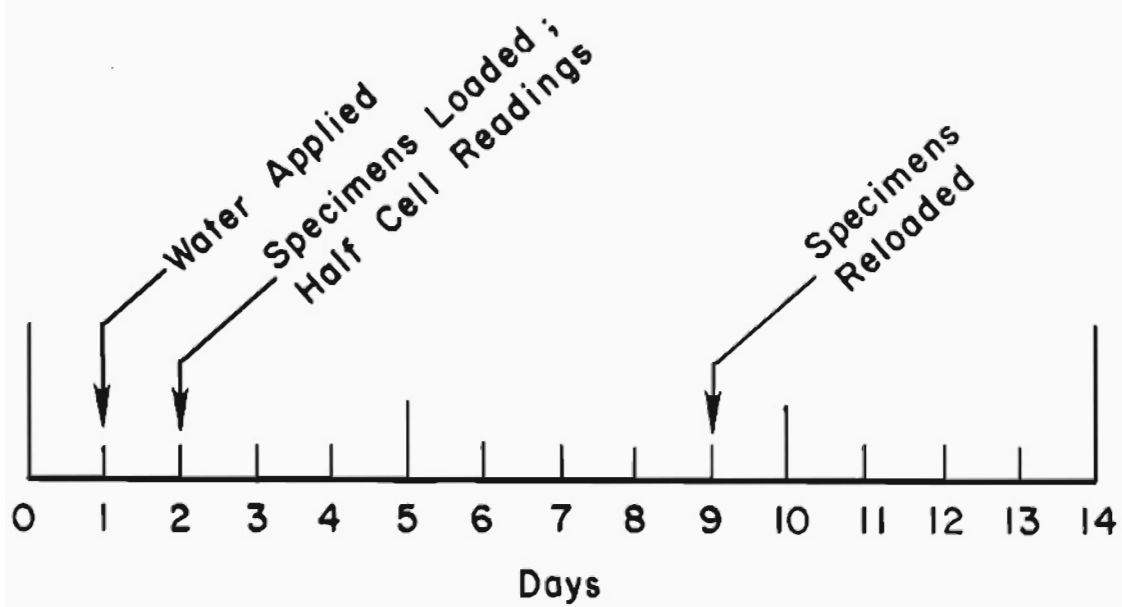


Fig. 3.21 Basic exposure cycle

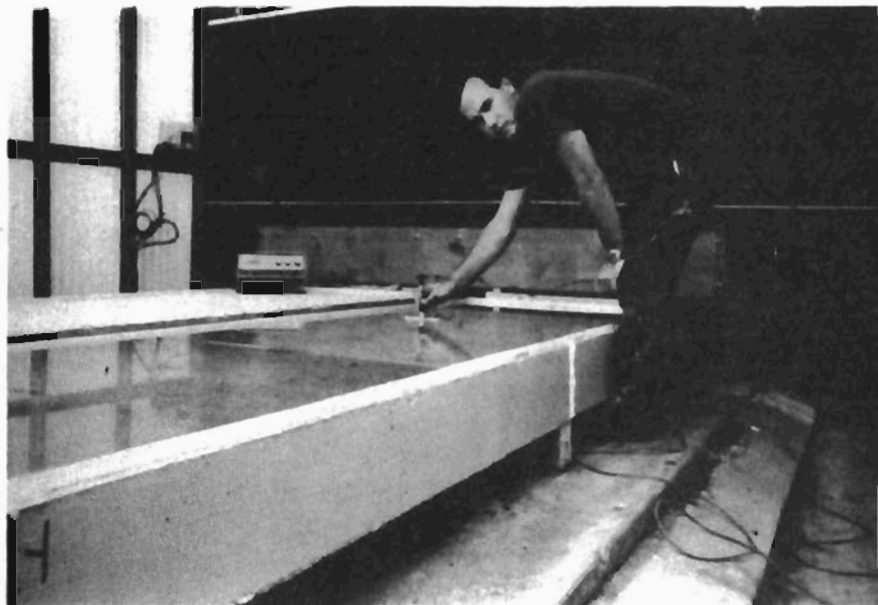


Fig. 3.22 Half cell potential readings

loaded end of the specimen. In a few cases, samples were taken at various depths in the specimen in order to determine a chloride content profile. Appendix A shows the locations where the concrete samples were taken for each specimen.

In order to visually examine the reinforcement, two saw cuts, the locations of which are shown in Appendix A for each specimen, were made approximately 4 to 6 in. apart at the crack locations using the concrete saw shown in Fig. 3.23. The concrete section removed from each specimen, as seen in Fig. 3.24, was broken apart in order to examine the steel for corrosion. A few specimens were jackhammered apart in order to examine the full length of all the top reinforcement as well as the anchorages.



Fig. 3.23 Saw used to crosscut specimens at crack zones

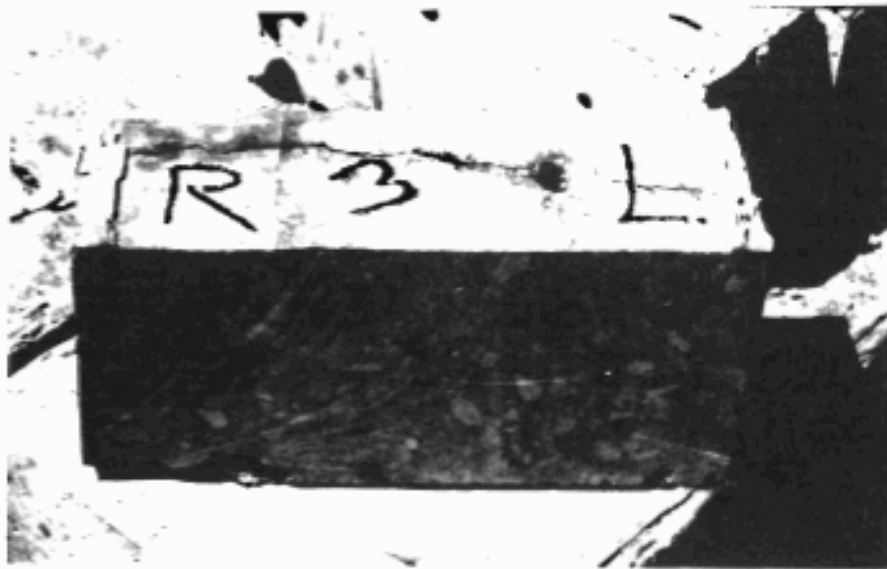


Fig. 3.24 Concrete section removed from crack zone

C H A P T E R 4

PRESENTATION OF DURABILITY TEST RESULTS

4.1 Introduction

The results of the durability tests are reported in this chapter. Results include cracking behavior of the durability specimens during the initial loading cycle to initiate cracking, followed by half cell potential readings during exposure. Finally, results from post-mortem analysis of the concrete to determine chloride penetration and visual inspection for evidence of corrosion on the embedded steel are presented. This chapter presents basic data. Chapter 5 will present a thorough evaluation of the data.

4.2 Specimen Initial Cracking Cycle

During initial load stages, induced cracking occurred on the top surface of the durability specimens in the interior support region. In all cases, one crack formed at or in the immediate vicinity of the interior support, as shown in Fig. 4.1a for Specimen 1 and in Fig. 4.1b for Specimen 13. In many cases, a second crack also formed within 8 to 12 in. of the first crack, as shown in Fig. 4.2a for Specimen 2 and in Fig. 4.2b for Specimen 18. Crack patterns for all specimens are provided in Appendix A. Except for the much higher cracking load and smaller crack widths, there was no apparent variation in crack distribution because of the presence of prestressing. There was no apparent difference between grouted or unbonded tendons. This was probably due to the presence of conventional nonprestressed reinforcement in all the specimens which controlled crack distribution as well as crack width.

Load versus crack width data were taken after initial cracking for Specimens 14, 15, 21, and 23, since each one represented a major variable classification, namely 2 in. and 3 in. cover and prestressed and nonprestressed specimens.

Nonprestressed specimens represent conditions typical in conventionally reinforced concrete members, in which, upon removal of applied load, existing cracks remain open. In contrast, in prestressed specimens, existing cracks which open upon loading will close upon load removal. The moments to initiate cracking are shown for the specimens in Fig. 4.3. Moment at the interior support versus surface crack width upon reloading after initial cracking for the

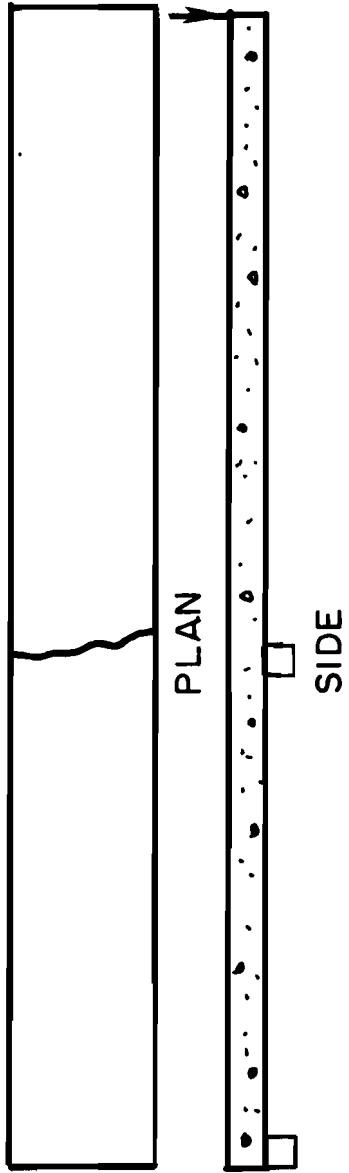


Fig. 4.1a Induced cracks for Specimen 1

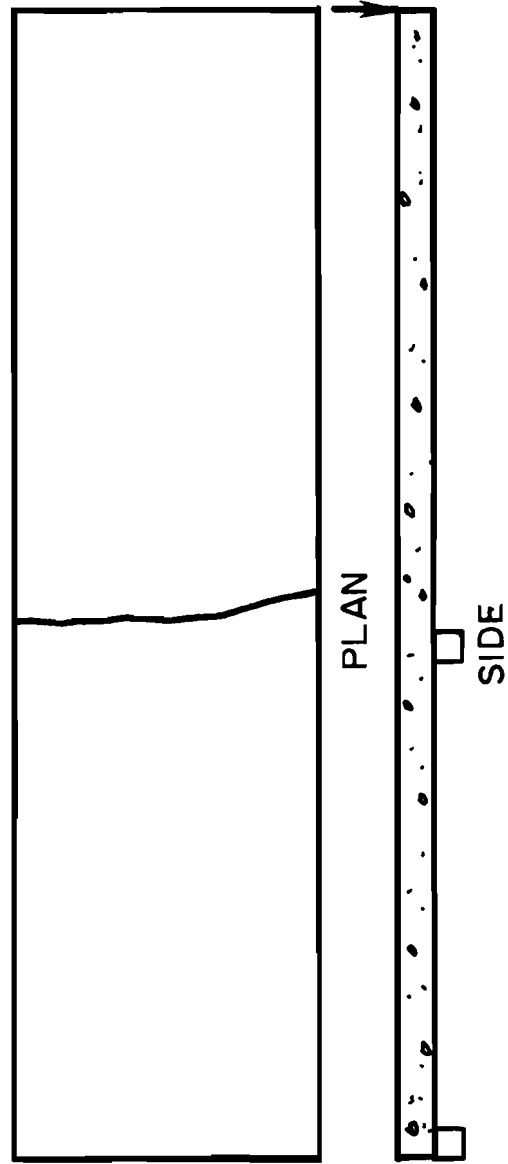


Fig. 4.1b Induced cracks for Specimen 13

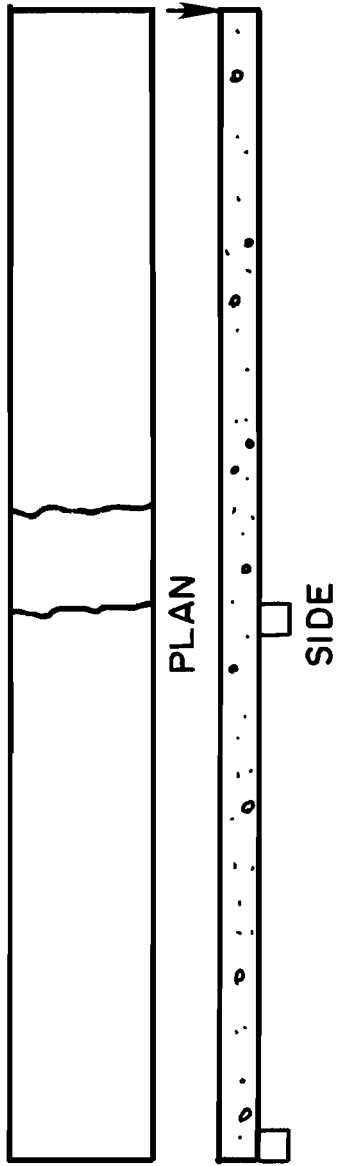


Fig. 4.2a Induced cracks for Specimen 2

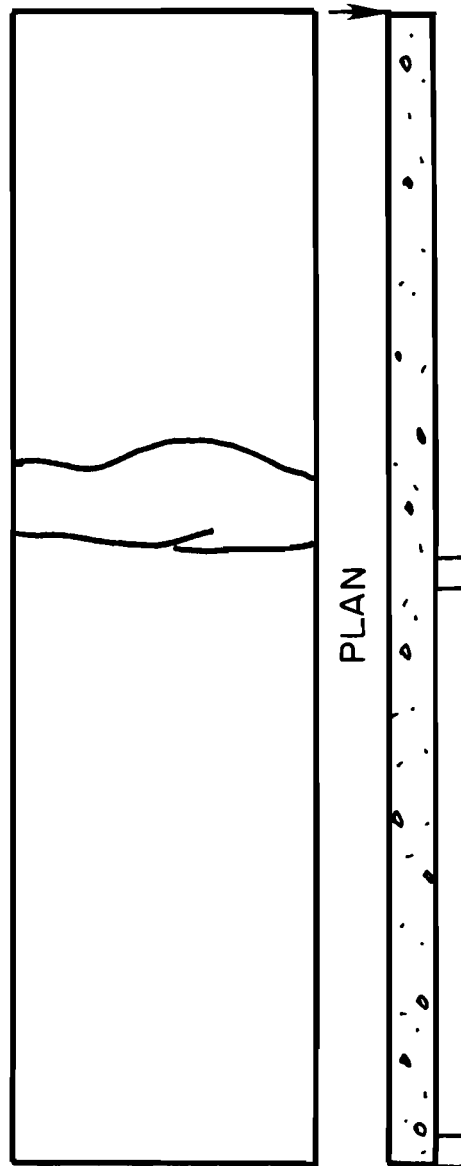


Fig. 4.2b Induced cracks for Specimen 18

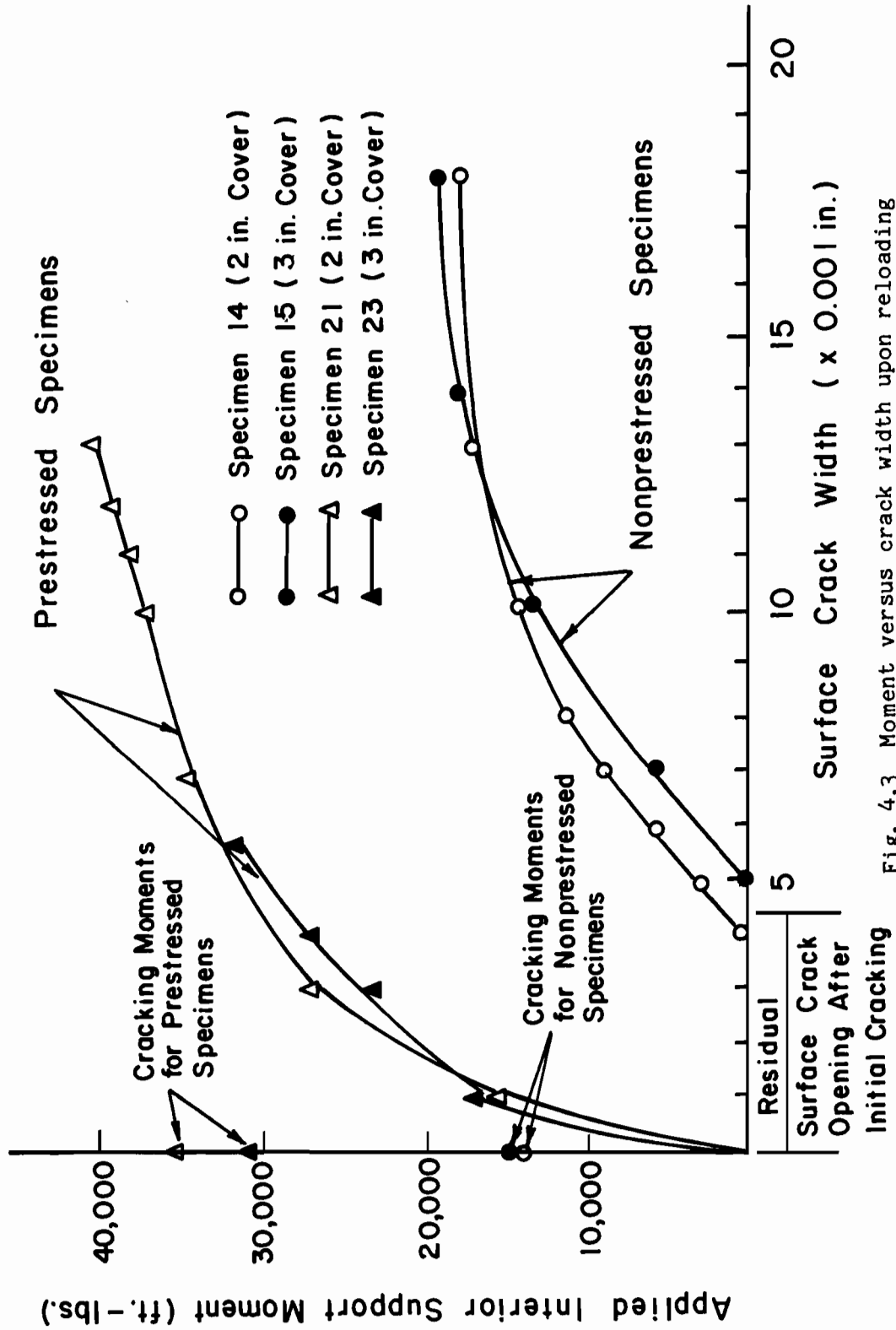


Fig. 4.3 Moment versus crack width upon reloading after initial cracking

four specimens are also shown in Fig. 4.3. As can be seen, the cracking moments for the two nonprestressed specimens were similar and substantially lower than for the two prestressed specimens. After initial cracking, the load was dropped to 0 before reloading. As is evident from Fig. 4.3, before reloading occurred, the residual surface crack opening was of the order of 0.004 in. to 0.005 in. for the nonprestressed specimens independent of cover. However, before reloading the prestressed specimens, the cracks were completely closed. Upon reloading, it is clear from Fig. 4.3 that for a given applied moment, the surface crack width for the prestressed specimens was much smaller than for the nonprestressed specimens and basically independent of concrete cover. The curves in Fig. 4.3 are believed to be representative. It can be concluded that the moment-surface crack width behavior for the specimens is dependent on whether the specimens were prestressed or nonprestressed, and independent of concrete cover.

Surface crack widths were measured after initial cracking under the full applied load (see Table 3.7 for load levels) at the crack location nearest the interior support for all other specimens. In all cases, the surface crack widths under the applied load were close to the values specified in Table 3.2, namely 0.002 in. or 0.015 in., for each of the specimens. These results additionally confirm that the surface crack widths were basically independent of whether tendons were unbonded or grouted because of the presence of conventional nonprestressed reinforcement.

4.3 Exposure Testing

Data taken during exposure testing consisted mainly of half cell potential readings and periodic visual examinations for any signs of corrosion and corrosion distress.

4.3.1 Half Cell Potential Readings. Half cell potential readings were taken referenced to the standard calomel electrode (SCE, 241 millivolts) and plotted in units of negative millivolts with respect to SCE. The half cell potential method was one method used for detecting corrosion. Typical curves for half cell potential readings versus time are presented in Figs. 4.2 and 4.3. At a given time, there was very little variation in the half cell potential reading at the different locations along a specimen as shown in Figs. 4.4 and 4.5. Figure 4.4 represents the half cell readings with time for the left reinforcing bar in Specimen 13. Similarly, Fig. 4.5 represents the half cell readings with time for the right bar of Specimen 11. Since the readings were referenced to the saturated calomel electrode potential, then according to Ref. 39 (and further discussed in Section 5.3.2), the results indicate that the left bar

13 LB GROUTED OPSI .015IN 2IN PL

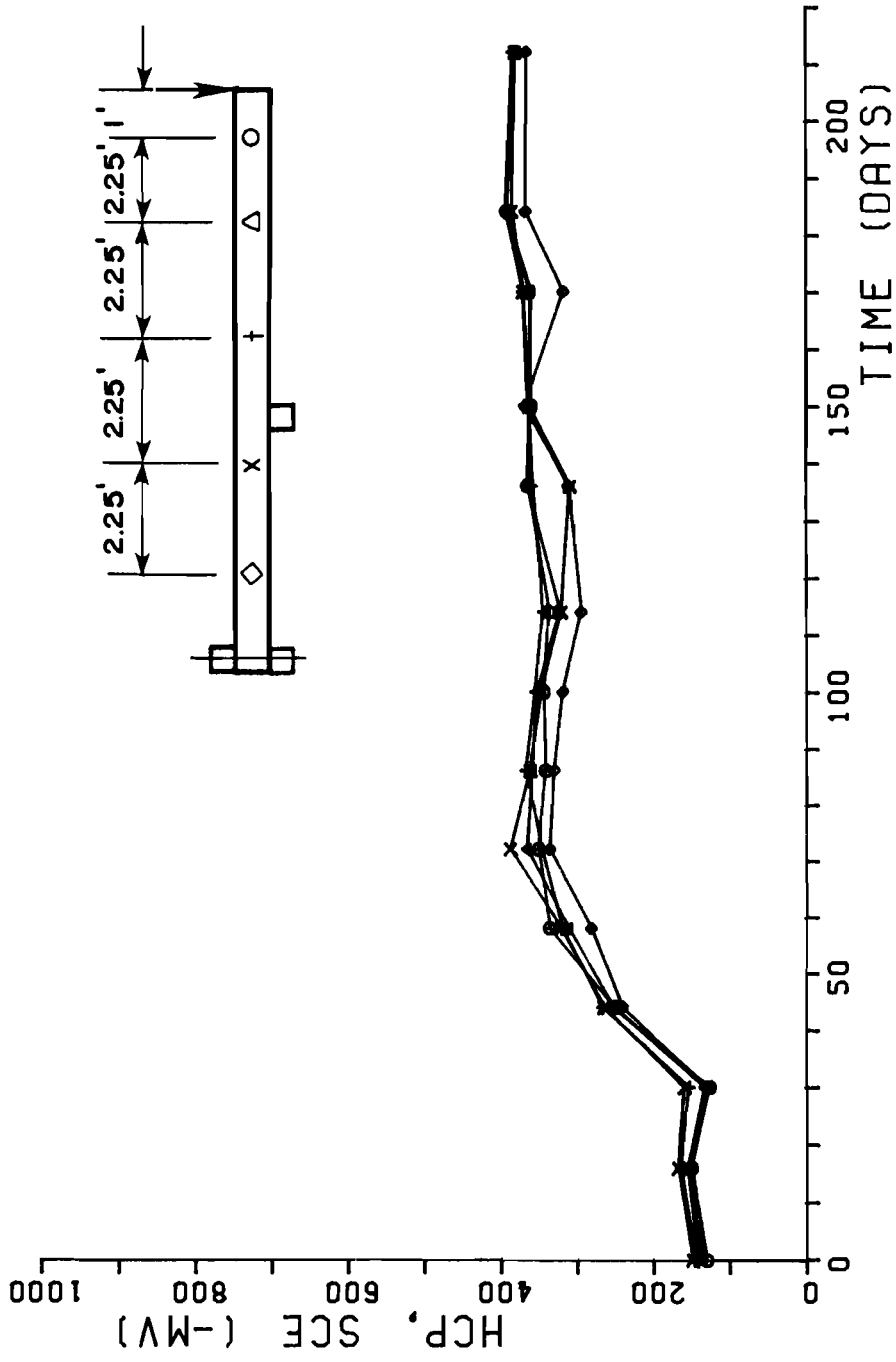


Fig. 4.4 Half cell potentials with time for left reinforcing bar in Specimen 13

11 RB UNBONDED 160PSI .002IN 3IN PL

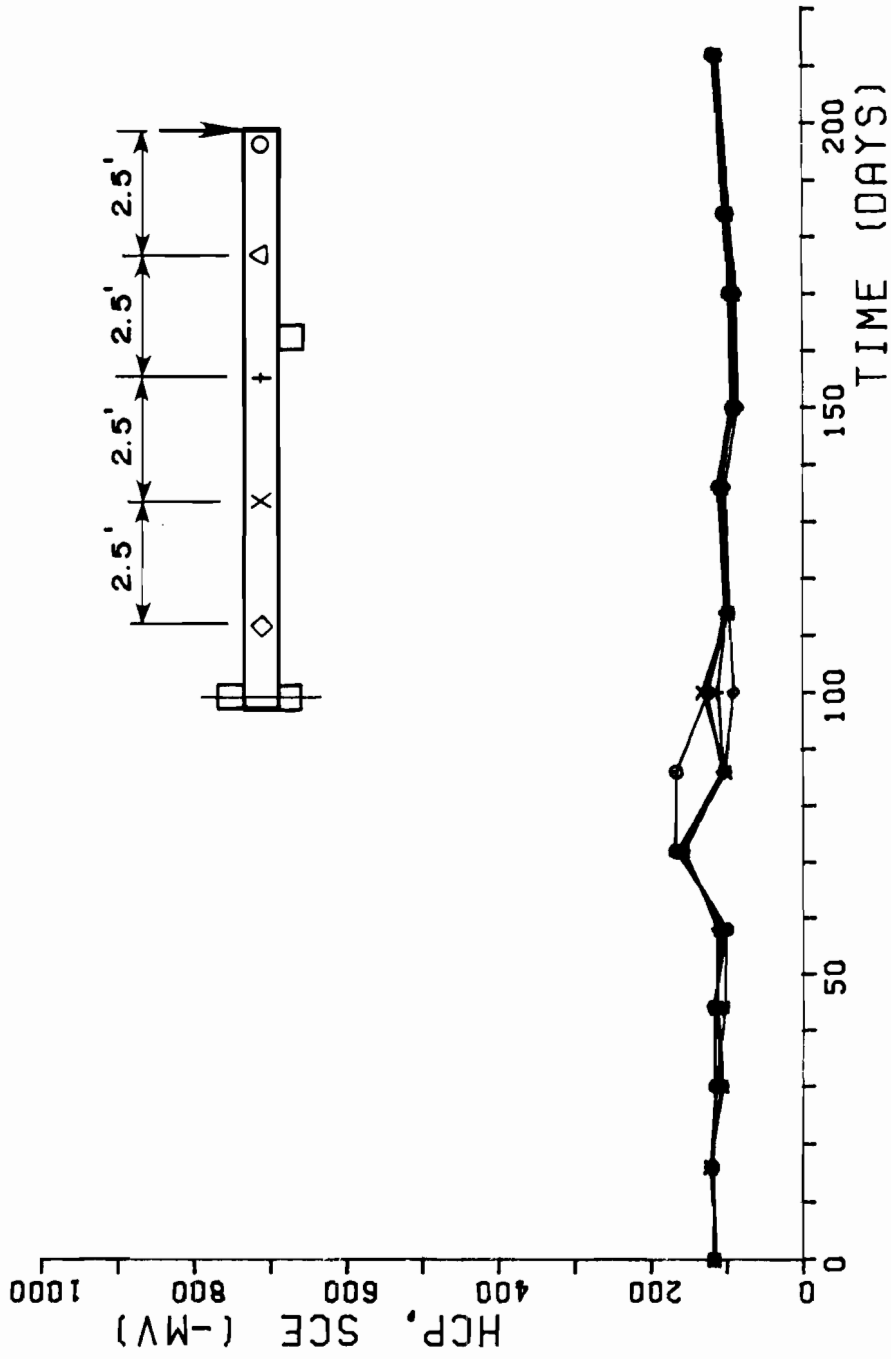


Fig. 4.5 Half cell potentials with time for right reinforcing bar in Specimen 11

of Specimen 13, in which the potential exceeded 290 millivolts, had a greater than 90% probability of being in an active state of corrosion after approximately 40 days of exposure testing. In comparison, the results indicate that there was a greater than 90% probability that no corrosion occurred for the right bar of Specimen 11 at any time during the testing since the potential did not exceed 140 millivolts. A thorough evaluation of these half cell potential readings will be presented in the next chapter.

4.3.2 Visual Examination. The only visual signs of corrosion noted throughout the exposure tests were in the form of surface rust stains as shown in Fig. 4.6 above the anchorage locations at the loaded end of Specimens 2, 5, and 9. The stains first appeared after several weeks of exposure. They were accompanied by a small surface splitting crack extending above the tendon and along the length direction of the specimen as illustrated in Fig. 4.7. This splitting crack was not present before exposure testing began.

In addition, during exposure testing, progressive discoloration of the mortar anchorage plug was noted in most of the unbonded specimens as shown in Fig. 4.8. The mortar used for the plug was a rich gray color at the start of exposure testing, indicative of a fairly rich cement content. However, after prolonged exposure, some cement appeared to be leached out of the mortar by the action of the salt water percolating through the specimen. Areas of the anchor plug turned golden-brown in color probably reflecting the coloration of the sand which remained in the mortar. The leaching of the cement out of the mortar plug was not necessarily a sign of corrosion distress, but did indicate the aggressive nature of the salt water.

4.4 Post-Mortem Examination

After exposure testing of the specimens was discontinued because of time constraints, a post-mortem examination of each of the specimens was conducted. The examination included chloride content determination and visual inspection of the reinforcement. Results from the post-mortem examination are presented in this section.

4.4.1 Chloride Content Determination. The chloride ion (Cl^-) content in the concrete samples taken from the durability specimens was determined by the Mineral Studies Laboratory (MSL) of the Bureau of Economic Geology of The University of Texas at Austin. MSL used a colorimetric procedure, which is summarized in Appendix B, for determination of Cl^- in the concrete samples. Both water soluble and acid soluble chloride contents were determined using the

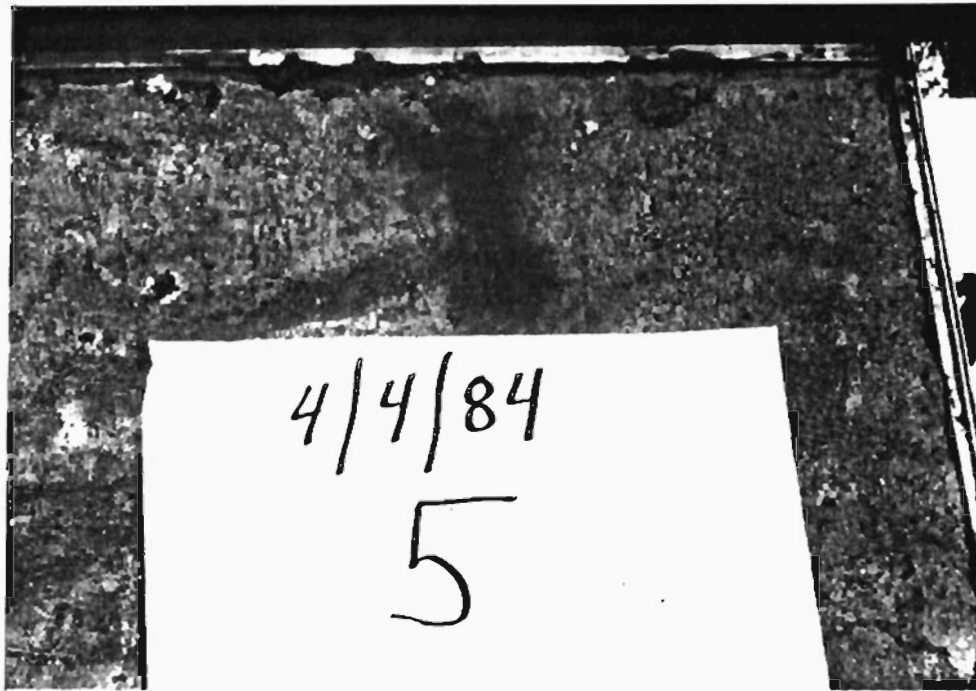
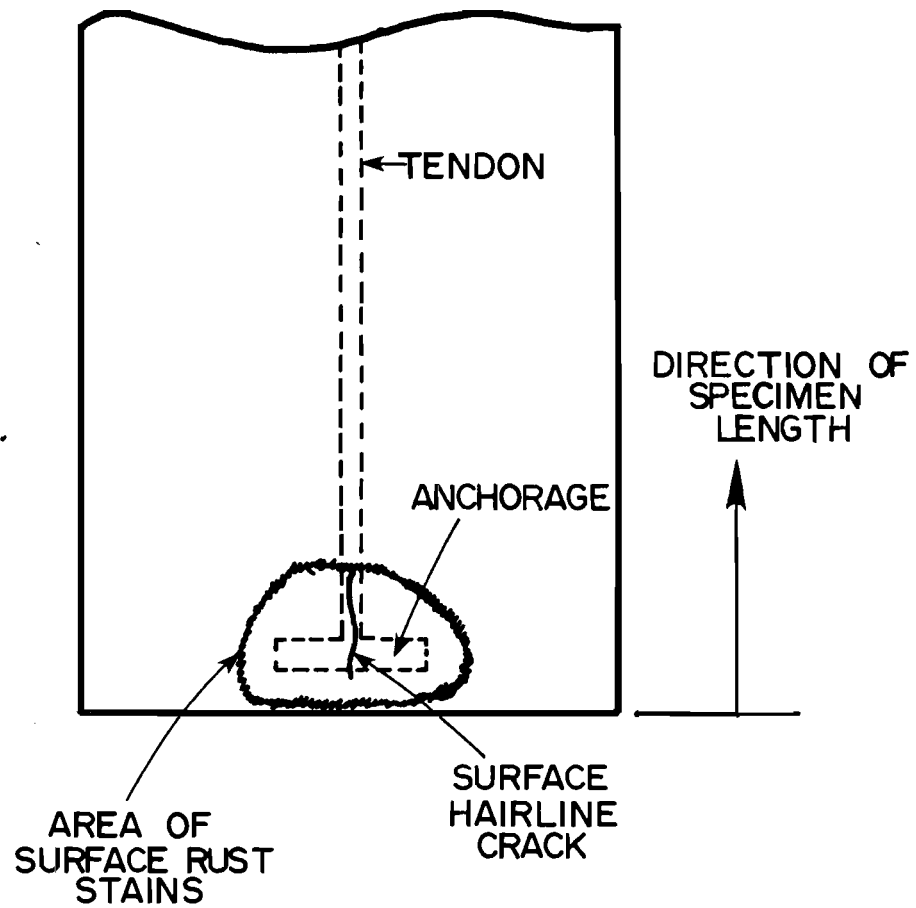


Fig. 4.6 Rust staining on specimen surface above anchorage



PLAN VIEW OF SPECIMEN END

Fig. 4.7 Surface rust staining and hairline crack along direction of specimen length



Fig. 4.8 ° Discoloration of mortar anchorage plug in some areas after prolonged exposure

colorimetric procedure. In addition, approximately 10% of the concrete samples were analyzed for water soluble chlorides using the more classical titration procedure as recommended by FHWA [42].

An acid soluble test is generally considered to represent the total chloride ion (Cl^-) content in concrete. A water soluble test measures the chloride ion (Cl^-) which is extractable in water, and probably better represents the actual amount of chloride available for corrosion. Generally, Cl^- content measured by a water soluble test will be between 70 to 80% of that measured by an acid soluble test. Both water and acid soluble tests are currently in wide use.

The results from the Cl^- analysis are presented in Table 4.1. The first number in the sample identification represents the specimen number. Appendix A shows the core locations from which the concrete samples were taken. "A" represents a sample taken from the core at the crack zone of a specimen, and "B" represents a sample taken from the core at the uncracked end of a specimen. The next number in the sample identification represents the approximate depth below the top surface of the specimen in inches at which the sample was taken. A "P" at the end of the sample identification denotes that the sample is part of a profile in which samples were taken at various depths in order to determine the Cl^- ion penetration with depth. The sample identifications which begin with "R" represent concrete samples taken from concrete cylinders cast from each of six different batches used to construct the durability specimens. The Cl^- contents measured in these samples represent the chlorides in the constituent materials before exposure testing began. The Cl^- levels are reported in both pounds of Cl^- per cubic yard of concrete and weight of Cl^- to weight of cement in percent.

4.4.2 Visual Inspection of Reinforcement. The conventional reinforcement, prestressing strand, and posttensioning duct were removed from the concrete section cut at the crack zones of the specimens and visually inspected. In addition, all of the top conventional reinforcement, prestressing tendons, and duct over the full length of the specimen as well as the anchorages for Specimens 1, 2, 3, 4, 9, 10, 11, 12, 13, 16, and 22 were removed and examined. The removal of all the top reinforcement in these specimens clearly indicated that corrosion was occurring only on the reinforcement in the immediate regions of the cracks. For example, the uncoated bars shown in Fig. 4.9, which show signs of heavy corrosion, were removed from specimens at crack locations. Consequently, it was unnecessary to remove the full length of the reinforcement from the other specimens.

TABLE 4.1 Chloride Ion (Cl⁻) Content in Concrete Samples Taken from Durability Specimens

Sample Identi- fication	Water Soluble Colorimetric		Acid Soluble Colorimetric		Water Soluble Titration	
	Lbs Cl ⁻	Wt Cl ⁻	Lbs Cl ⁻	Wt Cl ⁻	Lbs Cl ⁻	Wt Cl ⁻
	Yd ³	%	Yd ³	%	Yd ³	%
	Con	Wt Cem	Con	Wt Cem	Con	Wt Cem
1A2.0	12.2	1.99	13.7	2.25	11.8	1.93
1B1.OP	2.8	0.46	4.2	0.69		
1B2.OP	0.6	0.10	0.8	0.13		
1B4.OP	0.2	0.03	<0.2	<0.03		
1B6.OP	0.4	0.06	0.4	0.06		
2A2.0	19.8	3.24	21.9	3.59		
2B2.0	2.3	0.37	2.8	0.46		
3A3.0	20.7	3.39	21.8	3.57		
3B3.0	0.5	0.08	0.6	0.10		
4A3.0	13.7	2.25	14.7	2.41	12.9	2.11
4B3.0	0.5	0.09	0.5	0.08		
	(0.5)	(0.08)	(0.4)	(0.07)		
5A2.0	11.0	1.80	12.7	2.08		
5B2.0	0.5	0.09	0.6	0.10		
6A2.0	14.8	2.42	16.4	2.68		
6B2.0	1.7	0.28	2.2	0.37		
7A3.0	5.5	0.90	6.7	1.09		
7B3.0	0.5	0.09	0.7	0.11		
8A3.0	6.4	1.04	7.3	1.20		
8B3.0	0.6	0.10	0.6	0.10		
9A2.0	2.8	0.46	3.3	0.55		
9B1.0	23.8	3.89	23.4	3.82	23.3	3.81
9B2.OP	1.8	0.30	1.7	0.28		
9B3.OP	0.9	0.15	0.9	0.14		
9B4.OP	0.5	0.08	0.9	0.15		
9B6.OP	1.2	0.20	1.8	0.30		
10A2.0	3.5	0.57	4.8	0.78		
10B2.0	1.8	0.30	2.4	0.39		
11A3.0	19.0	3.12	18.5	3.02		
11B3.0	0.9	0.15	1.0	0.16		
	(0.7)	(0.11)	(0.7)	(0.12)		
12A3.0	7.7	1.25	8.6	1.41		
12B3.0	0.7	0.11	0.7	0.12	1.2	0.20

Parentheses indicate duplicate samples.

TABLE 4.1 Chloride Ion (Cl^-) Content in Concrete Samples
Taken from Durability Specimens (continued)

Sample Identi- fication	Water Soluble Colorimetric		Acid Soluble Colorimetric		Water Soluble Titration	
	Lbs Cl^-	Wt Cl^-	Lbs Cl^-	Wt Cl^-	Lbs Cl^-	Wt Cl^-
	Yd ³ Con	% Wt Cem	Yd ³ Con	% Wt Cem	Yd ³ Con	% Wt Cem
13A2.0	24.8	4.06	27.7	4.53		
13B1.0P	19.4	3.18	19.8	3.24		
13B2.0P	2.6	0.43	3.6	0.58	3.7	0.61
13B3.0P	0.7	0.11	1.4	0.23		
13B4.0P	0.4	0.07	0.6	0.10		
13B6.0P	1.5	0.24	2.0	0.33		
14A1.5	23.5	3.84	26.4	4.32		
14A3.0	16.7	2.73	18.6	3.05		
14B1.5	13.2	2.15	13.3	2.18		
14B3.0	0.4	0.07	0.5	0.08		
	(0.4)	(0.06)				
15A3.0	11.6	1.90	14.2	2.33	10.6	1.73
15B3.0	0.5	0.09	0.6	0.10		
16A3.0	10.4	1.70	11.3	1.84		
16B3.0	0.5	0.08	0.7	0.11		
17A2.0	14.9	2.44	14.7	2.41		
17B2.0	1.2	0.20	1.4	0.23		
18A2.0	10.6	1.74	12.6	2.06		
	(10.5)	(1.72)	(12.9)	(2.11)		
18B2.0	0.5	0.08	0.6	0.10		
19A3.0	21.2	3.47	23.2	3.79		
19B3.0	2.5	0.40	3.4	0.56		
	(2.6)	(0.42)				
20A3.0	22.6	3.69	24.7	4.05		
20B3.0	0.7	0.11	0.8	0.13		
21A2.0	5.4	0.88	6.7	1.09		
21B1.0P	13.5	2.22	15.1	2.47		
21B2.0P	1.3	0.21	1.4	0.23		
21B3.0P	0.4	0.06	0.5	0.08	0.7	0.12
21B4.0P	0.4	0.06	0.4	0.06		
	(0.5)	(0.08)	(0.5)	(0.08)		
21B6.0P	0.5	0.08	0.5	0.08		

Parentheses indicate duplicate samples.

TABLE 4.1 Chloride Ion (Cl^-) Content in Concrete Samples
Taken from Durability Specimens (continued)

Sample Identi- fication	Water Soluble Colorimetric		Acid Soluble Colorimetric		Water Soluble Titration	
	Lbs Cl^-	Wt Cl^-	Lbs Cl^-	Wt Cl^-	Lbs Cl^-	Wt Cl^-
	$\frac{\text{Yd}^3}{\text{Con}}$	$\frac{\%}{\text{Wt Cem}}$	$\frac{\text{Yd}^3}{\text{Con}}$	$\frac{\%}{\text{Wt Cem}}$	$\frac{\text{Yd}^3}{\text{Con}}$	$\frac{\%}{\text{Wt Cem}}$
22A2.0	4.0	0.66	4.4	0.71		
	(3.7)	(0.61)	(4.8)	(0.78)		
22B2.0	0.5	0.08	0.5	0.09		
23A3.0	0.2	0.04	0.4	0.07		
	(0.2)	(0.03)				
23B3.0	<0.2	<0.03	0.4	0.06		
	(0.4)	(0.05)	(0.5)	(0.08)		
24A2.0	5.4	0.88	6.9	1.13	6.4	1.05
24B2.0	2.2	0.35	2.4	0.39		
R1	0.7	0.11	0.7	0.11	1.4	0.22
R2	<0.2	<0.03	0.2	0.04		
	(<0.2)	(<0.03)	(<0.2)	(<0.03)		
R3	<0.2	<0.03	0.4	0.07		
	(<0.2)	(<0.03)	(0.4)	(0.06)		
R4	<0.2	<0.03	0.4	0.06		
R5	0.3	0.05	0.7	0.11	0.7	0.12
R6	0.4	0.06	0.4	0.06		

Parentheses indicate duplicate samples.

Figures 4.9a and 4.9b are indicative of the heavy corrosion observed on some of the uncoated nonprestressed reinforcement in the specimens. It is interesting to note that in these photographs the corrosion was not confined to a small area of just 3 bar diameters at the crack. This is the distance cited for localized corrosion [18]. Instead, the corrosion had obviously already spread along the bar since the corrosion extended 6 to 10 bar diameters in many cases.

In general, the epoxy-coated reinforcement examined showed very little sign of corrosion. In a few cases, such as illustrated in Fig. 4.10, it appeared that the epoxy-coating had chipped off the bar deformations at crack regions which resulted in very light surface corrosion at these locations.

Inspection of the galvanized duct in the grouted specimens revealed signs of surface corrosion as shown in Fig. 4.11. In general, the corrosion of the duct represented attack of the anodic zinc coating and not of the underlying steel.

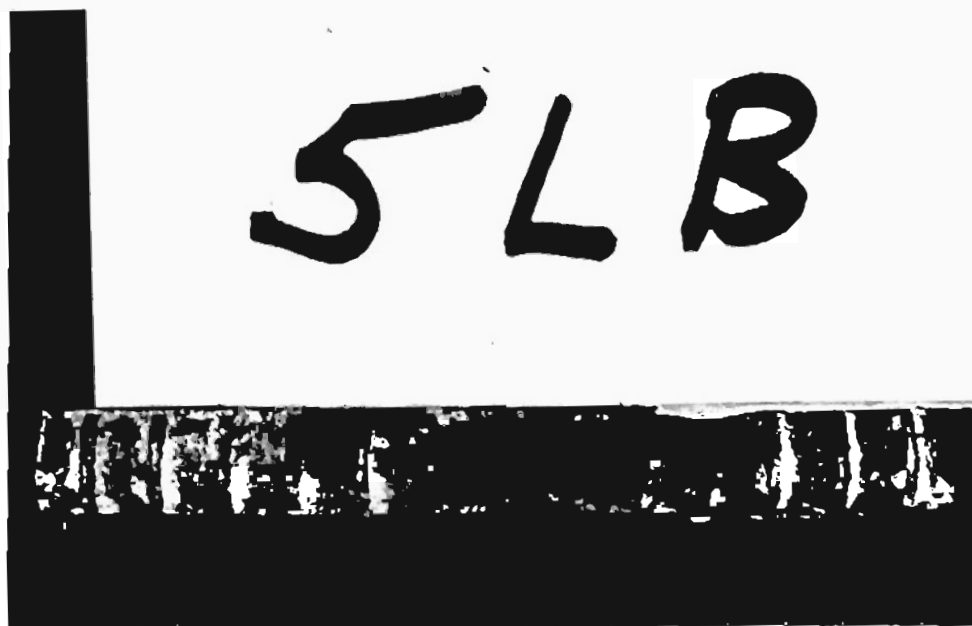
The prestressing tendons in all specimens showed little evidence of corrosion in the length between the anchorages. In Specimen 8, the prestressing tendon showed signs of initial stages of surface corrosion at a location where the plastic duct had been purposely slit, as shown in Fig. 4.12. However, the prestressing tendon extensions outside the anchorage on the loaded end of the unbonded specimens, which were protected only by the anchorage mortar plug, showed signs of heavy corrosion as seen in Fig. 4.13a.

Most of the anchorages on the loaded end of the unbonded specimens, whether the specimen was prestressed or nonprestressed, showed evidence of heavy corrosion as seen in Figs. 4.13a and 4.13b. In general, the heavy corrosion was observed for the outer areas of the anchorage casting; however, there was also some corrosion of the anchorage jaws and inner locations of the anchorage casting where the jaws bear against the casting. At these inner locations, the corrosion could be considered to be crevice corrosion, since this represents an area of geometric constraint.

It was necessary to develop a rating system in order to objectively evaluate by means of visual inspection the corrosion performance of the components removed from the specimens. The rating system which was developed is given in Table 4.2. It was important to include the length over which corrosion was occurring in the evaluation system in order to provide an indication of the pernicious spreading effect which is associated with more advanced stages of corrosion. For example, corrosion occurring within a short length, such as less than 1/2 in., implies that the corrosion is occurring very locally, whereas a longer length, such as greater than 2 in.,



a)



b)

Fig. 4.9 Typical heavy corrosion of uncoated nonprestressed reinforcement in the region near cracks



Fig. 4.10 Very light surface corrosion on epoxy-coated reinforcing bar



Fig. 4.11 Surface corrosion of zinc coating on galvanized duct of grouted specimens

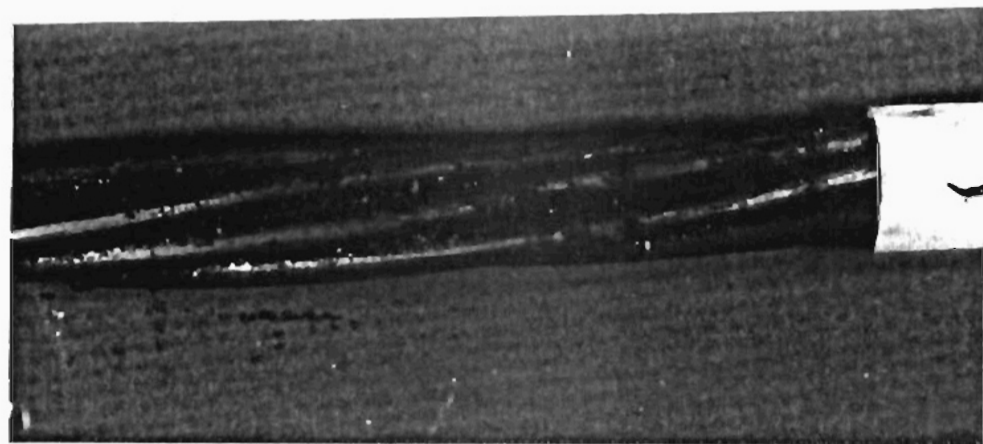
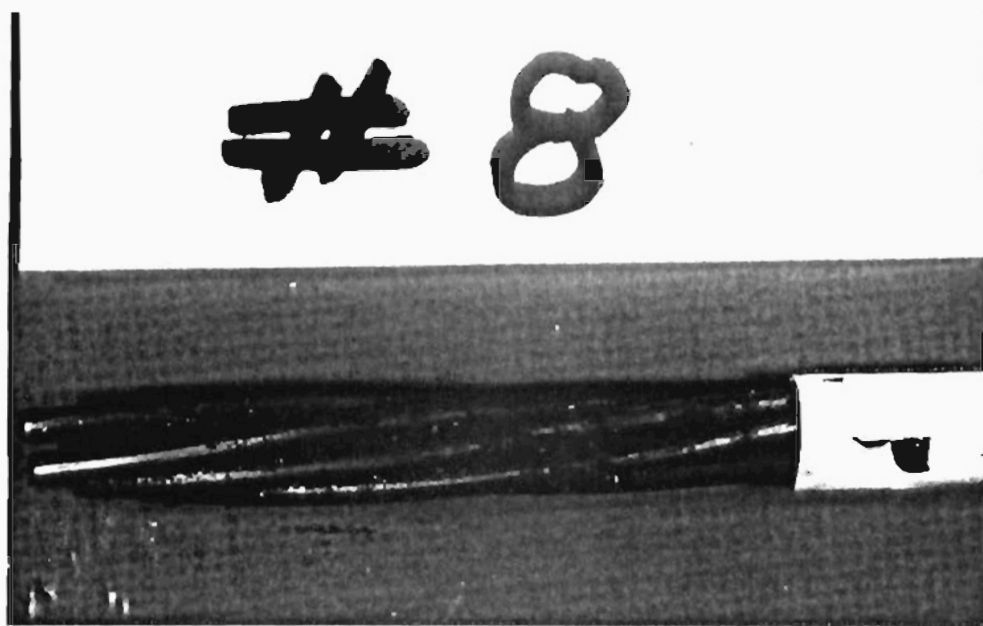
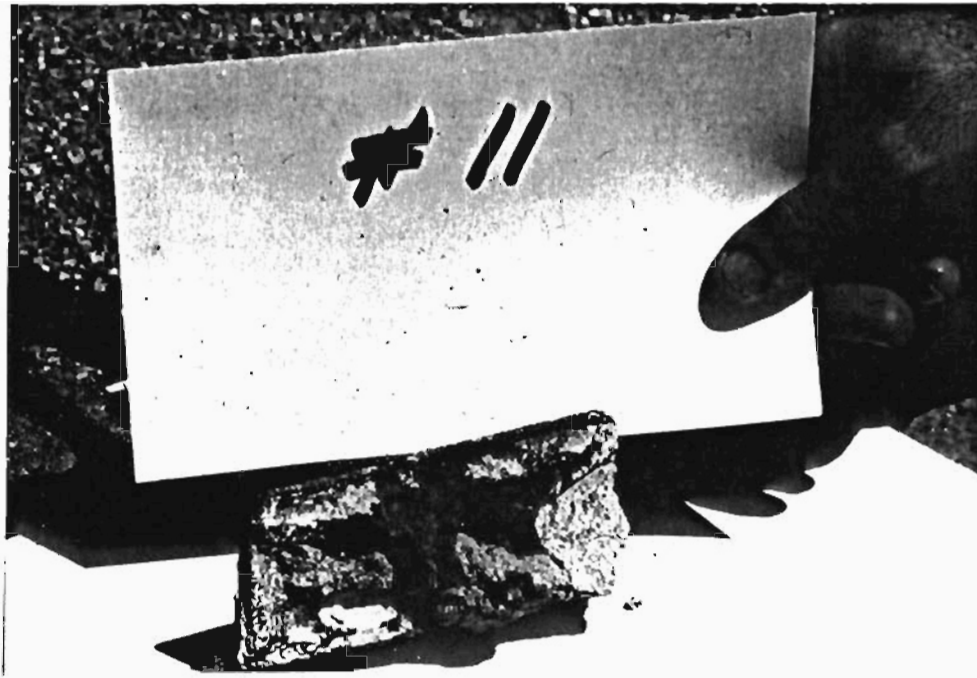
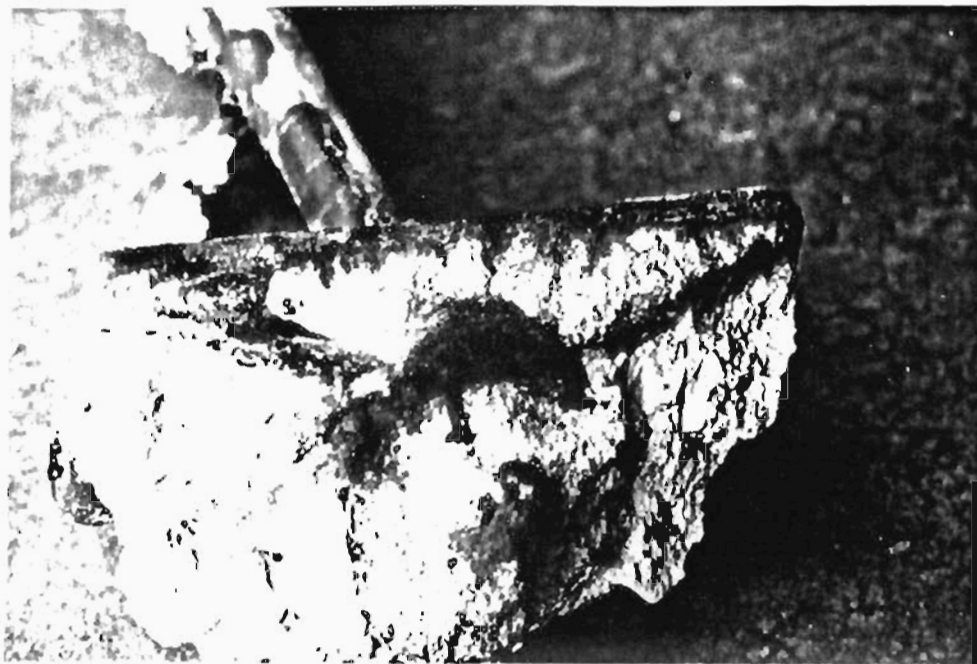


Fig. 4.12 Very light surface corrosion on unbonded tendon removed from Specimen 8



a)



b)

Fig. 4.13 Corrosion of loaded end anchorage of unbonded specimens

TABLE 4.2 Evaluation System for the Visual Inspection of the Components Removed from the Durability Specimens

Code	Meaning	Evaluation
NC	No corrosion	No evidence of corrosion
D	Discoloration	No evidence of corrosion, but some discoloration from original color
VL	Very light corrosion	Surface corrosion less than 1/4 in. in length at a location; no pitting.
L	Light corrosion	Surface corrosion greater than 1/4 in. in length at a location but less than 1/2 in. in length; no pitting.
M	Medium corrosion	Surface corrosion greater than 1/2 in. in length at a location but less than 1 in. in length, and/or shallow pits in the early stages of formation.
H	Heavy corrosion	Surface corrosion greater than 1 in. in length, but less than 2 in. in length at a location and/or presence of pitting.
VH	Very heavy corrosion	Surface corrosion greater than 2 in. in length at a location and/or presence of deep pitting.

suggests advanced stages of corrosion. The results of the inspection and evaluation of each component are presented in Table 4.3. The codes used to describe the components in Table 4.3 are described in Fig. 4.14.

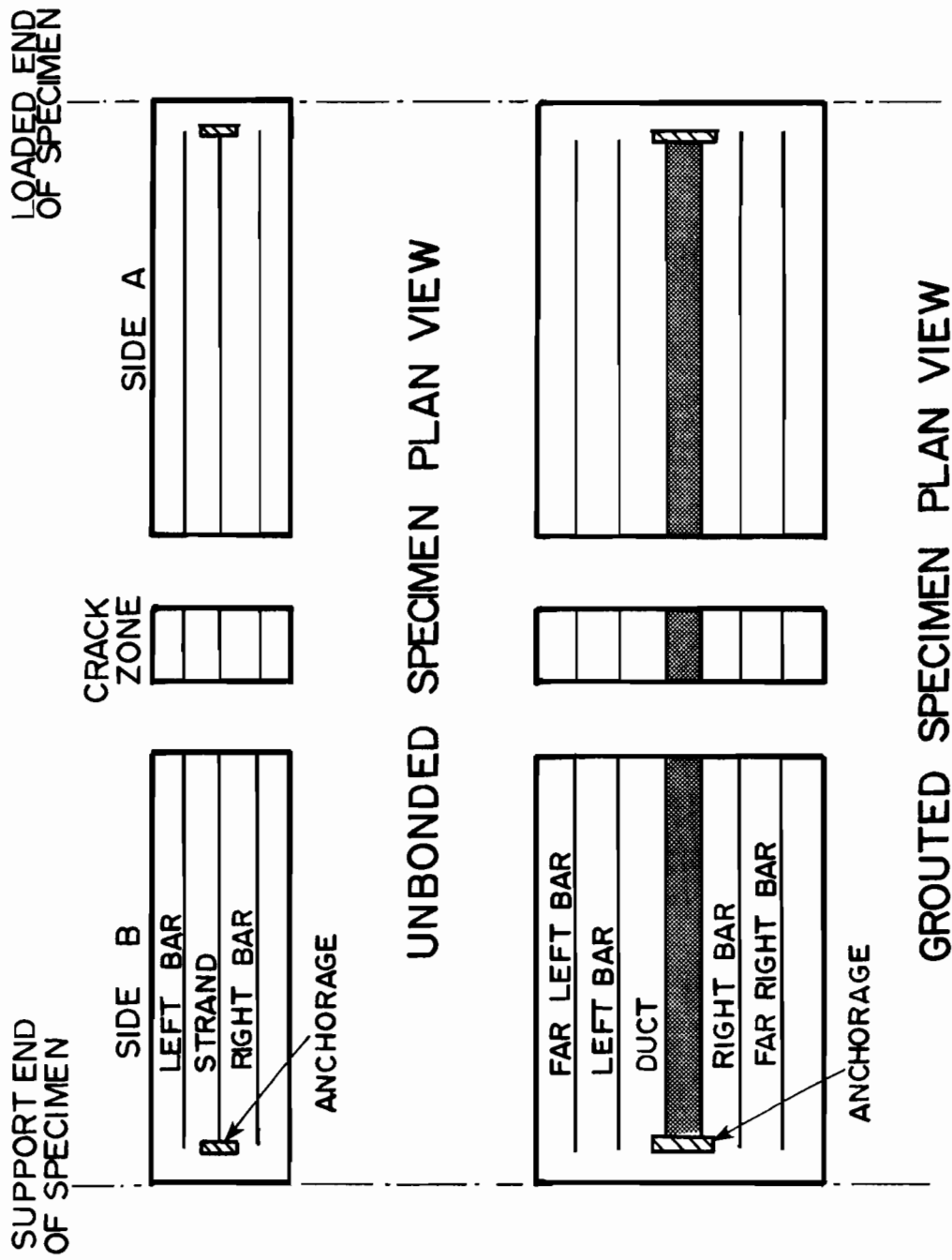


Fig. 4.14 Description of component codes used in Table 4.3

TABLE 4.3 Results of the Evaluation of the Components Removed from the Durability Specimens

Specimen No., Description	Component*	Region*	Evaluation**	Remarks
1 Unbonded prestressing system Nonprestressed specimen ≈ 0.015 surface width crack under load 2 in. concrete cover Uncoated nonprestressed reinforcement	Right bar	Side A	L and D	At end next to crack zone
	Right bar	Crack zone	VH	
	Right bar	Side B	D	
	Anchorage	Side A	H	
	Strand	Side A	NC	
	Strand	Crack zone	NC	
	Strand	Side B	NC	
	Anchorage	Side B	NC	
	Left bar	Side A	D	
	Left bar	Crack zone	VH	
Left bar	Side B	D		

* See Fig. 4.14

** See Table 4.2

TABLE 4.3 Results of the Evaluation of the Components Removed from the Durability Specimens
(continued)

Specimen No., Description	Component*	Region*	Evaluation**	Remarks
2		Side A	NC	
Unbonded prestressing system	Right bar	Crack zone	NC	
Nonprestressed specimen	Right bar	Side B	D	
≈ 0.015 in. surface crack width under load	Anchorage	Side A	H	
2 in. concrete cover	Strand	Side A	NC	
Epoxy-coated nonprestressed reinforcement	Strand	Crack zone	NC	
	Strand	Side B	NC	
	Anchorage	Side B	NC	
	Left bar	Side A	NC	
	Left bar	Crack zone	L	
	Left bar	Side B	NC	

* See Fig. 4.14

** See Table 4.2

TABLE 4.3 Results of the Evaluation of the Components Removed from the Durability Specimens
(continued)

Specimen No., Description	Component*	Region*	Evaluation**	Remarks
3 Unbonded prestressing system Nonprestressed specimen ≈ 0.015 in. surface crack width under load 3 in. concrete cover Uncoated nonprestressed reinforcement	Right bar	Side A	NC	
	Right bar	Crack zone	VH	
	Right bar	Side B	L and D	At end next to crack zone
	Anchorage	Side A	M	
	Strand	Side A	NC	
	Strand	Crack zone	NC	
	Strand	Side B	NC	
	Anchorage	Side B	NC	
	Right bar	Side A	NC	
	Right bar	Crack zone	VH	
Right bar	Side B	D		

* See Fig. 4.14

** See Table 4.2

TABLE 4.3 Results of the Evaluation of the Components Removed from the Durability Specimens
(continued)

Specimen No., Description	Component*	Region*	Evaluation**	Remarks
4	Right bar	Side A	NC	
Unbonded prestressing system	Right bar	Crack zone	L	
Nonprestressed specimen	Right bar	Side B	NC	
± 0.015 in. surface crack width under load	Strand	Side A	NC	
3 in. concrete cover	Strand	Crack zone	NC	
Epoxy-coated nonprestressed reinforcement	Strand	Side B	NC	
	Anchorage	Side B	NC	
	Left bar	Side A	NC	
	Left bar	Crack zone	NC	
	Left bar	Side B	NC	

* See Fig. 4.14

** See Table 4.2

TABLE 4.3 Results of the Evaluation of the Components Removed from the Durability Specimens
(continued)

Specimen No., Description	Component*	Region*	Evaluation**	Remarks
5	Right Bar	Crack zone	VH	
Unbonded prestressing system	Strand	Crack zone	NC	
Prestressed specimen	Left bar	Crack zone	VH	
≈ 0.015 in. surface crack width under load				
2 in. concrete cover				
Uncoated nonprestressed reinforcement				
6	Right bar	Crack zone	VL	
Unbonded prestressing system	Strand	Crack zone	NC	
Prestressed specimen	Left bar	Crack zone	NC	
≈ 0.015 in. surface crack width under load				
2 in. concrete cover				
Epoxy-coated nonprestressed reinforcement				

* See Fig. 4.14

** See Table 4.2

TABLE 4.3 Results of the Evaluation of the Components Removed from the Durability Specimens
(continued)

Specimen No., Description	Component*	Region*	Evaluation**	Remarks
7 Unbonded prestressing system Prestressed specimen ≈ 0.015 in. surface crack width under load 3 in. concrete cover Uncoated nonprestressed reinforcement	Right bar Strand Left bar	Crack zone Crack zone Crack zone	VH NC H	
8 Unbonded prestressing system Prestressed specimen ≈ 0.015 in. surface crack width under load 3 in. concrete cover Epoxy-coated nonprestressed reinforcement	Right bar Strand Left bar	Crack zone Crack zone Crack zone	NC M NC	

* See Fig. 4.14

** See Table 4.2

TABLE 4.3 Results of the Evaluation of the Components Removed from the Durability Specimens
(continued)

Specimen No., Description	Component*	Region*	Evaluation**	Remarks
9	Right bar	Side A	D and VL	
Unbonded prestressing system	Right bar	Crack zone	NC	
Prestressed specimen	Right bar	Side B	D	
≈ 0.002 in. surface crack width under load	Anchorage	Side A	VH	
2 in. concrete cover	Strand	Side A	NC	
Uncoated nonprestressed reinforcement	Strand	Crack zone	NC	
	Strand	Side B	NC	
	Anchorage	Side B	VL	
	Left bar	Side A	D	
	Left bar	Crack zone	NC	
	Left bar	Side B	D	

* See Fig. 4.14

** See Table 4.2

TABLE 4.3 Results of the Evaluation of the Components Removed from the Durability Specimens
(continued)

Specimen No., Description	Component*	Region*	Evaluation**	Remarks
10	Right bar	Side A	NC	
Unbonded prestressing system Prestressed specimen ≈ 0.002 in. surface crack width under load 2 in. concrete cover Epoxy-coated nonprestressed reinforcement	Right bar	Crack zone	NC	
	Right bar	Side B	NC	
	Anchorage	Side A	VH	
	Strand	Side A	NC	
	Strand	Crack zone	NC	
	Strand	Side B	NC	
	Anchorage	Side B	VL	
	Left bar	Side A	NC	
	Left bar	Crack zone	NC	
Left bar	Side B	NC		

* See Fig. 4.14

** See Table 4.2

TABLE 4.3 Results of the Evaluation of the Components Removed from the Durability Specimens
(continued)

Specimen No., Description	Component*	Region*	Evaluation**	Remarks
11	Right bar	Side A	D	
Unbonded prestressing system	Right bar	Crack zone	D	
Prestressed specimen	Right bar	Side B	D	
≈ 0.002 in. surface crack width under load	Anchorage	Side A	H	
3 in. concrete cover	Strand	Side A	NC	
Uncoated nonprestressed reinforcement	Strand	Crack zone	NC	
	Strand	Side B	NC	
	Anchorage	Side B	L and D	
	Left bar	Side A	NC	
	Left bar	Crack zone	M	
	Left bar	Side B	NC	

* See Fig. 4.14

** See Table 4.2

TABLE 4 3 Results of the Evaluation of the Components Removed from the Durability Specimens
(continued)

Specimen No., Description	Component*	Region*	Evaluation**	Remarks
12 Unbonded prestressing system Prestressed specimen ≈ 0.002 in. surface crack width under load 3 in. concrete cover Epoxy-coated nonprestressed reinforcement	Right bar	Side A	NC	
	Right bar	Crack zone	NC	
	Right bar	Side B	NC	
	Anchorage	Side A	H	
	Strand	Side A	NC	
	Strand	Crack zone	NC	
	Strand	Side B	NC	
	Anchorage	Side B	L	
	Left bar	Side A	NC	
	Left bar	Crack zone	NC	
Left bar	Side B	NC		

* See Fig. 4.14

** See Table 4.2

TABLE 4.3 Results of the Evaluation of the Components Removed from the Durability Specimens
(continued)

Specimen No., Description	Component*	Region*	Evaluation**	Remarks
13	Far right bar	Side A	NC	
Grouted prestressing system	Far right bar	Crack zone	VH	
Nonprestressed specimen	Far right bar	Side B	D	
≈ 0.015 in. surface crack width under load	Right bar	Side A	L	At end of bar next to crack zone
2 in. concrete cover	Right bar	Crack zone	VH	
Uncoated nonprestressed reinforcement	Right bar	Side B	NC	
	Anchorage	Side A	M	Strand exten- sions corroding

* See Fig. 4.14

** See Table 4.2

TABLE 4.3 Results of the Evaluation of the Components Removed from the Durability Specimens
(continued)

Specimen No., Description	Component*	Region*	Evaluation**	Remarks
13	Duct	Side A	D	
	Duct	Crack zone	D	
	Duct	Side B	D	
	Anchorage	Side B	NC	
	Left bar	Side A	NC	
	Left bar	Crack zone	VH	
	Left bar	Side B	L	At end of bar next to crack zone
	Far left bar	Side A	D	
	Far left bar	Crack zone	VH	
	Far left bar	Side B	H	At end of bar next to crack zone

* See Fig. 4.14

** See Table 4.2

TABLE 4.3 Results of the Evaluation of the Components Removed from the Durability Specimens
(continued)

Specimen No., Description	Component*	Region*	Evaluation**	Remarks
14 Grouted prestressing system Nonprestressed specimen ≈ 0.015 in. surface crack width under load 2 in. concrete cover Epoxy-coated nonprestressed reinforcement	Far right bar	Crack zone	VL	At end of bar next to crack
	Right bar	Crack zone	NC	
	Duct	Crack zone	D	
	Left bar	Crack zone	NC	
	Far left bar	Crack zone	NC	

* See Fig. 4.14

** See Table 4.2

TABLE 4.3 Results of the Evaluation of the Components Removed from the Durability Specimens
(continued)

Specimen No., Description	Component*	Region*	Evaluation**	Remarks
15 Grouted prestressing system Nonprestressed specimen ≈ 0.015 in. surface crack width under load 3 in. concrete cover Uncoated nonprestressed reinforcement	Far right bar	Crack zone	VH	
	Right bar	Crack zone	H	
	Duct	Crack zone	D	
	Left bar	Crack zone	NC	
	Far left bar	Crack zone	L	
16 Grouted prestressing system Nonprestressed specimen ≈ 0.015 in. surface crack width under load 3 in. concrete cover Epoxy-coated nonprestressed reinforcement	Far right bar	Side A	NC	
	Far right bar	Crack zone	NC	
	Far right bar	Side B	NC	
	Right bar	Side A	NC	
	Right bar	Crack zone	NC	

* See Fig. 4.14

** See Table 4.2

TABLE 4.3 Results of the Evaluation of the Components Removed from the Durability Specimens
(continued)

Specimen No., Description	Component*	Region*	Evaluation**	Remarks
16	Right bar	Side B	NC	
	Anchorage	Side A	NC	
	Duct	Side A	L	
	Duct	Crack zone	M	
	Duct	Side B	M	
	Anchorage	Side B	NC	
	Left bar	Side A	NC	
	Left bar	Crack zone	NC	
	Left bar	Side B	NC	
	Far left bar	Side A	NC	

* See Fig. 4.14

** See Table 4.2

TABLE 4.3 Results of the Evaluation of the Components Removed from the Durability Specimens
(continued)

Specimen No., Description	Component*	Region*	Evaluation**	Remarks
16	Far left bar	Crack zone	NC	
	Far left bar	Side B	NC	
17 Grouted prestressing system Prestressed specimen ≈ 0.015 in. surface crack width under load 2 in. concrete cover Uncoated nonprestressed reinforcement	Far right bar	Crack zone	VH	
	Right bar	Crack zone	VH	
	Duct	Crack zone	D	
	Left bar	Crack zone	NC	
	Far left bar	Crack zone	NC	

* See Fig. 4.14

** See Table 4.2

TABLE 4.3 Results of the Evaluation of the Components Removed from the Durability Specimens
(continued)

Specimen No., Description	Component*	Region*	Evaluation**	Remarks	
18 Grouted prestressing system Prestressed specimen ≈ 0.015 in. surface crack width under load 2 in. concrete cover Epoxy-coated nonprestressed reinforcement	Far right bar	Crack zone	NC		
	Right bar	Crack zone	NC		
	Duct	Crack zone	M		
	Left bar	Crack zone	NC		
	Far left bar	Crack zone	NC		
	Far right bar	Crack zone	VH		
19 Grouted prestressing system Prestressed specimen ≈ 0.015 in. surface crack width under load 3 in. concrete cover Uncoated nonprestressed reinforcement	Right bar	Crack zone	VH		
	Duct	Crack zone	VH	Top and bottom surfaces	
	Left bar	Crack zone	VH		
	Far left bar	Crack zone	VH		

* See Fig. 4.14

** See Table 4.2

TABLE 4.3 Results of the Evaluation of the Components Removed from the Durability Specimens
(continued)

Specimen No., Description	Component*	Region*	Evaluation**	Remarks
20 Grouted prestressing system Prestressed specimen ≈ 0.015 in. surface crack width under load 3 in. concrete cover Epoxy-coated nonprestressed reinforcement	Far right bar	Crack zone	NC	
	Right bar	Crack zone	M	
	Duct	Crack zone	VH	Top and bottom surfaces
	Left bar	Crack zone	NC	
	Far left bar	Crack zone	NC	
	Far right bar	Crack zone	NC	
21 Grouted prestressing system Prestressed specimen ≈ 0.002 in. surface crack width under load 2 in. concrete cover Uncoated nonprestressed reinforcement	Right bar	Crack zone	NC	
	Duct	Crack zone	D	
	Left bar	Crack zone	NC	
	Far left bar	Crack zone	NC	
	Far right bar	Crack zone	NC	
	Right bar	Crack zone	NC	

* See Fig. 4.14

** See Table 4.2

TABLE 4.3 Results of the Evaluation of the Components Removed from the Durability Specimens
(continued)

Specimen No., Description	Component*	Region*	Evaluation**	Remarks
22 Grouted prestressing system Prestressed specimen ≈ 0.002 in. surface crack width under load 2 in. concrete cover Epoxy-coated nonprestressed reinforcement	Far right bar	Side A	NC	
	Far right bar	Crack zone	NC	
	Far right bar	Side B	NC	
	Right bar	Side A	NC	
	Right bar	Crack zone	NC	
	Right bar	Side B	NC	
	Anchorage	Side A	NC	
	Duct	Side A	L	
	Duct	Crack zone	VL	
	Duct	Side B	NC	

* See Fig. 4.14

** See Table 4.2

TABLE 4.3 Results of the Evaluation of the Components Removed from the Durability Specimens
(continued)

Specimen No., Description	Component*	Region*	Evaluation**	Remarks
22	Anchorage	Side B	NC	
	Left bar	Side A	NC	
	Left bar	Crack zone	NC	
	Left bar	Side B	NC	
	Far left bar	Side A	NC	
	Far left bar	Crack zone	NC	
	Far left bar	Side B	NC	

* See Fig. 4.14

** See Table 4.2

TABLE 4.3 Results of the Evaluation of the Components Removed from the Durability Specimens
(continued)

Specimen No.	Component*	Region*	Evaluation**	Remarks
23	Far right bar	Crack zone	NC	
	Right bar	Crack zone	NC	
	Duct	Crack zone	NC	
	Left bar	Crack zone	NC	
	Far left bar	Crack zone	NC	
24	Far right bar	Crack zone	NC	
	Right bar	Crack zone	NC	
	Duct	Crack zone	NC	
	Left bar	Crack zone	NC	
	Far left bar	Crack zone	NC	

* See Fig. 4.14

** See Table 4.2

CHAPTER 5

EVALUATION OF DURABILITY STUDY TEST RESULTS

5.1 Introduction

This chapter presents an evaluation of the test results from the durability study, including a comparison of the effectiveness of the principal test variables in reducing chloride-induced corrosion of steel in concrete.

5.2 Initial Cracking

Cracking occurs in the tension zone of reinforced concrete members subjected to flexure or axial tension when the induced tensile stresses exceed the tensile strength of the concrete. In general, the tensile strength of concrete subjected to flexure is assumed to be equal to $7.5 \sqrt{f'_c}$, where f'_c is in psi. For the case of the durability specimens in this study, the applied loading produced a maximum negative moment at the location of the interior support, resulting in randomly distributed cracking near the interior support location as seen in the crack patterns in Appendix A. In many test specimens, two flexural cracks were observed in the support region at a spacing of approximately 8 in. It is believed that the cracks which developed in the specimens were representative of the type and distribution of flexural cracks which would occur in bridge decks if some bonded nonprestressed reinforcement is present.

One of the mechanisms by which it is suggested that deck prestressing would improve the durability of bridge decks was clearly illustrated upon specimen loading. The applied load to cause first flexural cracking was much larger for the prestressed specimens than for the nonprestressed specimens as shown in Fig. 5.1. This clearly shows that with proper design at service load levels, prestressed concrete is less likely to have cracks than conventional reinforced concrete.

The crack width data presented in Fig. 5.1 illustrate some additional advantages of prestressed concrete with regard to improved durability. Not only did it originally take a larger load to induce first cracking in the prestressed specimens, but once cracking occurred, a much larger load is required to produce a given crack width in the prestressed specimens. Or alternatively, once cracking has occurred, the crack width for a given load level is much smaller for the prestressed specimens than for the nonprestressed specimens.

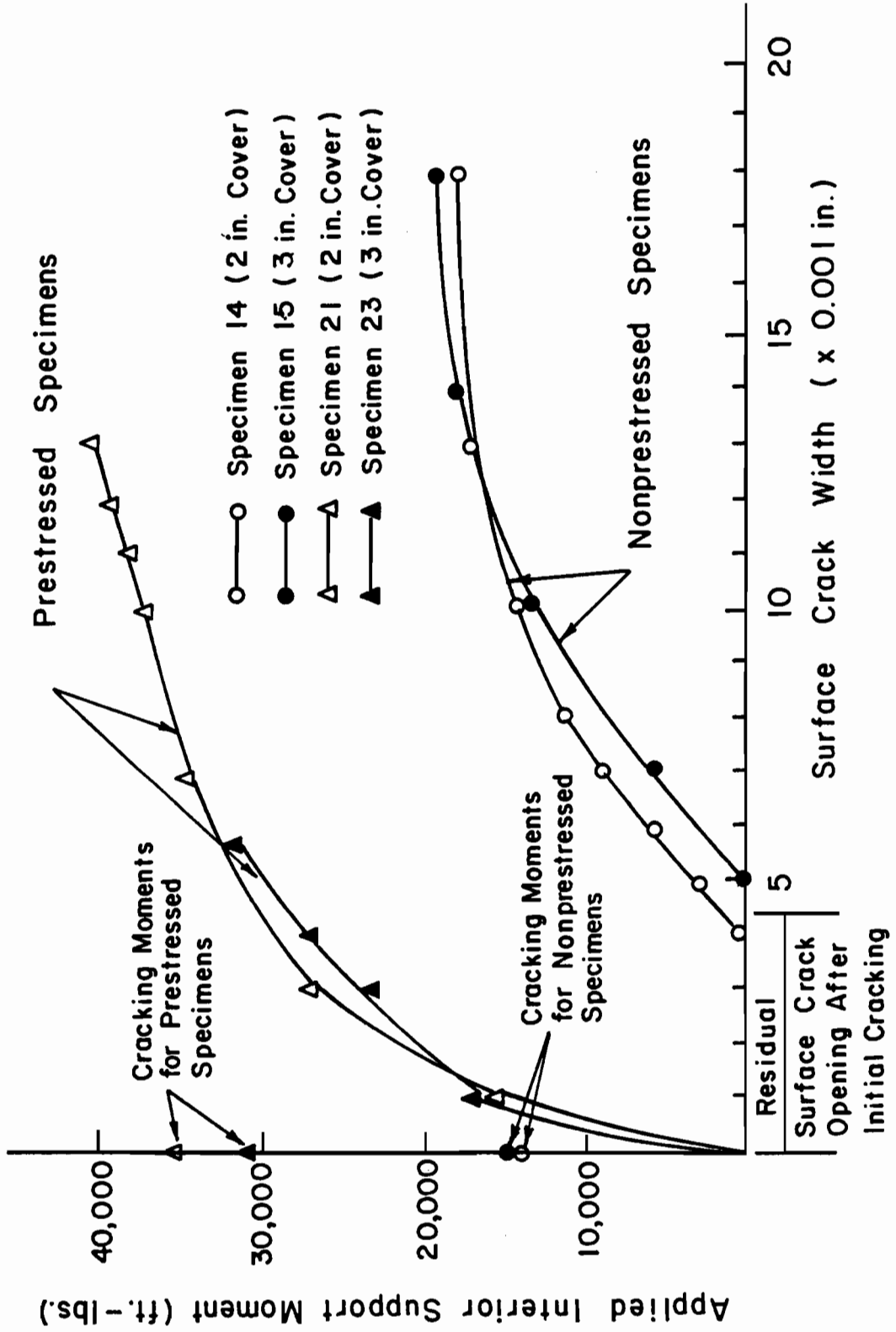


Fig. 5.1 Moment versus crack width upon reloading after initial cracking

Furthermore, Fig. 5.1 clearly shows that after cracking there is a residual crack width opening at zero load for the nonprestressed (i.e., only conventionally reinforced) specimens of about 0.005 in. In contrast, the cracks closed completely in the prestressed specimens.

5.3 Exposure Testing

In this section, the results obtained during the exposure testing of the durability specimens are evaluated. This includes an evaluation of the results from the visual inspections and the half cell potential readings.

5.3.1 Visual Inspection. As pointed out in Chapter 2, corrosion progressing to such an extent that rust stains appear on the concrete surface and cracking occurs suggests substantial distress. Thus, the staining which appeared above the unprotected anchorages in some of the specimens implies significant corrosion of the anchorage had occurred at the time of detection.

The heavy corrosion associated with the anchorages, as evidenced by rust staining in the anchorage region in the unbonded tendon specimens, is particularly distressful. This is so because visual inspection of the concrete surface by itself does not reveal whether the anchorage plate, jaws, and/or the tendon extensions were corroding. Corrosion of any or all of these components could lead to the loss of the load-carrying capability of the tendon. The post-mortem visual examination confirmed that the outer surfaces of the anchorage casting, strand extensions, jaws, and inner surfaces of the anchorage casting around the jaws had some forms of corrosion. For unbonded construction, the loss of any part of the anchorage is as critical as the loss of the tendon itself.

Further visual inspection did not indicate any other signs of corrosion distress at any other locations on the specimens. In particular, there was no evidence of distress at the location of the flexural cracks in any of the specimens. This means that any corrosion occurring in the reinforcement had not progressed to a stage that would cause surface rust stains or delaminations.

The results of the visual inspection presented in Chapter 4 revealed a gradual discoloration of the mortar in the anchorage recesses. The color changed from a rich gray to a golden-brown. The color change resulted from a leaching of some of the cement out of the mortar. This suggests a water migration path as shown in Fig. 5.2. The cement was leached out of the mortar by the aggressive percolating action of the salt water. However, at the end of the

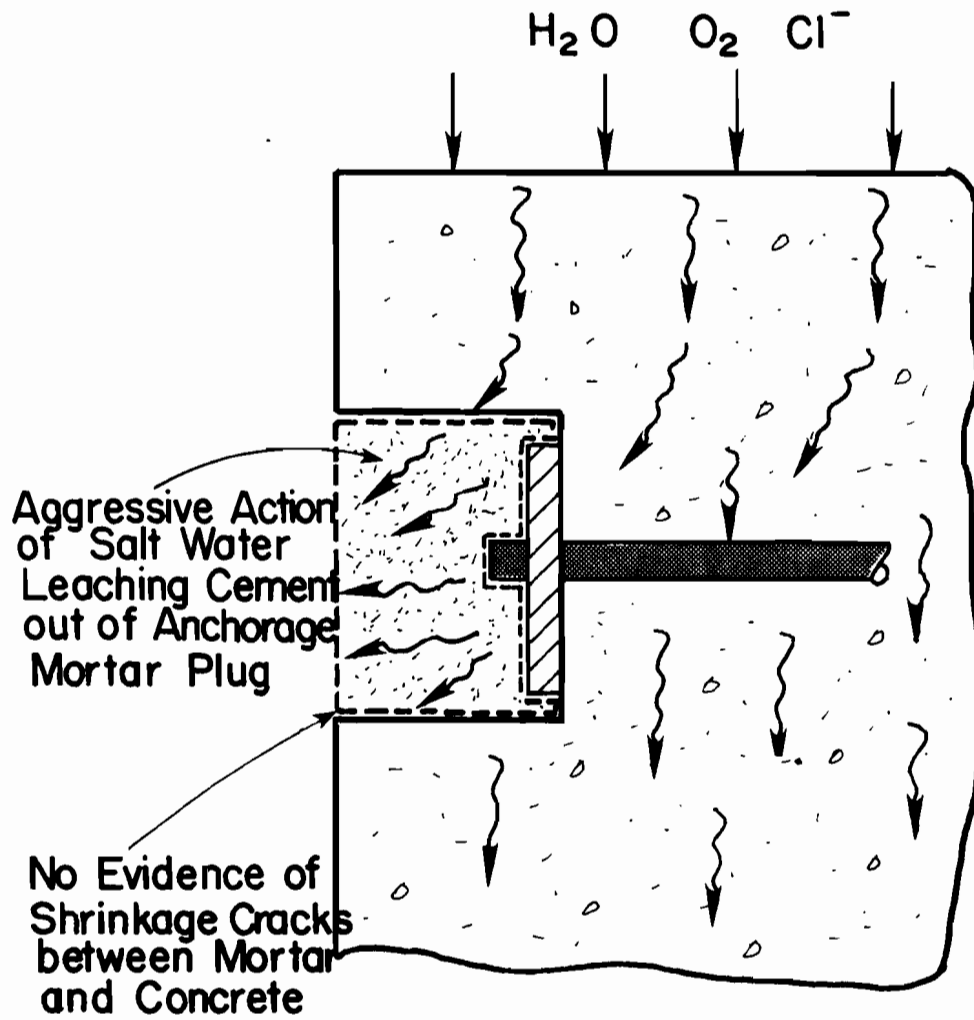


Fig. 5.2 Migration path of salt water

exposure testing, the unprotected mortar anchorage plugs were still intact, and showed no loss of soundness due to the cement lost by leaching. Thus, the discoloration appeared to have no significant effect with respect to the corrosion protection of the anchorage.

Inspection of the mortar plug also revealed that no shrinkage gaps existed between the mortar and concrete as shown in Fig. 5.2. This was particularly significant since the mortar mix used for the anchorage recesses did not contain an admixture which limited shrinkage, and was considered to be a typical mortar mix [41].

5.3.2 Half Cell Potentials for Nonprestressed Reinforcement. As described in Chapter 2, the measurement of half cell potentials provides a nondestructive means of determining if the steel reinforcement is in an active state of corrosion. Half cell potential measurements indicate corrosion in advance of severe forms of distress. Thus, the monitoring of half cell potentials provided a means of determining the likelihood of corrosion during the exposure testing period of the durability specimens. Since the half cell potentials were read periodically throughout the testing period, they also provided an indication of the onset of corrosion.

However, it is important to recognize that an evaluation using half cell potential measurements only indicates the likelihood of corrosion. No inference can be made as to the severity of corrosion distress when interpreting half cell potential readings. This is particularly true in the case of the epoxy-coated reinforcement where any corrosion which occurred was extremely light compared to the corrosion of the uncoated reinforcement.

The ASTM C-876 [39] criteria for evaluating half cell potential readings of mild steel reinforcement are summarized as follows:

1. "No": $|HCP| < |-140mV|$
(relative to SCE)

This classification represents a greater than 90% probability that no corrosion is occurring.

2. "UNCERTAIN": $|-140mV| < |HCP| < |-290mV|$
(relative to SCE)

This classification suggests that the corrosion activity is uncertain.

3. "YES": $|HCP| > |-290mV|$
(relative to SCE)

This classification represents a greater than 90% probability that corrosion is occurring.

Based on this ASTM criteria, the half cell potential readings for the nonprestressed reinforcing steel were evaluated. The results of this evaluation are presented in Table 5.1. The evaluations were based on the half cell potential (HCP) readings at the end of exposure testing. For those evaluations designated as "YES", the approximate time in days when the HCP readings numerically exceeded -290mV are also given in Table 5.1 under the heading "Time to Corrosion."

5.3.2.1 Predictive Capability. In the present research, the post-mortem examination, which included a visual inspection of the reinforcement after removal from the durability specimens, permitted a direct evaluation of the predictive capability of the half cell potential method. A comparison of the corrosion activity predicted by the half cell potential method to that actually observed during the visual inspection of the post-mortem examination is presented in Table 5.2. For the half cell potential predictions which are "YES" or "NO", this comparison reveals that the half cell potential method predicted the correct visual observation in approximately 85% of the cases. This is close to the 90% confidence limit applied by the ASTM C-876 [39] evaluation criteria.

It is interesting to note that in all but one case, an incorrect evaluation resulted from the interpretation of the half cell potentials for an epoxy-coated reinforcing bar. In all these cases, the half cell potential measurements suggested corrosion activity, whereupon the subsequent visual inspection indicated no corrosion. The reason for this is not known, since the half cell potential method correctly predicted some evidence of corrosion on the epoxy-coated reinforcing bars of other specimens. Considering only the uncoated bars, there was a 95% agreement between the HCP method and the visual inspection.

For those cases in Table 5.2 in which the half cell potential predictions were "UNCERTAIN", approximately 40% indicated corrosion by visual inspection, and about 60% indicated no corrosion. This is close to the 50%-50% split which is implied by the "UNCERTAIN" category for interpretation of half cell potential readings.

5.3.2.2 Comparisons. Table 5.3 presents the evaluation of the incidence of corrosion of the nonprestressed reinforcement based on an interpretation of half cell readings with visual observation

TABLE 5.1 Evaluation of the Half Cell Potentials for the Mild Reinforcement in the Specimens

Unbonded Single-Strand Specimens (USS)									
Prestress Level, psi	0		160		0		160		
Approximate Surface Crack Width under Load, in.	0.015		0.015		0.002		0.002		
Concrete Cover, in.	2		3		2		3		
Nonprestressed Reinforcement Type	UC	EC	UC	EC	UC	EC	UC	EC	
UC=Uncoated	/	/	/	/	/	/	/	/	
EC=Epoxy-coated	/	/	/	/	/	/	/	/	
Component	LB	RB	LB	RB	LB	RB	LB	RB	LB
LB=left reinforcing bar									
RB=right reinforcing bar									
Corrosion Activity*	Y	U	N	Y	Y	Y	Y	Y	Y
Y = Yes, N = No									
U = Uncertain									
Time to Corrosion** (days)	17	17	12	10	83	50	≈0	≈0	16
			113	78	70				13

* Based on ASTM C-876 criteria summarized in Section 5.3.2.1

** Time when HCP reading numerically exceeded -290mV relative to SCE

TABLE 5.1 Evaluation of the Half Cell Potentials for the Mild Reinforcement in the Specimens (continued)

GROUTED MULTI-STRAND SPECIMENS (GMS)		0		160		0		160				
Prestress Level, psi	Approximate Surface Crack Width under Load, in.	Concrete Cover, in.	Nonprestressed Reinforcement Type	Component	Corrosion Activity*	Time to Corrosion** (days)						
0	0.015	2	UC	UC	Y	56	65	50	128	128	126	62
			EC	EC	Y	56	65	50	128	128	126	62
0	0.015	3	UC	UC	Y	56	65	50	128	128	126	62
			EC	EC	Y	56	65	50	128	128	126	62
160	0.015	2	UC	UC	Y	56	65	50	128	128	126	62
			EC	EC	Y	56	65	50	128	128	126	62
160	0.015	3	UC	UC	Y	56	65	50	128	128	126	62
			EC	EC	Y	56	65	50	128	128	126	62
160	0.002	2	UC	UC	Y	56	65	50	128	128	126	62
			EC	EC	Y	56	65	50	128	128	126	62
160	0.002	3	UC	UC	Y	56	65	50	128	128	126	62
			EC	EC	Y	56	65	50	128	128	126	62

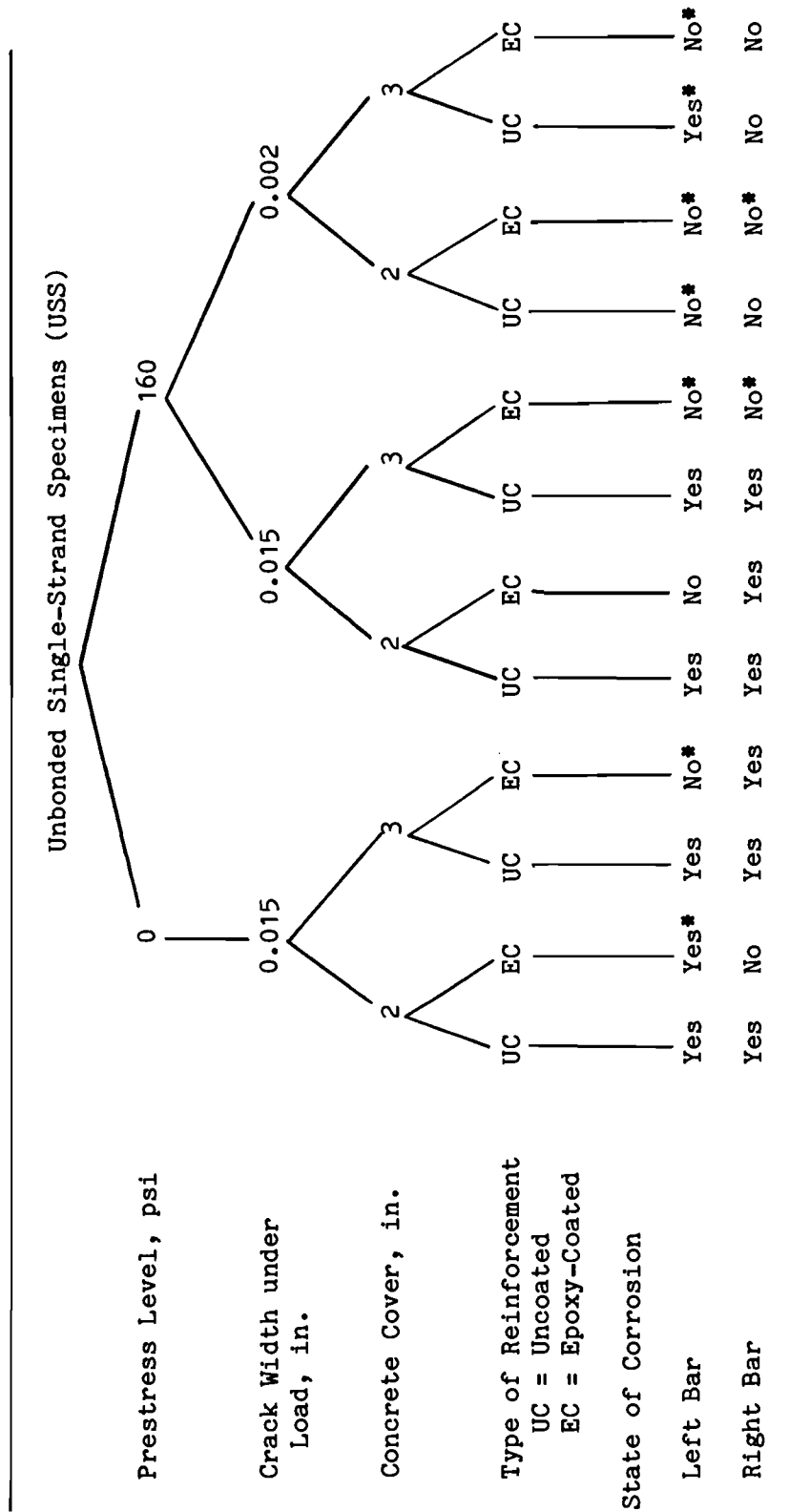
* Based on ASTM C-876 criteria summarized in Section 5.3.2.1

** Time when HCP reading numerically exceeded -290mV relative to SCE

TABLE 5.2 Comparison of Corrosion Activity by Half Cell Potential (HCP) Method to That Observed by Visual Inspection of the Exposed Steel (continued)

Grouted Multi-Strand Specimens (GMS)												
Prestress Level, psi	0		0.015		0.015		0.015		0.002		0.002	
Approximate Surface Crack Width under Load, in.	2		3		2		3		2		3	
Concrete Cover, in.	2		3		2		3		2		3	
Nonprestressed Reinforcement Type	UC	EC	UC	EC	UC	EC	UC	EC	UC	EC	UC	EC
UC=Uncoated	/	/	/	/	/	/	/	/	/	/	/	/
EC=Epoxy-coated	/	/	/	/	/	/	/	/	/	/	/	/
Component	LB	RB	LB	RB	LB	RB	LB	RB	LB	RB	LB	RB
LB=left reinforcing bar	/	/	/	/	/	/	/	/	/	/	/	/
RB=right reinforcing bar	/	/	/	/	/	/	/	/	/	/	/	/
HCP Prediction	Y	Y	N	Y	Y	N	Y	Y	N	U	Y	N
Y = Yes, N = No	Y	Y	N	N	Y	N	Y	Y	N	Y	N	N
U = Uncertain	Y	Y	N	N	Y	N	Y	Y	N	Y	N	N
Visual Inspection	Y	Y	N	N	Y	N	Y	Y	N	Y	N	N
Y = Yes, N = No	Y	Y	N	N	Y	N	Y	Y	N	Y	N	N
Agreement Between HCP and Visual Inspection	Y	Y	N	N	Y	Y	Y	Y	N	Y	Y	Y
Y=Yes	Y	Y	N	N	Y	Y	Y	Y	N	Y	Y	Y
N=No	N	N	Y	Y	N	N	N	N	Y	N	N	N

TABLE 5.3 Evaluation of Incidence of Corrosion of the Nonprestressed Reinforcement in the Durability Specimens



* Based on post-mortem visual inspection.

TABLE 5.3 Evaluation of Incidence of Corrosion of the Nonprestressed Reinforcement in the Durability Specimens (continued)

Grouted Multistrand Specimens (GMS)										
Prestress Level, psi	0		160		0.015		0.002		0.015	
Crack Width under Load, in.	0.015		0.015		0.015		0.015		0.015	
Concrete Cover, in.	2		3		2		3		3	
Type of Reinforcement	UC		EC		UC		EC		UC	
State of Corrosion	Yes		No*		No		No		No	
Left Bar	Yes		No*		No		No		No	
Right Bar	Yes		No*		Yes		No*		No	
Type of Reinforcement	UC	EC	UC	EC	UC	EC	UC	EC	UC	EC
State of Corrosion	Yes	No*	No*	No*	No	No	Yes	No	Yes	No
Left Bar	Yes	No	No*	No*	No	No	No	No	No	No
Right Bar	Yes	No	Yes	No*	No*	Yes	No*	-Yes	Yes*	No

* Based on post-mortem visual examination.

from the post-mortem examination. Table 5.3 is subdivided into the principal variables of study in the durability tests in order to more clearly identify the trends. The results indicate that there was approximately equal incidence of corrosion in the unbonded and grouted specimens, confirming that corrosion of the nonprestressed reinforcement is independent of prestressing system type.

Figure 5.3 clearly indicates that the epoxy-coated reinforcement had a much lower incidence of corrosion than the uncoated reinforcement independent of other test variables. Figure 5.3 reveals that only 17% of the epoxy-coated reinforcement showed evidence of corrosion compared to 63% of the uncoated reinforcement. It is apparent that epoxy-coated reinforcement drastically reduces the likelihood of corrosion.

Figure 5.4 shows the effect that prestressing and reinforcement type had on the incidence of corrosion. It is clear from this figure that the incidence of corrosion of the uncoated reinforcement was drastically reduced when the presence of prestressing limited the crack widths to about 0.002 in. For this case only 13% (actually only one reinforcing bar) showed signs of corrosion. This compares to an 88% incidence of corrosion of the uncoated reinforcement in the nonprestressed and prestressed specimens which were loaded to produce crack widths of approximately 0.015 in. This suggests that the incidence of corrosion in cracked concrete is proportional to crack width and that the prestress works in the 0.002 in. case by limiting crack width. It must be pointed out that 0.015 in. is an artificial case with prestress since a much higher load was required to produce this crack width as was indicated in Fig. 5.1. Figure 5.4 also indicates that there was no corrosion of the epoxy-coated reinforcement in the prestressed specimens with 0.002 in. crack widths. This compares to 25% corrosion incidence of the epoxy-coated reinforcement for the specimens in the other two classifications.

There are several other trends which are evident from Fig. 5.4. For the nonprestressed specimens (i.e., only conventionally reinforced), the use of epoxy-coated reinforcement reduced corrosion incidence. Thus, this result confirms the theories that the use of epoxy-coated reinforcement in conventionally reinforced decks would reduce the risk of corrosion. For the prestressed specimens in which crack widths were limited to 0.002 in., the corrosion incidence for uncoated and epoxy-coated reinforcement could be considered about equal. This result suggests that for a transversely prestressed bridge deck that epoxy-coated reinforcement would not be needed. Prestressing which limited cracking would be sufficient for corrosion protection of uncoated reinforcement.

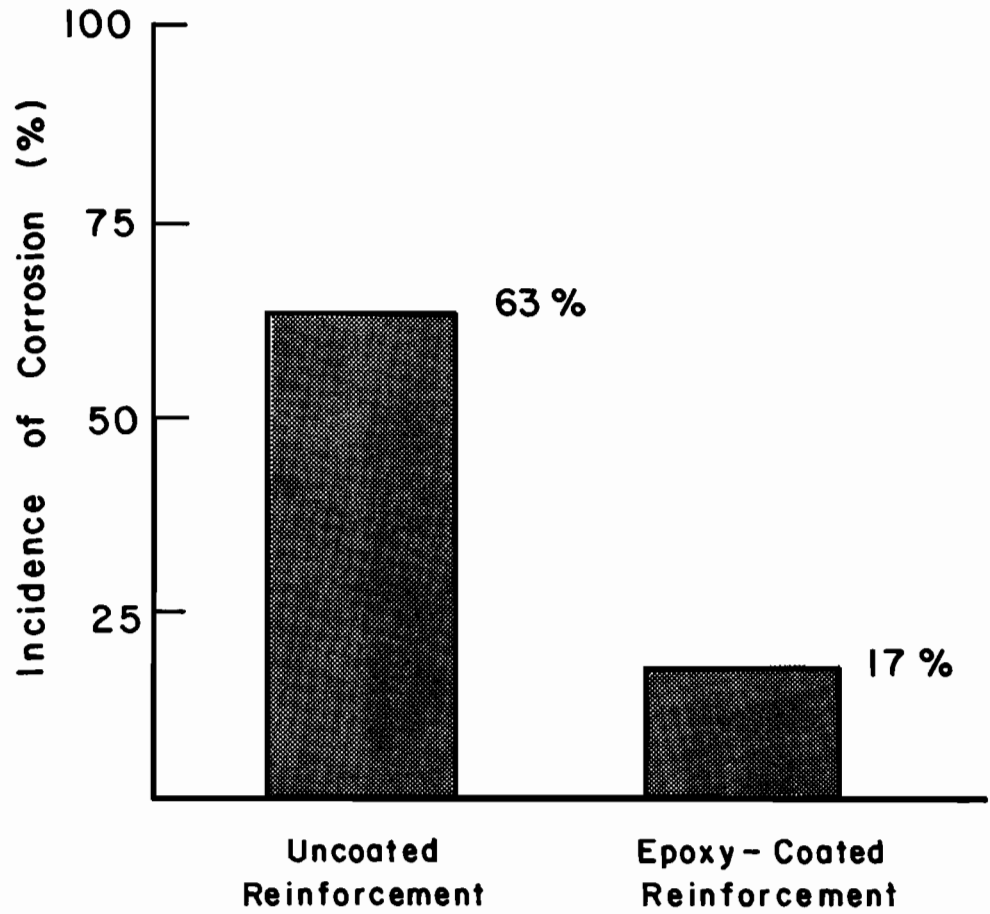


Fig. 5.3 Comparison of incidence of corrosion of uncoated and epoxy-coated reinforcement

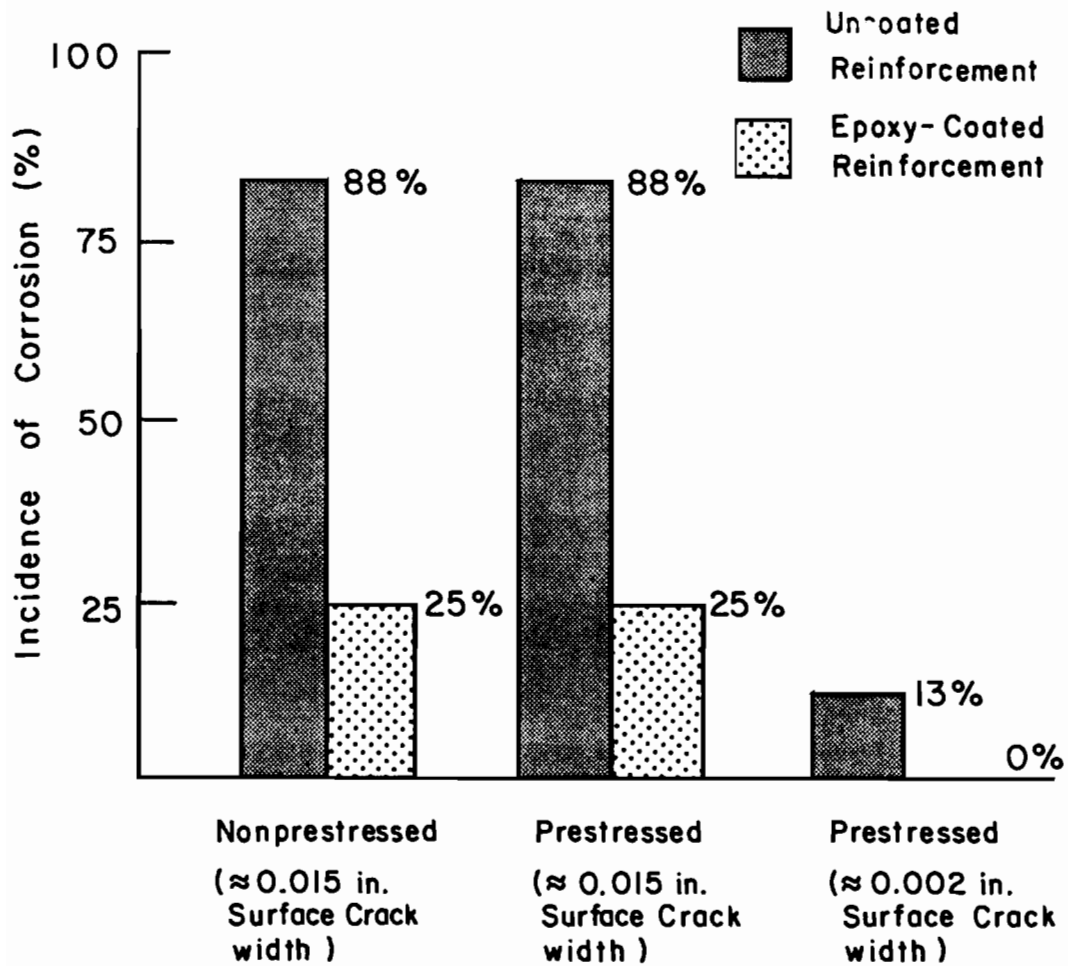


Fig. 5.4 Comparison of incidence of corrosion of reinforcement in nonprestressed and prestressed specimens

For this somewhat limited period of the exposure testing, Fig. 5.5 clearly indicates that without regard to other test variables the incidence of corrosion was independent of the concrete cover. There was about an equal incidence of corrosion of the reinforcement in the specimens with 2 in. concrete cover as in the specimens with 3 in. concrete cover. The concrete cover made little difference for the case of these durability specimens because the corrosion initiated on the reinforcement at the crack locations.

As discussed in Chapter 3, some of the uncoated reinforcement was precleaned of all mill scale before placement in the specimens. Figure 5.6 shows that the incidence of corrosion of the precleaned reinforcement was almost equal to that of the "not cleaned" reinforcement. Therefore, removing any heterogeneities on the surface of the reinforcement, and thereby removing any localized anodic locations which are prone to corrosive attack, apparently had no significant effect on the incidence of corrosion.

5.3.2.3 Time to Corrosion. An evaluation of the time to corrosion data presented in Table 5.2 reveals that the average time to corrosion of the reinforcement under these severe exposure conditions was approximately 30 days for the nonprestressed and prestressed specimens having similar crack widths. This implies that for crack widths of 0.015 in., the action of the prestressing closing cracks had little effect on the time to corrosion.

5.4 Post-Mortem Examination

In this section, the results obtained from the post-mortem examination are discussed. This includes an evaluation of the results from the tests for chloride content in the concrete as well as from the visual inspection of the reinforcement removed from the specimens.

5.4.1 Chloride Content. The chloride ion (Cl^-) content of a concrete sample measured using an acid soluble test is generally considered to represent the amount of total chloride in concrete. The only difference between the actual total chloride content and that measured using an acid soluble test is the presence of organically bound chloride. A water soluble chloride test determines the Cl^- which is extractable in water, and probably better represents the actual amount of chloride available for corrosion. In the present study, both water and acid soluble tests were conducted to determine Cl^- content in the concrete samples taken from the durability specimens.

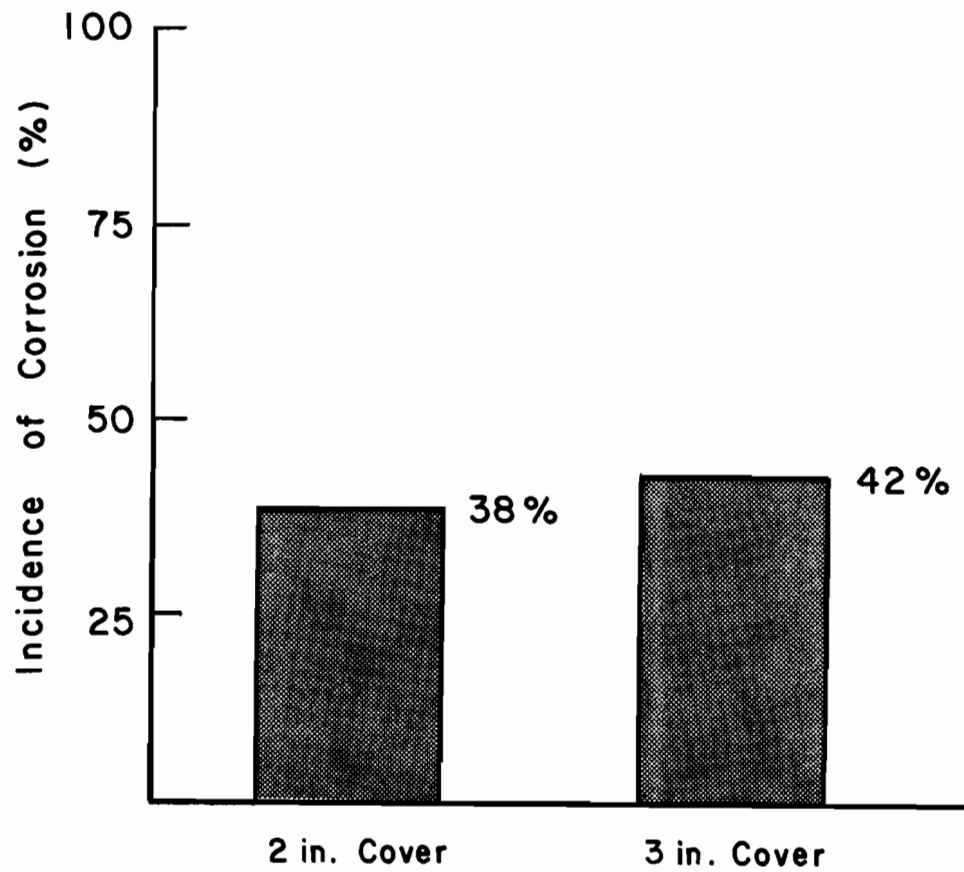


Fig. 5.5 Comparison of incidence of corrosion of reinforcement in specimens with 2 in. and 3 in. concrete covers without regard to other test variables

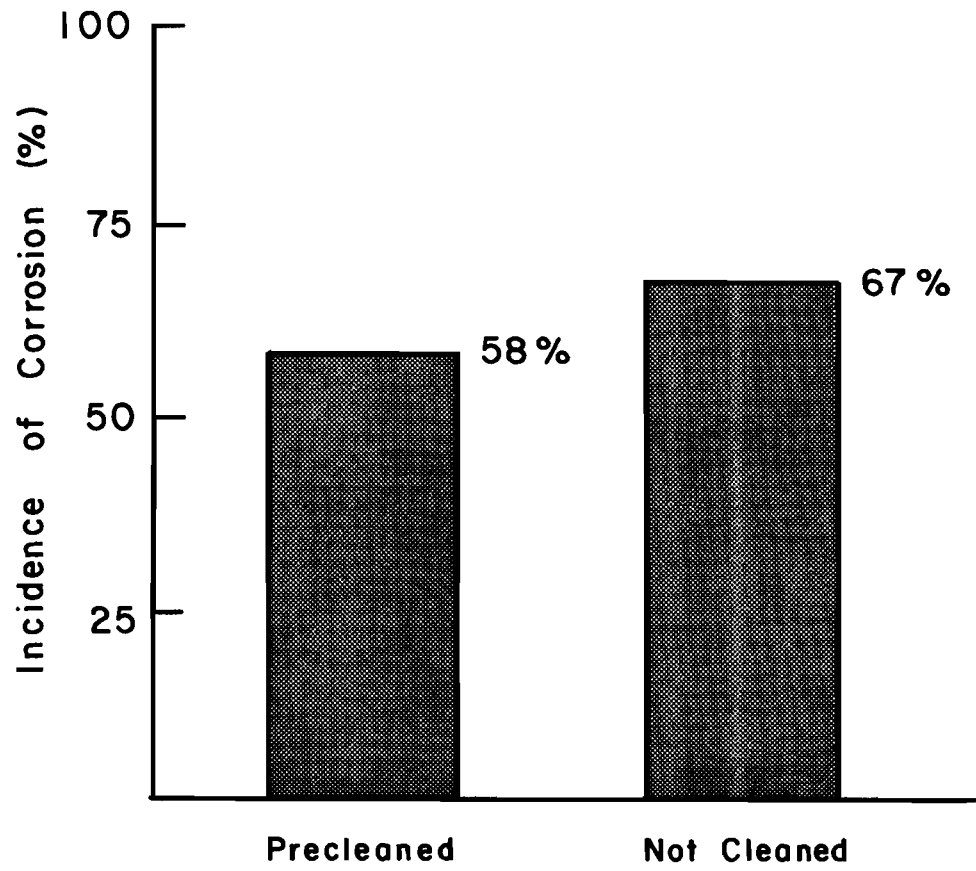


Fig. 5.6 Effect of precleaning uncoated reinforcement on incidence of corrosion

The water soluble chloride was determined according to the colorimetric procedure used by the Mineral Studies Laboratory (MSL) (see Appendix B). However, MSL also used both conventional titration procedures [42] and the colorimetric procedure for 10% of the concrete samples. In general, for large amounts of Cl^- , above 1 lb Cl^- /(cu.yd.concrete), the two methods give similar results. However, for Cl^- less than 1 lb/(cu.yd.concrete), on the average, the measured amounts of Cl^- using both methods differ by as much as 50%. For small Cl^- contents, it is believed that the colorimetric procedure is more accurate.

The average water soluble chloride content in the concrete samples was found to be about 90% of the acid soluble chloride content. This is slightly greater than the 75-80% range reported from other studies [43]. This implies that in the present study, most of the Cl^- found in the concrete samples was available for dissolution in water, and hence was available to cause corrosion.

For corrosion protection, the current ACI Building Code [29] recommends a maximum water soluble Cl^- concentration of 0.06% by weight of cement for prestressed concrete and 0.15% by weight of cement for reinforced concrete exposed to chlorides in service. The intent of this requirement is to minimize the risk of chloride-induced corrosion by limiting the amount of Cl^- in the hardened concrete before exposure to chlorides from the environment. Examination of Table 4.1 reveals that in this study only the concrete used for the first concrete batch (sample R1) exceeded the more restrictive prestressed concrete requirement. Other than this one case, the concrete used for the construction of the durability specimens met the ACI requirements, and should have been at low risk to chloride-induced corrosion according to ACI 318-83 recommendations.

5.4.1.1 Cracked Concrete. Results of the chloride content determination in the concrete samples taken at the level of the reinforcement in the cracked section of the specimens are given in Fig. 5.4 (see Appendix A for core locations). The cross-hatched bars in Fig. 5.7 represent cases in which corrosion of the reinforcement was observed at the crack location. Open bars represent cases in which no visible signs of corrosion occurred at the crack location. The generally accepted value of the minimum water soluble Cl^- content required to initiate corrosion is shown at 1.5 lbs Cl^- /(cu.yd. concrete) (see Section 2.4.2).

It is evident from Fig. 5.7 that the prestressed specimens in which crack widths were limited to about 0.002 in. had on the average a much lower Cl^- concentration at the crack location than the other specimens. However, for almost all specimens and independent

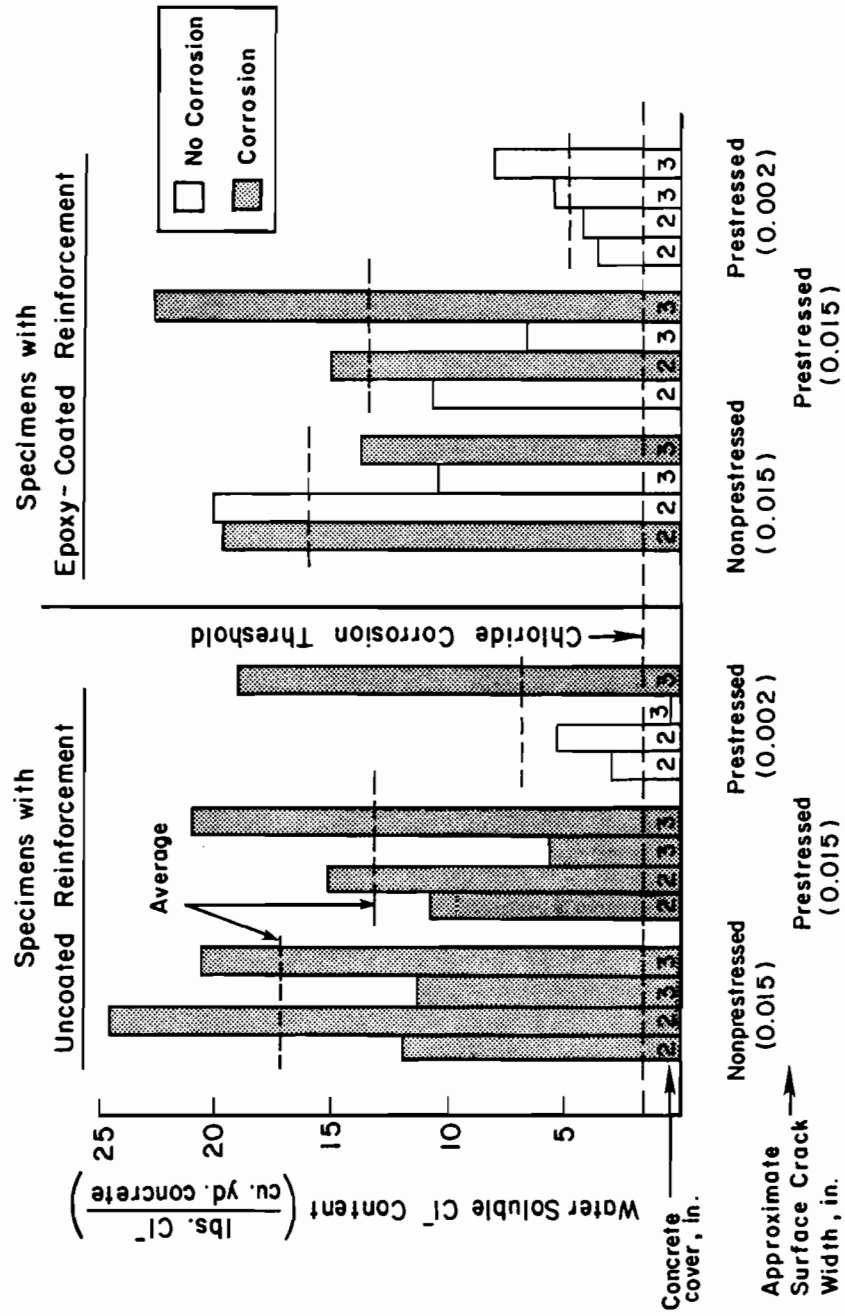


Fig. 5.7 Cl⁻ content at level of reinforcement at the crack location in the specimens (see Appendix A for crack locations)

of stress level and crack width, Fig. 5.7 also reveals that the Cl^- content at the crack location exceeded the generally accepted chloride corrosion threshold. The results from the half cell potential readings and the visual inspection indicated that virtually no corrosion of the nonprestressed reinforcement occurred in the prestressed specimens with 0.002 in. cracks, as evidenced by the open bars in Fig. 5.7. The one incidence of corrosion in this category had a Cl^- content of about 19 lbs Cl^- /(cu.yd.concrete), which greatly exceeds the chloride corrosion threshold. Since the Cl^- concentration exceeded that which is generally regarded as necessary to initiate corrosion, it is then concluded that other environmental conditions necessary to cause corrosion were in general not present. The action of the prestressing force which was sufficient to control crack widths and completely close cracks apparently limited the ingress of oxygen which is required for corrosion to take place. This conclusion is substantiated by evidenced cited in Refs. 44 and 45 in which concrete submerged in seawater with chloride contents ranging from 13 to 34 lbs Cl^- /(cu.yd.concrete) showed very little evidence of corrosion primarily because of the lack of oxygen. A chloride level exceeding the chloride corrosion threshold is not enough in itself to cause corrosion.

There are several other trends which are evident from Fig. 5.7. The water soluble Cl^- concentration at the crack locations appears to be independent of 2 in. and 3 in. cover as evidenced by the random nature of the bar data. It is also clear that epoxy-coating on reinforcement substantially reduced the incidence of corrosion even though the Cl^- levels were greater than the generally accepted value of the chloride corrosion threshold. Or it might be suggested from Fig. 5.7 that the chloride corrosion threshold for the epoxy-coated reinforcement is higher than that for uncoated reinforcement. For epoxy-coated reinforcement, corrosion only occurred when the Cl^- levels were above 12 lbs Cl^- /(cu.yd.concrete).

The one case in which corrosion was observed for a prestressed specimen with 0.002 in. crack width had an excessive amount of Cl^- . In this case, the prestress level was probably not as great as was assumed (i.e., 160 psi) and thus in actuality the cracks in that specimen may have opened to levels greater than 0.002 in.

5.4.1.2 Uncracked Concrete. Figure 5.8 presents the water soluble Cl^- concentrations in the concrete samples taken at the level of the reinforcement in an uncracked section of the specimens (see Appendix A for core locations). In this figure, no differentiation is made with respect to reinforcement type since there was no evidence of corrosion of any reinforcement at uncracked concrete locations. The figure clearly shows that prestressing had little direct effect on the Cl^- penetration in the uncracked regions of the

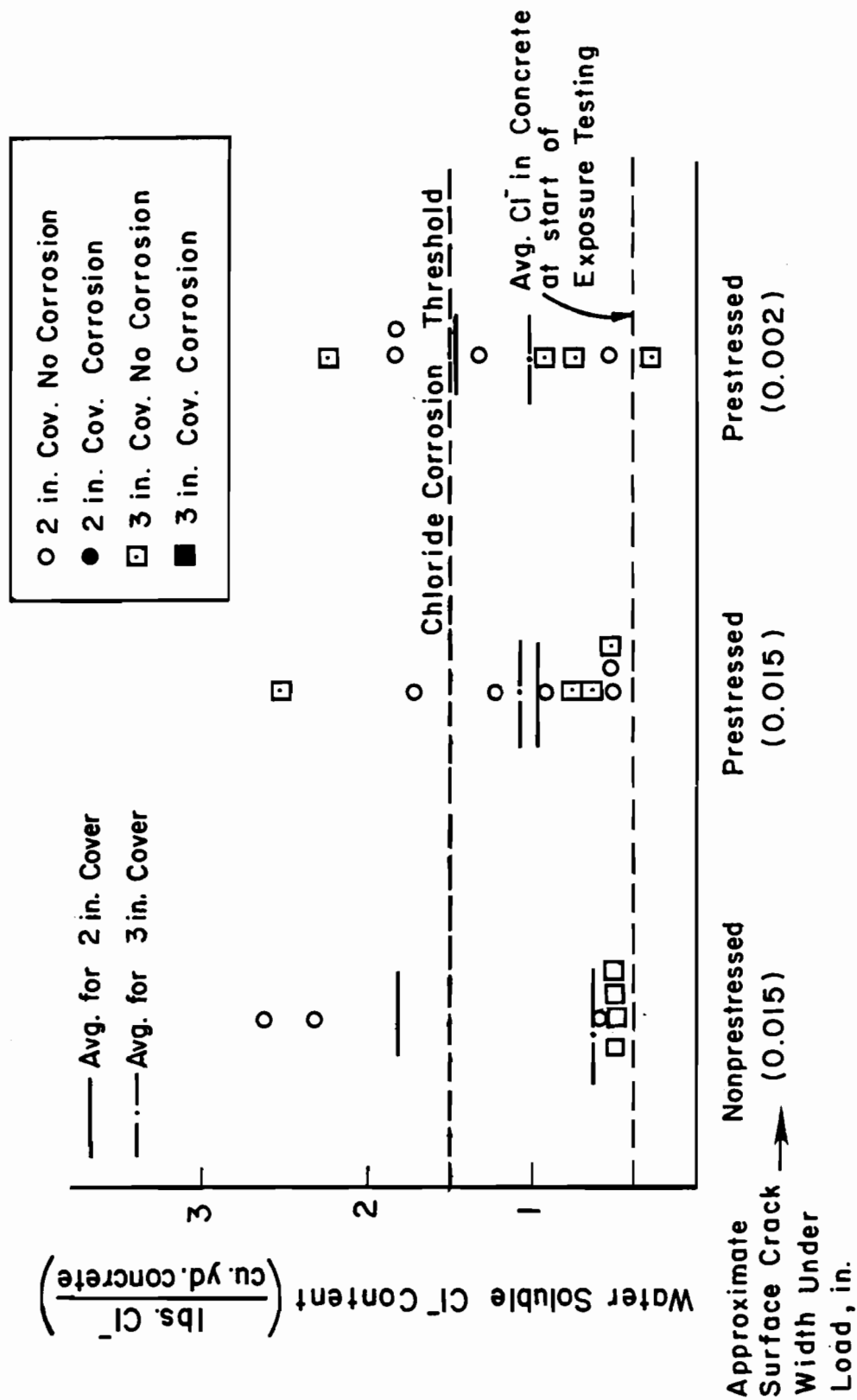


Fig. 5.8 Cl⁻ content at level of reinforcement at the uncracked location in the specimens (see Appendix A for core locations)

concrete. However, it must be remembered that prestressing has an indirect effect since for the same load a prestressed structure is more likely to be uncracked throughout than one that is only conventionally reinforced. Thus, in actuality, Fig. 5.8 shows the effect of what occurs if cracking is prevented. For both the 2 in. and 3 in. cover specimens, the average Cl^- content is similar for nonprestressed and prestressed specimens. Figure 5.8 also shows the Cl^- content was, on the average, at or below the chloride corrosion threshold. This probably explains why no corrosion of the nonprestressed reinforcement occurred in the uncracked regions of the specimens.

Figure 5.8 also reveals that the average Cl^- concentration at a depth of 3 in. is less than that at a depth of 2 in. The figure also indicates that in all but one case, the Cl^- level is substantially above the average amount at the start of exposure testing. The additional amount represents the Cl^- introduced from the salt water exposure. Since no corrosion of reinforcement occurred in uncracked concrete, it can be concluded that on the average this additional amount of Cl^- was less than that required to initiate corrosion.

5.4.1.3 Penetration with Depth. Figure 5.9 presents the water soluble Cl^- content with depth for the four profile cores which were taken at an uncracked concrete location (those samples ending with a "P" in Table 4.1). Two of the Cl^- penetration profiles are from nonprestressed specimens, and two from prestressed specimens. This figure clearly indicates the rapid decrease in Cl^- penetration with depth in the uncracked concrete. This figure also shows that prestressing had little direct effect on Cl^- penetration in the uncracked concrete as was previously indicated by Fig. 5.8. At a depth of about 2.5 in., all Cl^- values were less than the chloride corrosion threshold.

5.4.1.4 Relationship Between Chloride Level and Concrete Quality. Figure 5.10 presents a comparison between the average water soluble Cl^- content with depth taken from the profile cores of the durability specimens and that obtained by Clear in a previous research study [43]. Clear obtained Cl^- content data with depth for water-cement ratios of both 0.40 and 0.50. Since $W/C = 0.44$ for the concrete used in the durability specimens, the Cl^- levels with depth should ideally fall between Clear's data. Even though this was not the case, considering the differences in testing conditions, the Cl^- levels with depth from both tests are very similar. The rapid decrease of Cl^- with depth is evident from both sets of data.

Table 5.4 shows the requirements in the current ACI Building Code [29] regarding concrete cover and concrete quality for

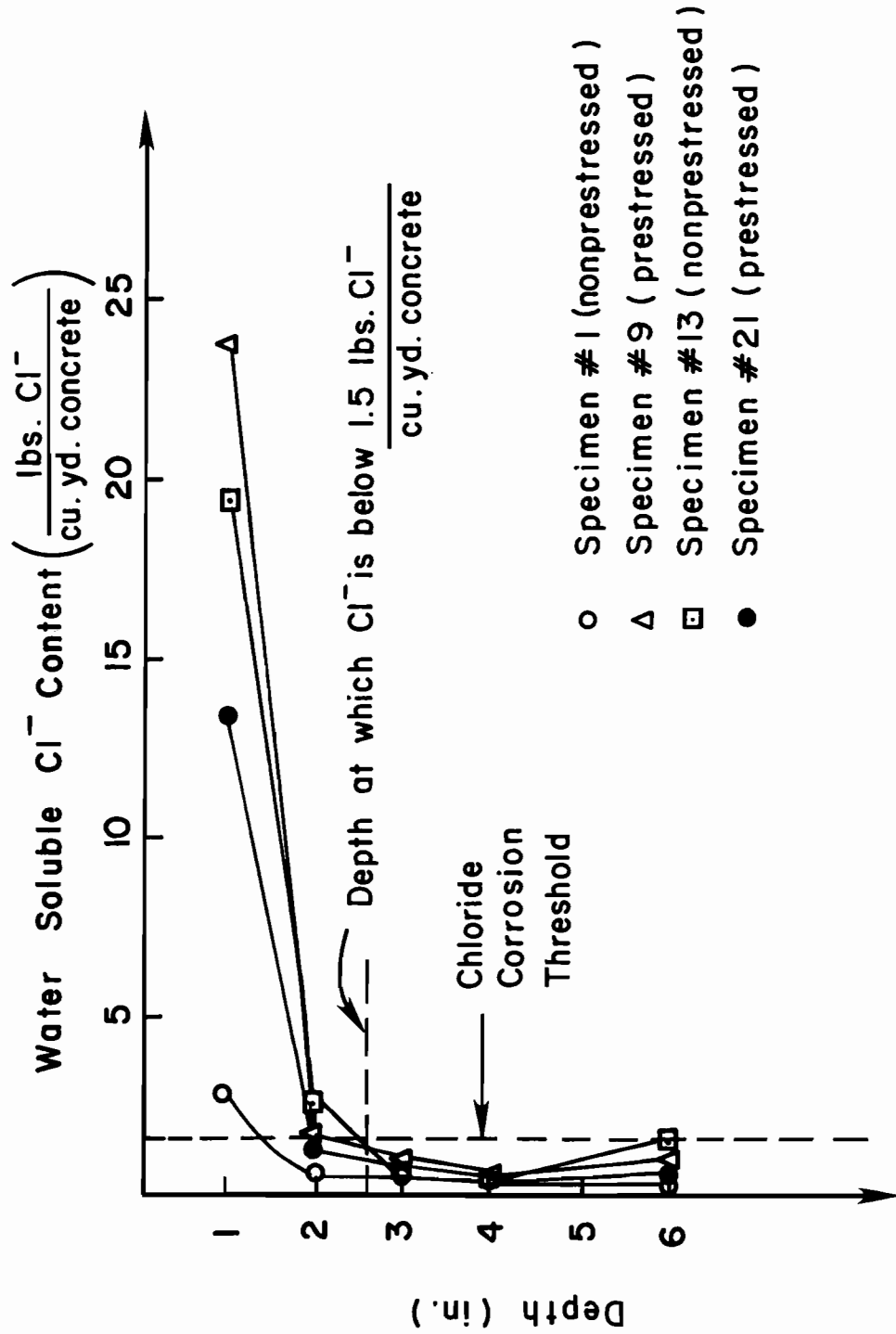


Fig. 5.9 Cl⁻ penetration with depth in uncracked concrete

reinforced and prestressed concrete slabs exposed to corrosive environments. These provisions suggest that a reduction in concrete cover of 0.5 in. is permissible with the use of a prestressed concrete slab. However, the results shown previously in Fig. 5.8 suggest that for uncracked concrete, Cl^- content is independent of prestressing, and therefore a reduction in cover for prestressed concrete is not consistent with the trends observed in this study. The effect of prestressing is to control cracking. However, ACI recommendations do appear consistent with observed trends regarding a decrease in concrete cover for a decrease in water-cement ratio (i.e., increase in concrete quality). Clear's data shown in Fig. 5.10 indicate that for a given concrete depth, the Cl^- concentrations decrease with an increase in concrete cover. Thus, the different combinations of W/C ratio and concrete cover in Table 5.4 provide similar protection from chloride-induced corrosion if the concrete is uncracked.

The results shown in Fig. 5.10 from the exposure tests of this research indicate that the combination of W/C = 0.44 and a 2 in. cover was on the average sufficient in keeping the Cl^- concentrations in the uncracked concrete below the chloride corrosion threshold for the exposure conditions of these relatively short time tests. As shown in Table 5.4, this is approximately the same combination recommended by ACI to ensure protection for prestressed concrete slabs exposed to corrosive environments. However, it is important to recognize that the ACI recommendations assume that the concrete is uncracked and do not envision the ingress of large amounts of chlorides at crack locations as is indicated by the results shown in Fig. 5.7. For cracked concrete, concrete quality and cover have little effect on Cl^- penetration.

5.4.2 Visual Inspection. Visually inspecting reinforcement which has been removed from concrete provides the most conclusive verification of corrosion activity. Moreover, visual inspection represents one of the few methods which can be used to quantify corrosion intensity.

The nonprestressed reinforcement, prestressing tendon and duct were removed from the crack zones in all the specimens. In addition, the full length of all reinforcement as well as anchorages were removed from selected specimens. The results of the visual inspection for corrosion of these components were presented in Table 4.3.

A close examination of the results from the visual inspection reveals that corrosion only occurred on the nonprestressed reinforcement which was removed from the crack zones. The

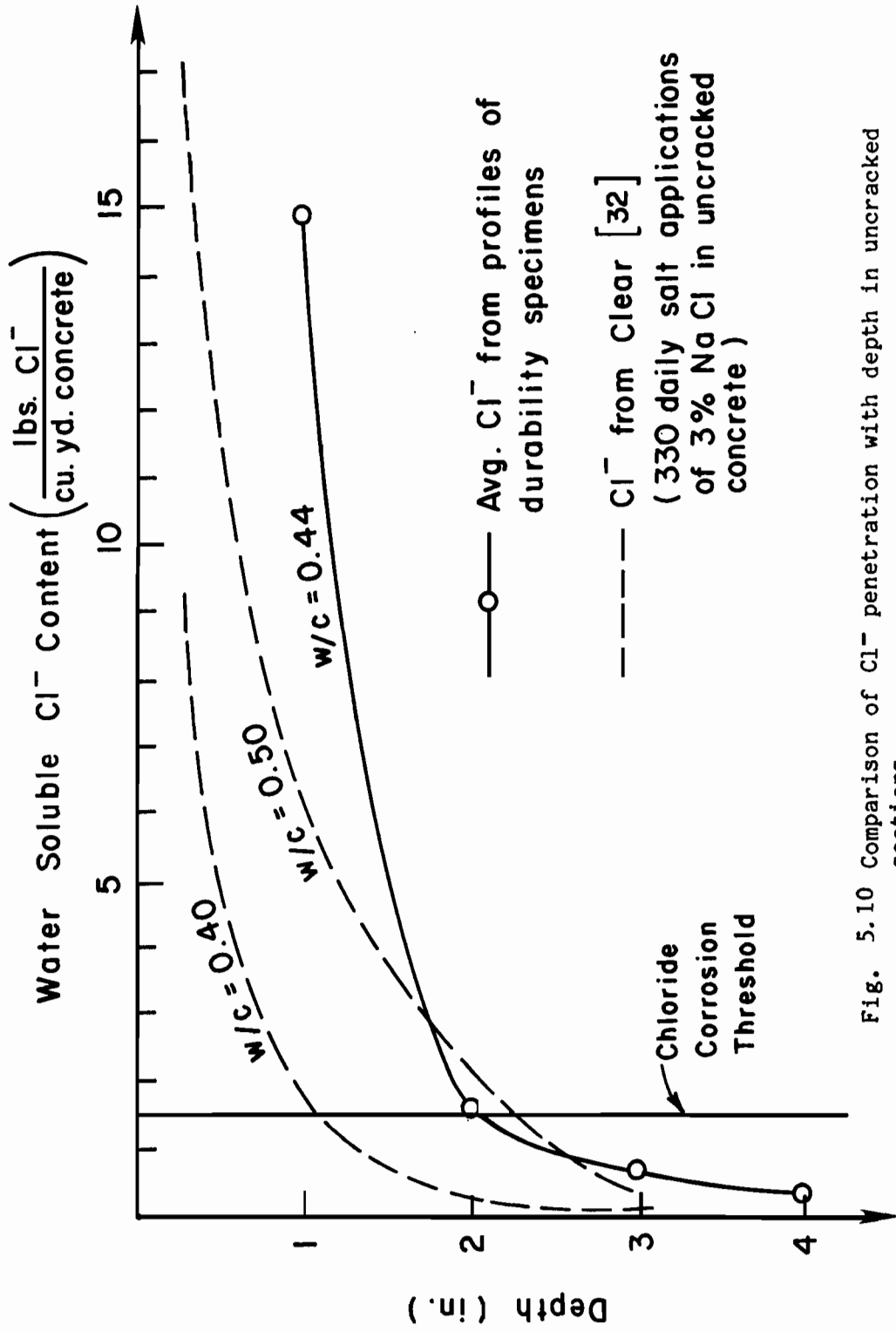


Fig. 5.10 Comparison of Cl⁻ penetration with depth in uncracked sections

TABLE 5.4 ACI Recommendations [29] for Reinforced and Prestressed Concrete Slabs Exposed to Corrosive Environments

	W/C Ratio	Minimum Cover (in.)
Reinforced Concrete Slabs	0.40	2.0
	0.45	2.5
Prestressed Concrete Slabs	0.40	1.5
	0.45	2.0

reinforcement outside the crack zone regions was well protected by the concrete during exposure testing.

Cracks in concrete are thought to have differing roles in the corrosion of reinforcing steel. From one viewpoint, cracks provide access to the steel for corrosion-producing substances. In this case it is thought that cracks accelerate the onset of corrosion. Another viewpoint suggests that while cracks accelerate corrosion, such corrosion is localized. Eventually, chloride ions penetrate even the uncracked concrete and initiate more widespread corrosion of steel. The result is that after a few years there is little difference between the amount of corrosion in cracked and uncracked concrete.

Clearly, in the present study, the cracks did accelerate the onset of corrosion. Since the exposure did not last for several years, it is uncertain whether corrosion would have eventually resulted in widespread corrosion of the reinforcement away from the crack zones in the specimens. However, it is believed that the test exposure conditions represented a more severe condition than would exist in practice, and thus can be viewed as representing a much longer exposure period than indicated by the actual test duration. Yet the fact is that corrosion of the nonprestressed reinforcement only occurred at the crack zones in the specimens. The results from the present study with a very aggressive environment for a relatively short time (112 to 196 days) show that corrosion only occurred at crack locations, and that the incidence of corrosion was substantially reduced by limiting crack widths with the use of prestressing.

The visual inspection of the uncoated nonprestressed reinforcement also clearly indicated the destructive spreading effect of more advanced stages of corrosion. As shown in Fig. 5.11, the corrosion initiated at the crack locations in the concrete, but then spread along the length of the bar. The length the corrosion had spread was greater than three bar diameters, which is the distance often cited for the occurrence of very localized corrosion [18]. In many cases, the corrosion had spread over a distance as much as 6 to 10 bar diameters. It is expected that allowed enough time the corrosion probably would have spread even further along the bar resulting in cracking of the concrete along the reinforcing steel bar.

Figures 5.12 through 5.14 present histograms for different categories of damage of the nonprestressed reinforcement. The categories of damage were summarized in Table 4.2. In the histograms, N represent the total number of occurrences for all categories. The histograms are based on all the top reinforcement which was removed from the crack zones of the specimens.

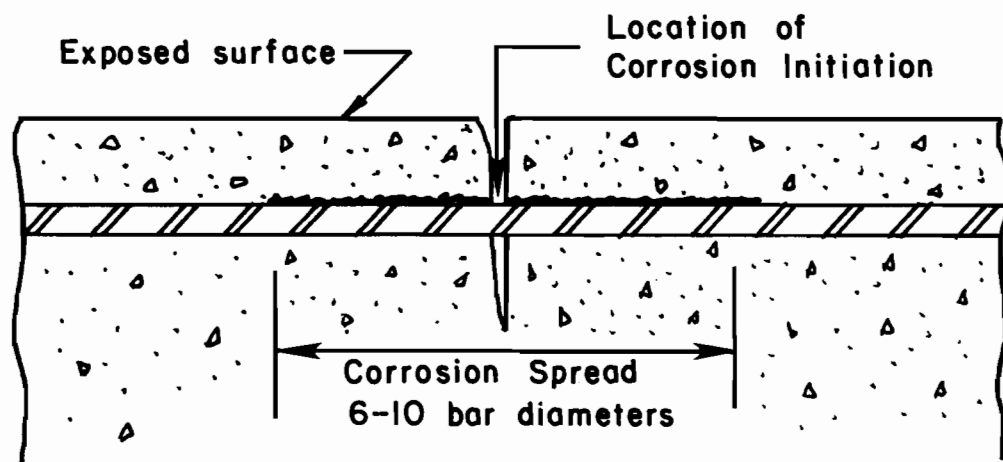


Fig. 5.11 Spreading effect of corrosion of uncoated reinforcement

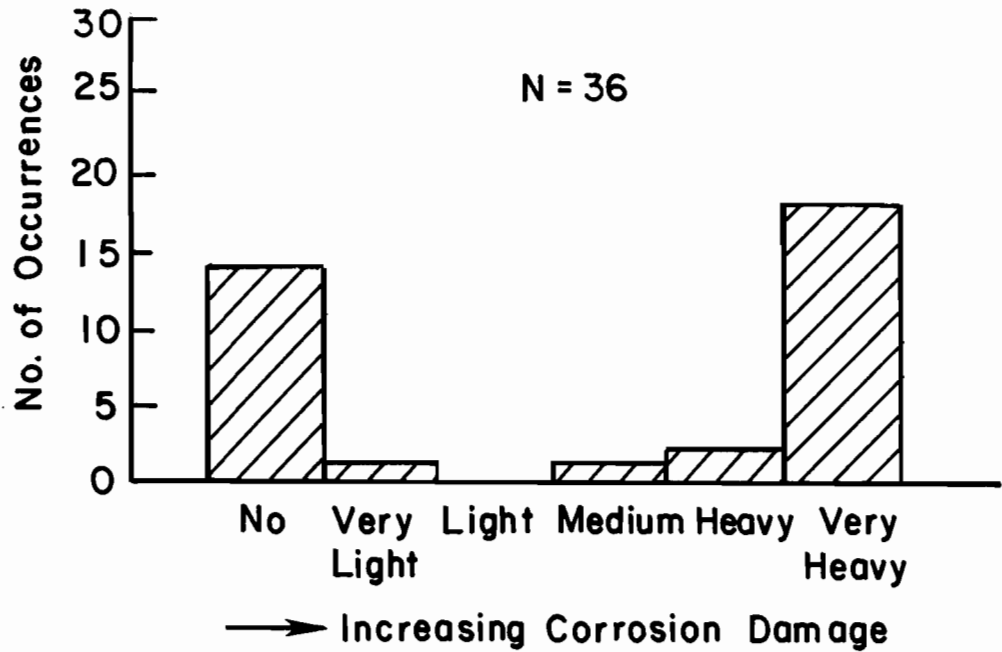


Fig. 5.12a Histogram of corrosion of uncoated reinforcement

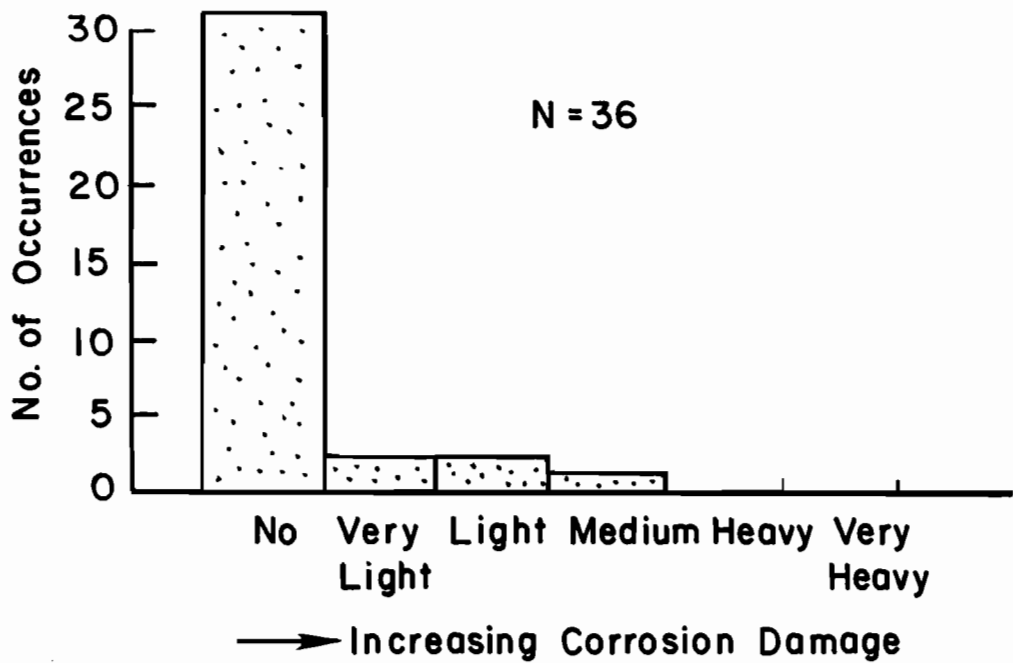


Fig. 5.12b Histogram of corrosion of epoxy-coated reinforcement

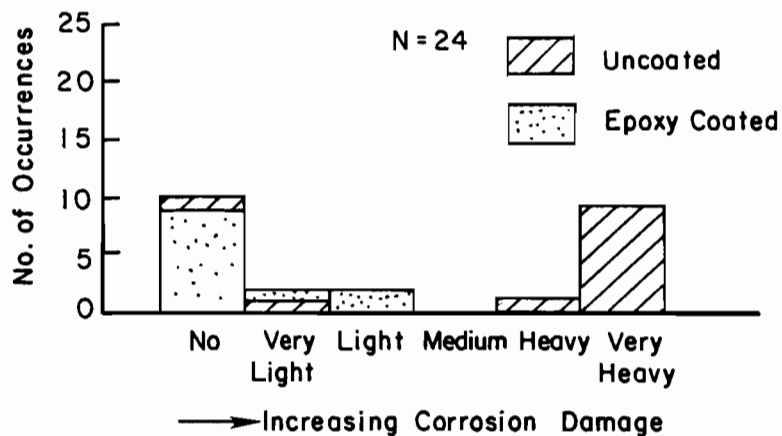


Fig. 5.13a Histogram of nonprestressed reinforcement corrosion in specimens (≈ 0.015 in. surface crack width)

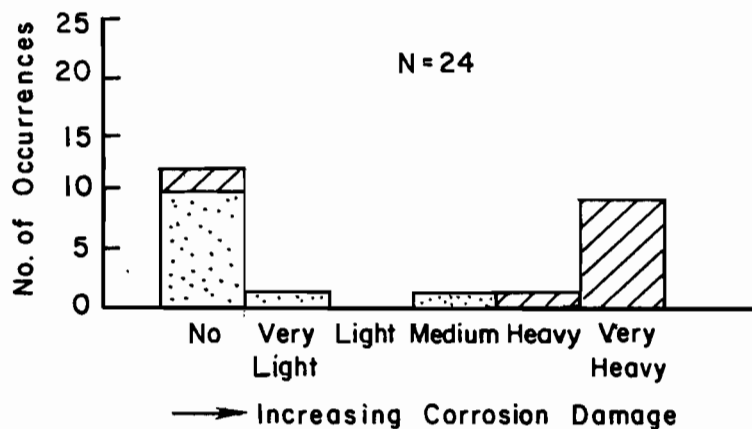


Fig. 5.13b Histogram of nonprestressed reinforcement corrosion in prestressed specimens (≈ 0.015 in. surface crack width)

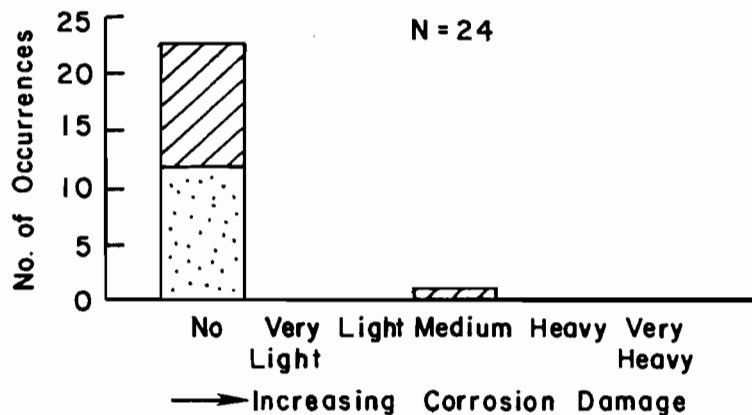


Fig. 5.13c Histogram of nonprestressed reinforcement corrosion in prestressed specimens (≈ 0.002 in. surface crack width)

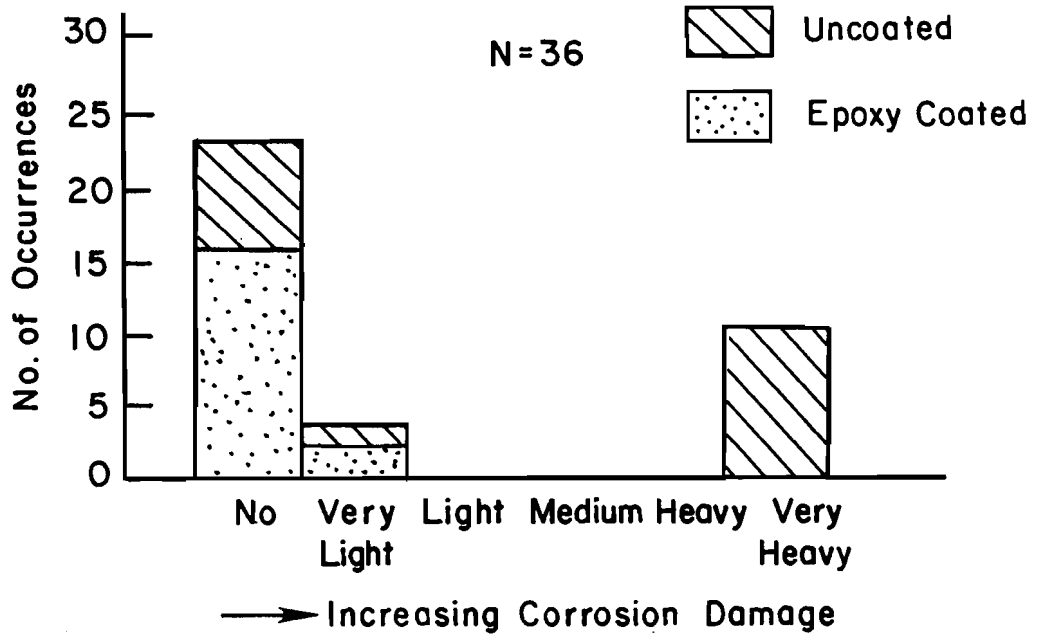


Fig. 5.14a Histogram of nonprestressed reinforcement corrosion with 2 in. cover

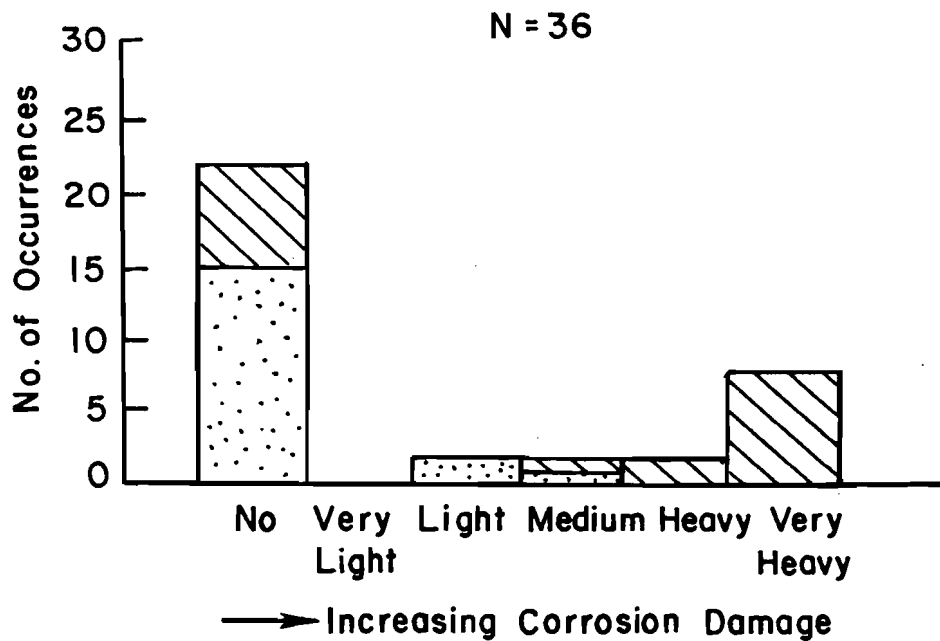


Fig. 5.14b Histogram of nonprestressed reinforcement corrosion with 3 in. cover

Figure 5.12 clearly shows that the extent and the occurrence of corrosion was substantially reduced with the use of epoxy-coated reinforcement as compared to the use of uncoated reinforcement.

Examination of Figs. 5.13a and 5.13b reveals that the distribution of corrosion damage for the nonprestressed specimens and the prestressed specimens with large crack widths (≈ 0.015 in.) is practically identical. This comparison suggests that prestressing does little to reduce corrosion if crack widths are comparable to those in reinforced concrete. However, Fig. 5.13c indicates that prestressing reduced the occurrence and extent of corrosion damage when crack widths were limited to approximately 0.002 in. This result substantiates the claim that prestressing limits corrosion by controlling cracking.

Figure 5.14 reveals that the increasing concrete cover did little to reduce the occurrence and extent of corrosion damage. This implies that for the length of exposure in this study, the corrosion of the nonprestressed reinforcement in the specimens was independent of the concrete cover between 2 in. and 3 in.

Figures 5.12b and 5.13c suggest that the epoxy-coated reinforcement, and prestressing which controlled crack widths to 0.002 in., were the factors most responsible for reducing both the incidence and extent of corrosion. There was virtually no corrosion which occurred in either epoxy-coated or uncoated reinforcement in the specimens which were prestressed and had a maximum surface crack width opening under load of 0.002 in. Therefore, for the durability tests, it can be concluded that prestressing which controlled cracking to this level was just as effective in reducing and controlling corrosion as epoxy-coated reinforcement.

The results presented in Table 4.3 show that, in general, the prestressing tendons in the unbonded specimens were well protected by the plastic duct. However, there was one case, Specimen 8, in which the unbonded tendon showed signs of localized surface corrosion at a location where the plastic duct had been purposely slit in the crack zone. This single instance of corrosion of a tendon, even if only very light, suggests the need for ensuring that there is no damage of the plastic duct after tendon placement.

Visual inspection of the galvanized duct which was removed from the crack zone of the grouted specimens did not reveal any clear trends in the corrosion pattern. There seemed to be less corrosion damage of the duct in the prestressed specimens with 0.002 in. crack widths, as compared to the other specimens. In all cases in which corrosion of the duct occurred, the corrosion was limited to the zinc coating (galvanizing) covering the duct. The galvanizing worked well in its intended function of controlling corrosion. The corrosion of the duct was evaluated as very heavy (VH) in many cases because it

occurred over a large area even though it was only the zinc coating which corroded. In actuality, the steel duct below the galvanizing was well protected, as were the prestressing tendons which were grouted in the duct.

The performance of the anchorages clearly revealed the need for special attention to ensure adequate corrosion protection. The unprotected anchorages of the unbonded specimens were heavily corroded, particularly on the castings. In addition, the jaws and inner surfaces of the anchorage castings around the jaws showed signs of corrosion. The clear concrete cover over the anchorages in the unbonded specimens varied between $7/8$ in. and $1-7/8$ in. depending on the required clear cover over the reinforcement. Other than for the concrete cover, the unbonded specimen anchorages were otherwise unprotected. As a result, the concrete cover alone proved ineffective in providing adequate corrosion protection of the anchorage.

The heavy corrosion which occurred on the strand extensions outside the unprotected anchors additionally suggests the need for anchorage protection. The corrosion of the tendon extensions is particularly distressful in the case of an unbonded tendon, since the loss of the tendon results in a loss of its ability to carry load. The need for complete encapsulation of the tendon system in a corrosion resistant barrier and the need for adequate auxiliary bonded reinforcement to ensure adequate structural integrity are emphasized in the design recommendation in Report 316-3F.

CHAPTER 6

CONCLUSIONS AND RECOMMENDATIONS

6.1 Conclusions

This report summarizes the results of a durability study involving accelerated exposure testing of full size segments of bridge decks with and without deck prestressing. While the actual time period was limited, very aggressive exposures were simulated. This accelerated exposure testing is considered adequate for determination of relative corrosion effects in cracked concrete but would not necessarily furnish conclusive evidence of relative corrosion effects in uncracked concrete. Based on the limited specimens and exposures, the following summarizes the major results and conclusions from the durability study.

1. Corrosion of nonprestressed reinforcement initiated and occurred only at the location of flexural cracks.
2. The incidence and extent of corrosion was much greater for uncoated reinforcement than for epoxy-coated reinforcement.
3. For the exposure conditions of the durability tests, the prestressed specimens in which crack widths were limited to approximately 0.002 in. under load resulted in virtually no corrosion of nonprestressed reinforcement.
4. Both nonprestressed and prestressed specimens which were loaded to produce crack widths of approximately 0.015 in. had a similar incidence and extent of corrosion damage to the nonprestressed reinforcement.
5. For the time period and exposure of this study, the incidence and extent of corrosion of the nonprestressed reinforcement at the crack zones was independent of the concrete cover between 2 and 3 in.
6. There was no advantage to "precleaning" the uncoated reinforcement prior to casting on the incidence and extent of corrosion.
7. Prestressing had a significant effect in reducing the penetration of Cl^- at crack locations in which crack widths were limited to 0.002 in. However, in all specimens, the Cl^- concentration at crack locations was substantially greater than the generally accepted chloride corrosion threshold.

8. The prestressed specimen in which the crack widths were limited to 0.002 in. apparently reduced chloride-induced corrosion by limiting the penetration of oxygen.
9. Prestressing had little effect on the Cl^- penetration with depth in uncracked concrete.
10. The combination of $\text{W/C} = 0.44$ and a 2 in. cover provided adequate protection of the nonprestressed reinforcement in uncracked concrete for the limited time exposure conditions of the test.
11. ACI and AASHTO recommendations for concrete cover and concrete quality assume that concrete is uncracked. These recommendations do not envision the ingress of large amounts of chlorides at crack locations. For cracked concrete, concrete quality and concrete cover had little effect on Cl^- penetration. Cracked concrete with wide cracks (0.015 in.) had substantial Cl^- penetration. Thus, the main benefit of prestressing is to eliminate and to greatly control cracking so as to restrict the Cl^- and oxygen penetration.
12. In general, concrete by itself proved inadequate in protecting prestressing anchorages and strand extensions from corrosion.
13. In general, both the grease-filled plastic duct and the grouted galvanized duct adequately protected the prestressing tendons in the length between the anchorages. When materials were received for the test specimens, a considerable amount of the plastic duct was heavily damaged. In addition, it would be more difficult to protect and inspect the plastic ducting on the job site. Complete encapsulation of the sheath and anchorage system are required for corrosion protection. These considerations, as well as the need for increased bonded reinforcement for general structural integrity when unbonded tendons are used, indicate that the grouted, bonded system is preferable for bridge deck applications.




6.2 Recommendations

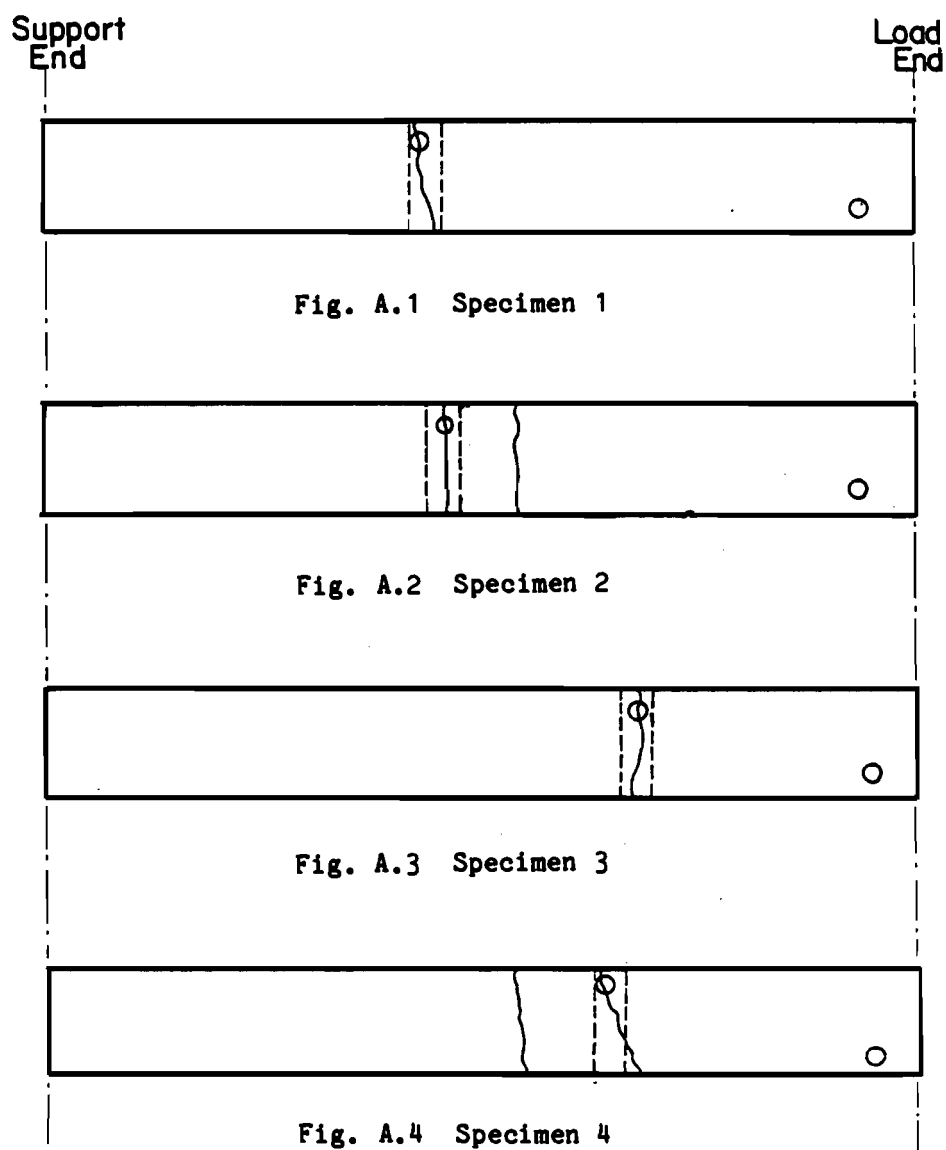
In carrying out the durability study as a portion of the overall project, the number of cycles of exposure to the harsh artificial environment was necessarily limited by overall time restraints. In addition, at the time the specimens were designed several later developments in tendon protection were unknown. It would add considerable value to the study and be a logical followup

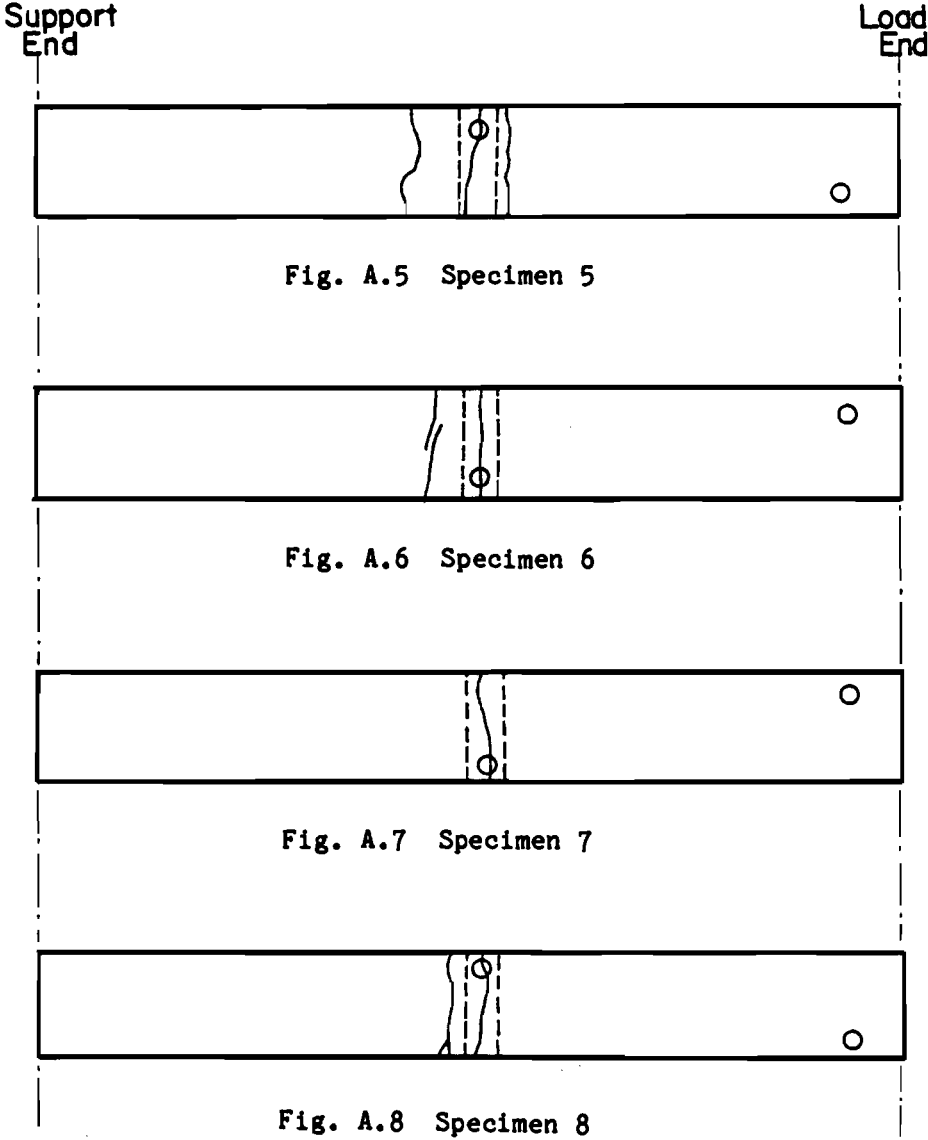
to plan to carry out a similar series of exposure tests subjected to a very high number of cycles over a longer time period. This series should employ the more recent details and requirements such as used in conjunction with the experimental full scale structure at LaGrange. We recommend that the State Department of Highways and Public Transportation seriously consider funding such a study in conjunction with extended detailed observation of the LaGrange, Texas bridge decks.

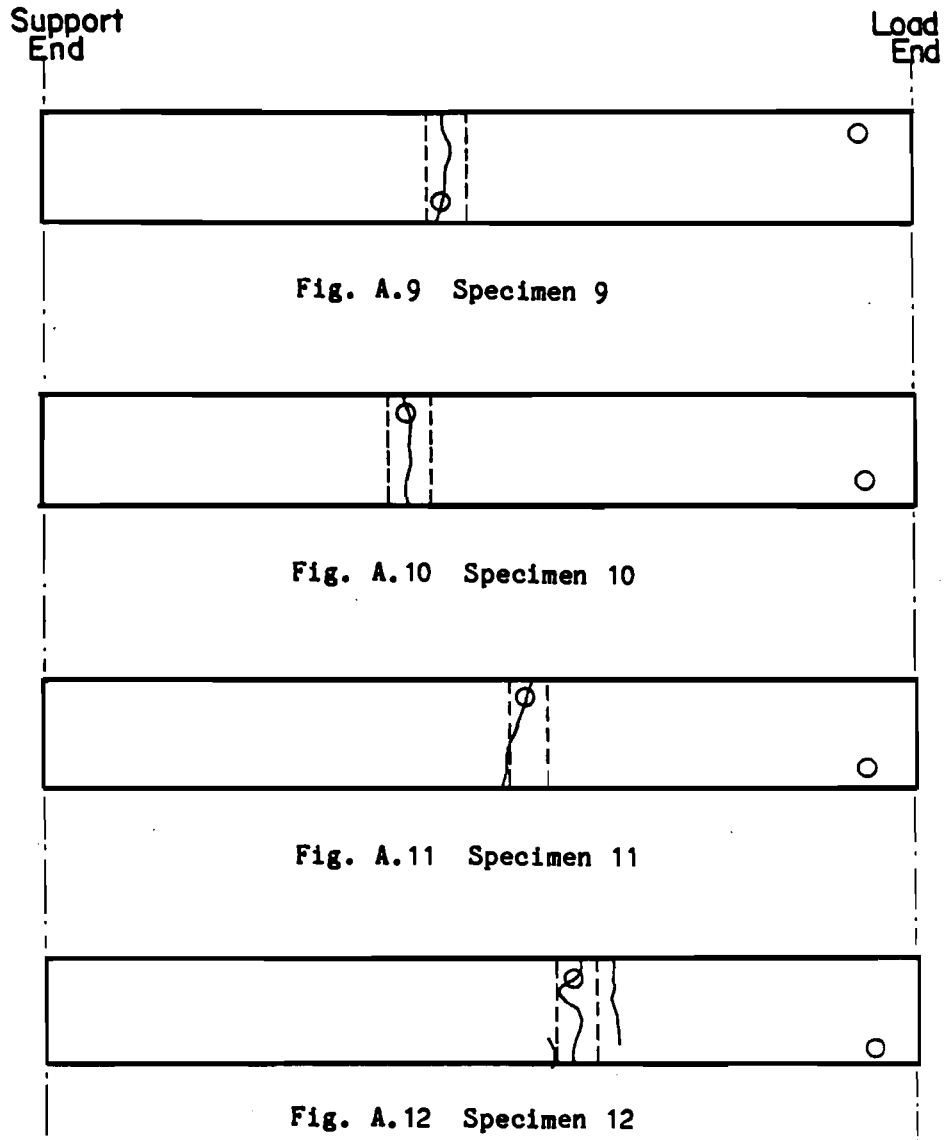
APPENDIX A

**SPECIMEN CRACK MAPS, SAW CUT LOCATIONS, AND CONCRETE SAMPLE
LOCATIONS FOR CHLORIDE CONTENT TESTS**

-  Crack
-  Saw Cuts
-  Sample Locations







Support End Load End

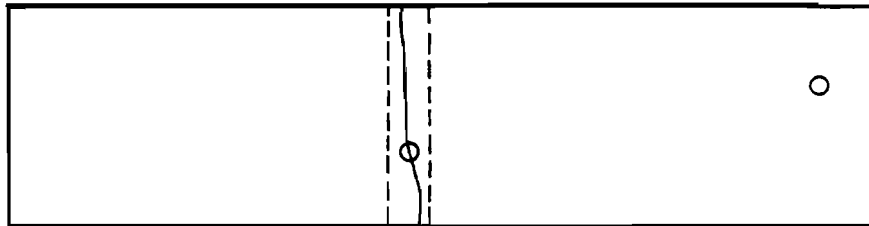


Fig. A.13 Specimen 13

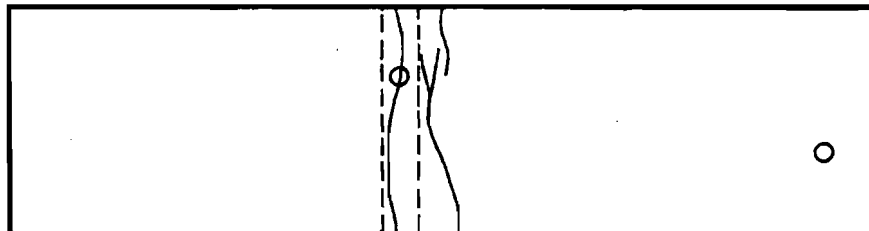


Fig. A.14 Specimen 14

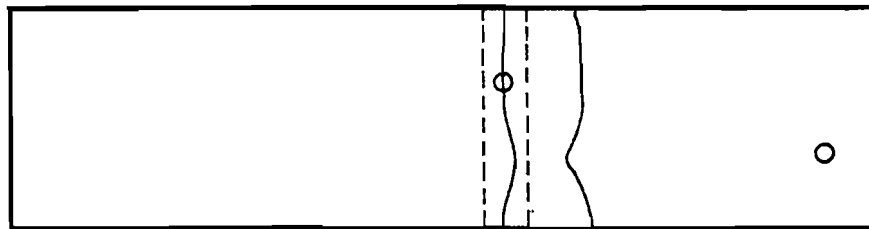


Fig. A.15 Specimen 15

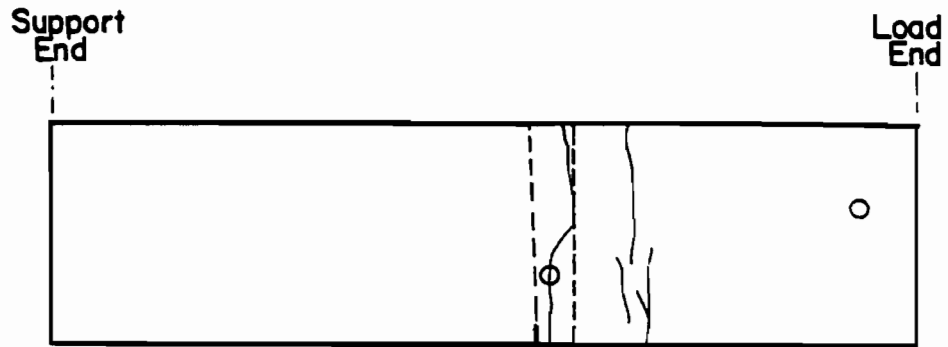


Fig. A.16 Specimen 16

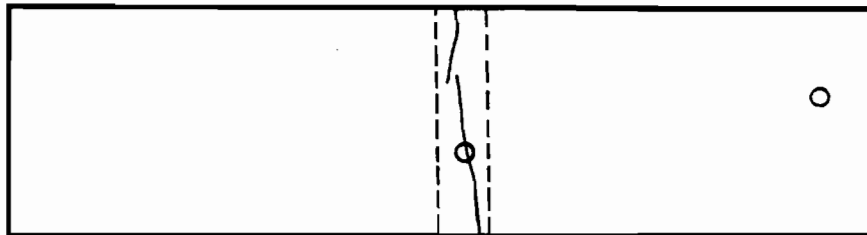


Fig. A.17 Specimen 17

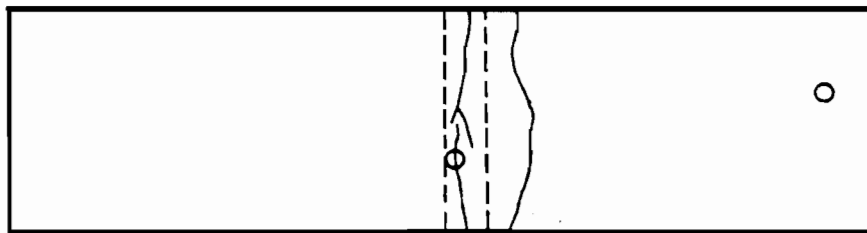


Fig. A.18 Specimen 18

Support End Load End

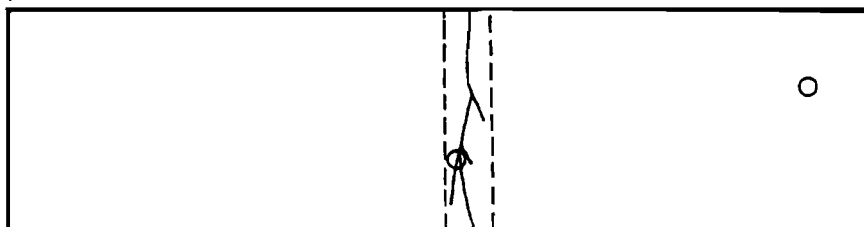


Fig. A.19 Specimen 19

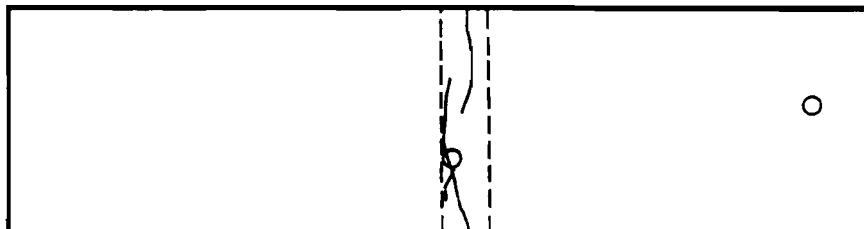


Fig. A.20 Specimen 20

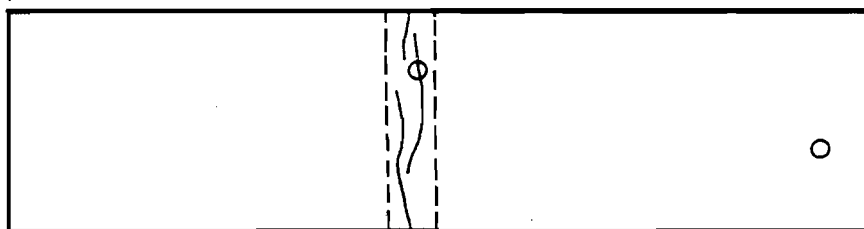


Fig. A.21 Specimen 21

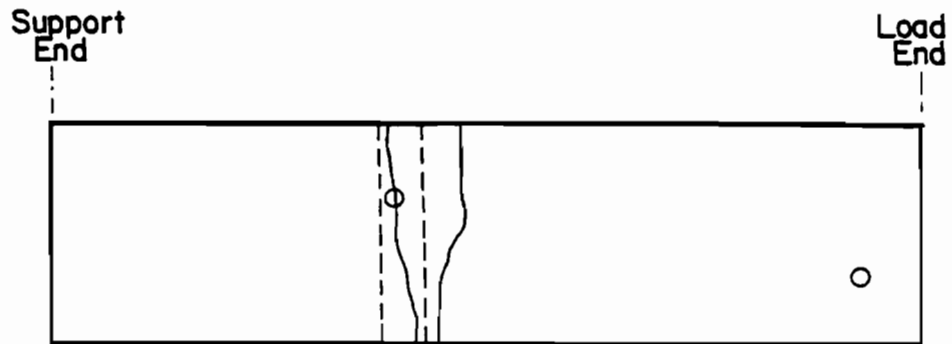


Fig. A.22 Specimen 22



Fig. A.23 Specimen 23



Fig. A.24 Specimen 24

APPENDIX B

SUMMARY OF MINERAL STUDIES LABORATORY (MSL) PROCEDURE FOR
DETERMINATION OF CHLORIDE (Cl^-) CONTENT IN CONCRETE

B.1 Residual Chloride of Colorimetric Method

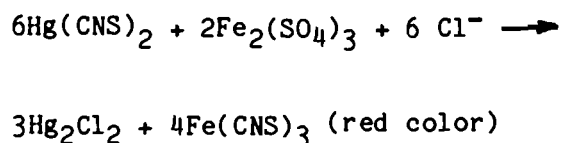
B.1.1 Reagents.

1. Ferric ammonium sulfate solution: Dissolve 6.0 g of $\text{FeNH}_4(\text{SO}_4)_2 \cdot 12\text{H}_2\text{O}$ in water in a 100-mL volumetric flask, and add 35.5 mL concentrated HNO_3 . Make up to 100-mL volume by adding water.
2. Saturated mercury thiocyanate solution: Weigh 0.35 g of $\text{Hg}(\text{CNS})_2$ into a 100-mL volumetric flask. Make up to 100 mL by adding 95 percent ethanol. The $\text{Hg}(\text{CNS})_2$ remains in suspension form. New solution should be prepared every few days.
3. Dilute HNO_3 (5 percent or 0.8N) for sample dissolution: Dilute 50 mL of concentrated HNO_3 with H_2O to make a 1000 mL solution.

B.1.2 Sample Dissolution. Weigh 0.5 g of sample into a 50-mL culture tube and add 5 mL of 4 percent HNO_3 . Heat content at 85°C on a Technicon BD40 digester to dissolve carbonates, anhydrite, and to release chloride. A boiling-point temperature and a high acid concentration must be avoided to prevent loss of chloride as HCl .

B.1.3 Procedure. Calibration standards and blanks: Prepare a chloride standard of 10 ug Cl/mL (Appendix A-1, Preparation of standard stock solution) by diluting 1 mL of the stock solution with H_2O to 100 mL in a 100-mL volumetric flask. Pipet 0, 2, 5, 8, and 10 mL of the 10 g/mL standard into 25-mL volumetric flasks.

Pipet an aliquot of sample solution containing between 20 to 100 μg of Cl^- into 25-mL volumetric flasks. All sample solutions and standard solutions must be acidified with HNO_3 to a pH of approximately 1 before addition of $\text{Hg}(\text{SCN})_2$. Shake the saturated mercury thiocyanate to bring it into suspension. Pipet 4 mL of the suspension into each flask followed by adding 2 mL of ferric ammonium sulfate to each. Mix content well and make up to 25 mL volume with water and mix again. Let the following reaction take place in 10 minutes, but do not allow the reaction to go for more than 30 minutes.



Remove colloidal particles by centrifuging a portion of the red-colored solution at 10,000 rpm. Measure absorbance of the clear solution at 460 nm on a spectrophotometer. Plot absorbance versus Cl^- concentration in ($\mu\text{g}/25 \text{ mL}$) on a linear scale; a straight line is obtained.

Calculation:

$$\text{Cl}^- (\mu\text{g/g}) = \frac{C \frac{V_t}{V_a} \times f}{\text{wt.}}$$

where: C: the amount of Cl^- (in $\mu\text{g}/25 \text{ mL}$) obtained from calibration curve (that is, the amount of Cl^- in the aliquot of sample used for analysis)

- V_a : aliquot of sample (in mL) used for analysis
- V_t : total volume (in mL) of sample solution
- wt: weight of sample (in grams) dissolved in total volume of V_t
- f: dilution factor

B.1.4 Comments. Mercury thiocyanate ($\text{Hg}(\text{CNS})_2$) is slightly soluble in ethanol; thus it is essential that a freshly prepared suspension of $\text{Hg}(\text{CNS})_2$ in alcohol be used for reaction. MSL's experience shows that if an aged suspension is used, a faint reddish color will develop at the levels of Cl^- concentration given. This phenomenon results from insufficient amounts of $\text{Hg}(\text{CNS})_2$ in the ethanol solution for complete reaction with Cl^- . It has also been found that if the excess amounts of $\text{Hg}(\text{CNS})_2$ in suspension are allowed to react with $\text{Fe}_2(\text{SO}_4)_3$ for a long time, even in the absence of Cl^- , an intense reddish color will develop, indicating reaction between $\text{Hg}(\text{CNS})_2$ and $\text{Fe}_2(\text{SO}_4)_3$ and leading to formation of the reddish $\text{Fe}(\text{CNS})_3$.

B.2 Dissolution of Samples

B.2.1 Acid Soluble Test.

<u>Wt. of Sample</u>	<u>Acid Dissolution</u>	<u>Heating Temperature</u>	<u>Direction of Heating</u>	<u>Final Volume</u>
1 gm	5 mL H_2O + 1.5 ml conc. HNO_3	95-100°C	1-2 hrs	50 mL with H_2O

B.2.2 Water Soluble Test.

<u>Wt. of Sample</u>	<u>Acid Dissolution</u>	<u>Heating Temperature</u>	<u>Direction of Heating</u>	<u>Final Volume</u>
1 gm	25 ml H ₂ O	95-100°C	1-2 hrs	50 ml with H ₂ O

B.3 Quality Assurance

To ensure reliability of the method, results on reference samples (EPA and standard seawater) were also obtained. These results were as follows:

Standard Seawater:

Found	Certified
20.00 gm/l	19.834 gm/l

EPA-478

Found	Certified
70.4 µg/ml	70.2 µg/ml

R E F E R E N C E S

1. Bellito, A., "The Civil Engineer and the Decay of America's Infrastructure," Civil Engineering, ASCE, December 1983, p. 56.
2. Federal Highway Administration, "Our Nation's Highways Selected Facts and Figures," U. S. Department of Transportation, Office of Highway Planning, No. HHP-41/4-83(50M), 1983.
3. Tonini, D., and Dean, S., Eds., Chloride Corrosion of Steel in Concrete, American Society for Testing and Materials, STP629, 1977.
4. "Cathodic Deck Protection for Bridges Come Slowly," Engineering News-Record, September 6, 1979, pp. 22-24.
5. Blaha, B., "Idea Packed Segmental Bridge Connects the Florida Keys," Concrete Products, August 1980.
6. Tedesko, A., "Bridge Decks: Transverse Post-Tensioning and Other Successful Experiences," ACI Journal, December 1976, pp. 665-670.
7. Cusens, A. R., and Abbasi, A. F., "The Influence of Transverse Prestress on the Strength of Prestressed Concrete Bridge Slabs," Magazine of Concrete Research, London, Vol. 15, No. 44, July 1963, pp. 107-114.
8. Rawles, R. H., "Dallas Bridge Has Post-Tensioned Concrete Deck," Civil Engineering, ASCE April 1973, pp. 74-77.
9. Stollendorf, D., "Application of Transverse Prestressing for Bridge Decks," RRC Conference, Williamsburg, Virginia, December 1979.
10. American Association of State Highway and Transportation Officials, Standard Specifications for Highway Bridges, Twelfth Edition, 1977.
11. Brown, R., and Kessler, R., "Fundamentals of Corrosion," unknown source.
12. Fontana, M., and Greene, N., Corrosion Engineering, McGraw-Hill, New York, 1978.
13. American Concrete Institute, Corrosion of Metals in Concrete, Publication SP-49, Detroit, Michigan, 1975.

14. Carter, C., Hyatt, M., and Cotton, J., "Stress-Corrosion Susceptibility of Highway Bridge Construction Steel," Federal Highway Administration Report No. FHWA-RD-73-3, April 1972.
15. Cornet, I., Pirtz, D., Polivka, M., Gau, Y., and Shimizu, A., "Effect of Stray Electric Current on the Corrosion of Prestressed Concrete in Sea Water," Offshore Technology Conference Proceedings, 1978, pp. 1251-1256.
16. Niemann, J., "Investigation of Mechanism of Delayed Failure of Prestressing Steel," Aerojet-General Corporation, Final Report, July 1968.
17. Mozer, J., Bianchini, A., and Kesler, C., "Corrosion of Reinforcing Bars in Concrete," ACI Journal, August 1965, pp. 909-930.
18. Beeby, A. W., "Corrosion of Reinforcing Steel in Concrete in Its Relation to Cracking," The Structural Engineer, Vol. 56A, No. 3, 1978, pp. 77-81.
19. Beeby, A., "Cracking, Cover, and Corrosion of Reinforcement," Concrete International, Vol. 5, No. 2, February 1983, pp. 35-40.
20. ACI Committee 222, "Corrosion of Metals in Concrete," ACI Journal, Vol. 82, No. 1, January-February 1985, pp. 3-32.
21. Abeles, P. W., "Study of Crack Widths and Deformation under Sustained and Fatigue Loading," PCI Journal, Vol. 10, No. 4, December 1965, pp. 43-52.
22. Abeles, P. W., and Filipek, S. J., "Corrosion of Steel in Finely Cracked Reinforced and Prestressed Concrete," PCI Journal, Vol. 10, No. 2, April 1965, pp. 36-41.
23. Gerwertz, N. W., "Causes and Repair of Deterioration to a California Bridge Due to Corrosion of Reinforcing Steel in a Steel Environment: Part I, Methods of Repair," Highway Research Board, No. 182, pp. 1-16, 1958.
24. Houston, J., Atimtay, E., and Ferguson, P., "Corrosion of Reinforcing Steel Embedded in Structural Concrete," Center for Highway Research, The University of Texas at Austin, Report 3-5-68-112-1F, March 1972.
25. Rehm, G., and Rauen, P., "Korrosion von Stahl in Beton," Jahrbuchdes Bauwesens, September 1966, pp. 1-25.

26. Thornton, J., "Tensile Crack Exposure Tests," Technical Memorandum No. 6-412, Report 4, Structures Laboratory, U. S. Army Engineer Waterways Experiment Station, March 1984.
27. Suzuki, K., and Ohno, Y., "Calculation of Crack Width and Crack Control Design of PPC Members," Advanced Research Workshop on Partial Prestressing, Sponsored by NATO Scientific Affairs Division, Paris, France, June 1984.
28. Gjørsv, O., "Steel Corrosion in Reinforced and Prestressed Concrete Structures," Nordisk Betong, 2-4: 1982, pp. 147-151.
29. American Concrete Institute, Building Code Requirements for Reinforced Concrete (ACI 318-83), American Concrete Institute, Detroit, 1983.
30. Moore, D., Klodt, D., and Hensen, R., "Protection of Steel in Prestressed Concrete Bridges," National Cooperative Highway Research Program Report 90, 1970.
31. Rehm, G., "Corrosion of Prestressing Steel," General Report submitted at FIP Symposium on Steel for Prestressing, Madrid, Spain, 1968.
32. Mindess, S., and Young, J., Concrete, Prentice-Hall, New Jersey, 1981.
33. Mehta, P., and Gerwick, B., "Cracking-Corrosion Interaction in Concrete Exposed to Marine Environment," Concrete International, October 1982, pp. 45-51.
34. Overman, T., "Flexural Fatigue Behavior of Pretensioned Concrete Girders," unpublished Master's thesis, The University of Texas at Austin, December 1984.
35. Spellman, D., and Stratfull, R., "Concrete Variables and Corrosion Testing," Highway Research Record, No. 423, pp. 27-45.
36. Stratfull, R., Jurkovich, W., and Spellman, D., "Corrosion Testing of Bridge Decks," Transportation Research Record, No. 539, 1975, pp. 50-59.
37. Stratfull, R., "Corrosion Autopsy of a Structurally Unsound Bridge Deck," Highway Research Record, No. 433, 1973, pp. 1-11.
38. Stratfull, R., "Half-Cell Potentials and the Corrosion of Steel in Concrete," Highway Research Record, No. 433, 1973, pp. 12-21.

39. American Society for Testing and Materials, Standard Test Method for Half Cell Potentials of Reinforcing Steel in Concrete, C876-80, 1980.
40. Texas State Department of Highways and Public Transportation, Standard Specification for Construction of Highways, Streets, and Bridges, September 1982.
41. Etienne, C., Binnekamp, D., Copier, W., Hendrick, R., and Smit, C., "Corrosion Protection of Unbonded Tendons," HERON, Vol. 26, No. 3, 1981.
42. Clear, K., and Harrigan, E., "Sampling and Testing for Chloride Ion in Concrete," Federal Highway Administration, Report No. FHWA-RD-77-85, August 1977.
43. Clear, K. C., "Time-to-Corrosion of Reinforcing Steel in Concrete Slabs," Vol. 3, Performance After 830 Daily Salt Applications, Report No. FHWA-RD-76-70, FHWA, 1976.
44. Beaton, J., Spellman, D., and Stratfull, R., "Corrosion of Steel in Continuously Submerged Reinforced Concrete Piling," Highway Research Record, No. 204, pp. 11-21.
45. Stratfull, R., discussion of article "Cracking, Cover, and Corrosion of Reinforcement," by A. Beeby, Concrete International, Vol. 5, No. 12, December 1983, pp. 67-68.